Industrialization of Selective Laser Melting for the Production of Porous Titanium and Tantalum implants

Ruben WAUTHLE

Supervisors:
Prof. dr. ir. Jean-Pierre Kruth
Prof. dr. Michiel Mulier
dr. ir. Jan Schrooten

Members of the examination committee:
Prof. dr. ir. Jean-Pierre Celis, chairman
Prof. dr. ir. Jan Van Humbeeck
dr. ir. Peter Mercelis
(3D Systems – LayerWise NV)
Prof. dr. ir. Harry Van Lenthe, secretary
Prof. dr. ir. Harrie Weinans
(TU Delft – UMC Utrecht)

Dissertation presented in partial fulfilment of the requirements for the degree of PhD in Engineering Science

November 2014

Funded by:

Industrial partner:

Uitgegeven in eigen beheer, RUBEN WAUTHLE, LEUVEN

ISBN 978-94-6018-908-1

D/2014/7515/132

Acknowledgements

Let's go back to July 2009. I just graduated as a mechanical engineer from KU Leuven and I was excited to start working in an industrial and commercial environment. I wanted to do something in which I could use my engineering skills and something that would keep me personally interested and involved. Doing a PhD wasn't part of that plan.

Through my Master thesis I had been in contact with the metal 3D printing company LayerWise and I really wanted to start working there. But at that time they had no jobs, so I graduated without knowing what my future would look like. About one week later, I got a call from Peter Mercelis, asking me if I would want to apply for an IWT Baekeland mandate on medical applications. A PhD? On medical applications, having no medical background? Well, if this would be the only way to start working at LayerWise: why not?

So I started working at LayerWise in September 2010 and here I am: The past 4 years I managed several challenging projects, worked with interesting people, travelled around the world and most importantly, liked what I did. And at the same time I obtained my PhD. The pleasure I had working at LayerWise and doing research for my PhD wouldn't be possible without the help and support of some people whom I would like to express my gratitude to.

For me, it all started thanks to Peter Mercelis and Jonas Van Vaerenbergh from LayerWise. You guys gave me the opportunity to work at a very interesting and dynamic company and I am still glad to be part of it. Peter, thank you for your faith and support and for guiding me through the medical device industry. Jonas, I really enjoyed our sometimes heavy technical discussions, often resulting in nice solutions.

During my PhD, I had the luxury and pleasure of having three supervisors, all of them renowned in their research field. Jean-Pierre, I realize that I have not been a role model for a PhD student, but thank you for your blind faith and keeping my feet on the ground at times when I was too ambitious. Michiel, you

are one of the few people I know that can talk in such an enthusiastic and inspiring way about their work, and I really appreciate the time and effort you have put in training me on my medical knowledge. I promise we will continue our discussions to create some innovative orthopedic solutions in the future. Jan, thank you for the many follow-up meetings we had and your down-to-earth approach. I look forward to that first whisky tasting invitation!

I would also like to express my gratitude to the members of the examination committee. Prof. Jan Van Humbeeck was actually only assigned as an assessor, but I had the pleasure of working with him on many interesting projects. Jan, thank you for the many discussions and your critical comments and instant feedback on my work. My history with Prof. Harrie Weinans goes back to June 2011, but ever since then I had the honor of working with him and his team. Harrie, thank you for your enthusiasm and our pleasant collaboration throughout these years. Furthermore, I would like to thank prof. Harry Van Lenthe for his critical and useful comments on my manuscript. Your comments have definitely contributed to the final quality of the work I present here. And in addition, I would like to thank Prof. Jean-Pierre Celis for chairing the committee.

Besides having great people for guidance and supervision of my dissertation, this work would not have been possible without the support of IWT. This research was established by funding of the agency for Innovation by Science and Technology (IWT) of the Flemish government through Baekeland mandate 'IWT 100228' at the company LayerWise N.V.. The animal experiment in Chapter 3 was funded by Project P2.04 BONE-IP of the research program of the BioMedical Materials Institute, co-funded by the Dutch Ministry of Economic Affairs.

A very special word of thanks goes to the researches under the supervision of Prof. Harrie Weinans and Prof. Amir Abbas Zadpoor. Some of the results of Chapters 2, 3 and 4 were obtained by collaboration between LayerWise N.V., KU Leuven, Erasmus Medical Centre, TU Delft and UMC Utrecht. Johan, Saber, Mohammad and Gianni, thank you guys for the almost perfect collaboration we had. I believe together we realized some great work which resulted in many publications. Thank you for continuously pushing me to make more test samples or to finish my manuscripts. A big part of my dissertation wouldn't be there without your help.

Not only abroad, but also at KU Leuven, I worked with great people. I would like to thank Lore Thijs and Bey Vrancken from MTM and Stijn Clijsters from PMA for the thesis projects we supervised together. Also thanks to my thesis students Maria, Tian, Evelina, Britt and Karl, and thanks to Simon Van Bael, Maarten Moesen, Gregory Pyka, Paul Crabbé, Bart Pelgrims, Kris Van de Staey, and many others I have worked with.

Once upon a time there was a bunch of 'LayerKwieten' at the good old Kapeldreef 60. They now moved to Grauwmeer 14, and have increased rapidly over the past 4 years, but I still do enjoy working with them. To all my colleagues at LayerWise, thank you for all the nice moments from making kick-ass metal AM parts to a 'fleske' on Friday evening.

As you may have noticed, I enjoyed every bit of what I did in my professional life so far and I strongly believe this is necessary in order to be successful. But at the same time I believe that having a healthy personal life is as least as important. I really like to travel around the world, go to a bar or a restaurant, do some sports or go for a walk, listen to music or go to festivals, live in Leuven or just have a beer and have fun. And that's what I have my friends for. Dear friends, thank you for your support, but most of all thank you for all the enjoyable moments.

I am very proud of what I have achieved so far and five years ago I never imagined I would be standing right here, right now. I don't know what my future will bring, but I do know that whatever I do or wherever I go, I will always be supported by my parents. Thank you for all your love, support, and advice.

And right at the moment when I least expected it, I meet this wonderful woman. Anna, thank you for all your love and support over the past few weeks. I really look forward enjoying life together with you.

Ruben Wauthle
31 oktober 2014

Abstract

As the number of orthopedic surgeries is increasing, so is the need for implants that not only can reconstruct a mechanical stable joint, but also serve as bone replacement material since the availability of transplant bone is rather limited. Already more than two decades porous metal implants have been a solution to address this need since they can exhibit mechanical properties close to human bone and thus provide sufficient implant strength and stability while at the same time they allow for bone to grow inside the pores, ensuring a long-term implant fixation.

Only now, with the introduction of additive manufacturing or 3D printing techniques like selective laser melting it has become possible to manufacture on an industrial scale porous metallic structures in a controlled and reproducible manner. In this dissertation three types of porous metallic implants made by selective laser melting have been evaluated: porous implants made from Ti6Al4V, tantalum and pure titanium.

Today, Ti6Al4V is still the material of choice since it is a mechanically strong material with a proven clinical track record. But in order to select the right implant design and processing steps, it is important to identify all the variables that influence the final result. This dissertation presents and discusses probably the largest experimental data set on the influence of geometrical variables (structure relative density and unit cell geometry) and processing variables (build orientation, heat treatment, bio-functionalizing surface treatments) on the mechanical and biological implant performance.

Tantalum, on the other hand, is an interesting metal since it has a very good biocompatibility, but because of its high price and difficulty to process, the use of tantalum for porous implants is not that obvious. In this dissertation it is shown for the first time that selective laser melting can be successfully used to manufacture porous tantalum implants with interesting mechanical properties and promising *in vivo* performance. Since porous pure titanium implants

showed very similar mechanical behavior, this could potentially lead to a revival of the use of pure titanium for dynamically loaded porous implants.

But in the end, the manufacturing cost is also important for the acceptance of this new technology to produce porous metallic implants on a commercially suitable level. Therefore significant productivity improvements have been achieved to lower the production costs of porous implants made by selective laser melting.

Samenvatting

Samen met het toenemende aantal orthopedische heelkundige ingrepen stijgt ook de nood aan implantaten die niet enkel een mechanisch stabiel gewricht kunnen reconstrueren, maar die ook kunnen dienen als botvervangend materiaal, aangezien de beschikbaarheid van getransplanteerd bot eerder beperkt is. Poreuze metalen implantaten bieden al meer dan twee decennia een oplossing om aan deze nood tegemoet te komen, aangezien ze mechanische eigenschappen kunnen bezitten die dicht aanleunen bij die van menselijk bot, waardoor ze voldoende sterkte en stabiliteit bezitten. Tegelijkertijd staan de implantaten toe dat bot in de porositeit groeit, zodat een langdurige implantaat-fixatie gegarandeerd is.

Met de introductie van additieve productietechnieken of zogenaamde 3D printing technieken, zoals het selectief laser smelten, is het nu mogelijk om op een industriële schaal poreuze metalen structuren te produceren op een gecontroleerde en reproduceerbare manier. In dit doctoraatsproefschrift zijn drie types poreuze metalen implantaten onderzocht, namelijk implantaten gemaakt uit Ti6Al4V, uit tantalum en uit zuiver titanium. Alle drie zijn ze vervaardigd via selectief laser smelten.

Tot op heden is Ti6Al4V het materiaal dat de voorkeur wegdraagt, aangezien het materiaal mechanisch sterk is en bovendien biocompatibel is. Om het juiste implantaatontwerp en de bijhorende verwerkingsstappen te kunnen kiezen is het echter belangrijk om alle variabelen die het uiteindelijke resultaat kunnen beïnvloeden te identificeren. Dit proefschrift presenteert en bespreekt wat wellicht de grootste experimentele dataverzameling is die de invloed karakteriseert van geometrische variabelen (de relatieve structuurdensiteit en de eenheidscel geometrie) en van procesvariabelen (bouworiëntatie, warmtebehandeling en bio-functionalizerende oppervlaktebehandelingen) op de mechanische en biologische implantaat prestatie.

Tantalum anderzijds is een interessant metaal doordat het een bijzonder goede biocompatibiliteit bezit. Door de hoge kostprijs en moeilijkheid om het te

verwerken is het gebruik van tantalum voor poreuze implantaten echter niet zo evident. In dit proefschrift wordt voor de eerste keer aangetoond dat selectief laser smelten succesvol kan gebruikt worden om poreuze tantalum implantaten te vervaardigen, die bovendien interessante mechanische eigenschappen bezitten en veelbelovende in vivo resultaten vertonen. Omdat poreuze, uit zuiver titanium vervaardige implantaten een zeer gelijkaardig mechanisch gedrag vertonen, zou dit mogelijk tot een heropleving kunnen leiden van het gebruik van zuiver titanium voor dynamisch belastte poreuze implantaten.

Om uiteindelijk de productie van poreuze metalen implantaten op een industriële schaal commercieel interessant te maken, is het belangrijk om alle directe en indirecte kosten in rekening te brengen. In dit proefschrift worden er significante productiviteitsverbeteringen behaald om de productiekost van poreuze implantaten vervaardigd via selectief laser smelten te reduceren.

List of Abbreviations

3D	Three-Dimensional
AB	As Built
AcAl	Acid-Alkali
AlAcH	Alkali-Acid-Heat treated
AM	Additive Manufacturing
CAD	Computer Aided Design
CP	Commercially Pure
CT	Computed Tomography
DIA	Diagonal
DoE	Design of Experiments
EBM	Electron Beam Melting
EDM	Electric Discharge Machining
ELI	Extra Low Interstitial
HA	Hydroxyapatite
HIP	Hot Isostatic Pressing
HOR	Horizontal
LENS	Laser Engineered Net Shaping
LOM	Light Optical Microscope
OEM	Original Equipment Manufacturer
RSA	Roentgen Stereophotogrammetry
SEM	Scanning Electron Microscope
SLM	Selective Laser Melting
SR	Stress Relieved
TM	Trabecular Metal
VER	Vertical

List of Symbols

Arabic Symbols

e_{frac}	strain at fracture [%]
e_{ple}	strain at plateau end [%]
e_s	elongation of solid material [%]
E	stiffness [GPa]
E_s	Young's Modulus of solid material [GPa]
h	hatch spacing [µm]
N	cycles to failure [-]
P	laser power [W]
t	layer thickness [µm]
v	scan speed [mm/s]
S	maximum stress [MPa]
S_f	fatigue strength [MPa]
$S_{f,s}$	fatigue strength of solid material [MPa]

Greek Symbols

ρ	density [g/cm³]
ρ_{rel}	structure relative density [-]
ρ_s	density of solid material [g/cm³]
σ_{130}	stress at plateau end [MPa]
σ_{pl}	plateau stress [MPa]
σ_y	yield strength [MPa]
$\sigma_{y,s}$	yield strength of solid material [MPa]

Table of Contents

1. Introduction

This chapter briefly introduces the background and motivation of the doctoral research by first explaining some basic principles and ideas. The research questions and the main achievements will be depicted in the next section, while the introduction chapter ends with outlining the dissertation in a chapter by chapter overview.

1.1. Motivation

Metal 3D printing or so called Additive Manufacturing (AM) is a collection of relatively new manufacturing technologies that can be used to process metals in a layer by layer manner that allows new and unexplored design possibilities. One example of the many possibilities of AM is the ability to manufacture porous structures that can be incorporated in implant designs. The Selective Laser Melting (SLM) technology is a promising AM technique that has been used to manufacture porous Titanium (Ti) and Tantalum (Ta) implants in this dissertation.

1.1.1. Porous implants

The use of certain implant materials has changed over time due to several reasons. Biocompatible metals have been used for decades as implant materials, mainly because of their high strength. This high strength and stiffness, however, also cause stress-shielding effects for implants under load-bearing conditions like e.g. orthopedic implants for joint replacements or spinal implants for fusion purposes.

For this reason, porous metallic implants are of interest since they exhibit lower strength and stiffness compared to the solid metals and are more in the range of the properties of human bone, still providing sufficient implant strength. Also, the initial fixation is improved by a high coefficient of friction and the long term stability is ensured by the ability for the bone to grow into the open, interconnected porosities.

These advantages of porous metal implants have driven the major orthopedic device manufacturers to introduce their own porous metallic biomaterials by means of a porous coating on top of a solid implant or by stand-alone porous bone substitutes. Figure 1.1 gives two examples of some of the commercial porous metallic implant materials that are available today.

Figure 1.1: Examples of commercially available porous orthopedic implants: *Trabecular Metal*™ revision hip cups and augments (top, image courtesy: Zimmer Inc, Warsaw, IN, USA) and a *Regenerex*™ primary tibial tray (bottom, image courtesy: Biomet Inc, Warsaw, IN, USA).

One of the major disadvantages of these porous implants is the manufacturing method. Traditional processing techniques like plasma spraying or foaming techniques, do not allow to create regular porous structures with controlled geometrical and mechanical properties in any desirable shape. AM techniques like SLM make it possible to overcome these disadvantages.

1.1.2. Selective Laser Melting

Selective Laser Melting is an additive manufacturing technique that melts thin layers of metal powder together by using a focused laser beam in order to create full dense and functional metal parts. The SLM process is schematically represented in Figure 1.2.

Thanks to the very thin layers in the range of 20-90 µm and the very accurate positioning of the laser beam, SLM is perfectly suited to manufacture highly porous structures with a high level of detail and good reproducibility.

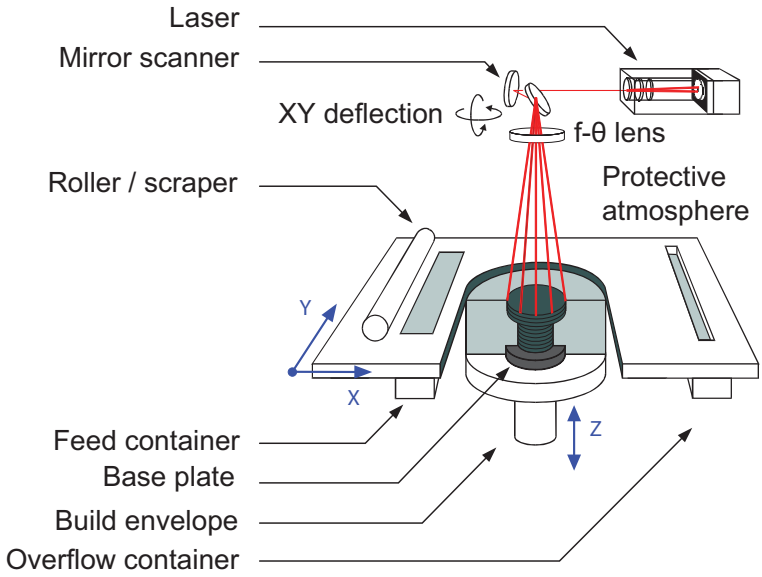

Figure 1.2: Schematical representation of the SLM process. A thin laser beam that gets deflected by the scanner selectively melts thin layers of metal powder together. Once the scanning of a layer is completed, the base plate lowers one layer thickness and the scraper deposits a new layer of powder before the scanning of the new layer starts. This process is repeated until the complete part is created.

One of the first metals that could be successfully processed using SLM is Ti6Al4V, and still today the SLM material portfolio is expanding rapidly. To name a few, several grades of titanium and titanium alloys, stainless steels, cobalt-chromium alloys and exotic metals like tantalum and tungsten are currently available for SLM manufacturing.

1.1.3. Titanium and tantalum

Several metals can be considered as the base material for porous implants made by SLM, but certain requirements have limited the selection of metals used in this dissertation. First, the selected materials should have a proven clinical track record to illustrate their biocompatible behavior and accelerate the clinical acceptance. Secondly, since highly porous structures are of interest, the selected

metals should have sufficient strength. And finally, it should be possible to process these materials by SLM.

These three requirements have narrowed the selection of metals down to Ti6Al4V, tantalum and pure titanium. The properties of these selected metals processed in a conventional way are summarized in Table 1.1 and will be used for further reference throughout this dissertation.

Material	ρ_s [g/cm³]	$\sigma_{y,s}$ [MPa]	$\sigma_{UTS,s}$ [MPa]	E_s [GPa]	e_s [%]	$S_{f,s}$ [MPa]
CP Ti grade 1	4.51	170-241	240-331	103	30	270
CP Ti grade 2	4.51	280-345	340-434	103	28	330
CP Ti grade 3	4.51	380-448	450-517	103	25	350
CP Ti grade 4	4.51	480-586	550-662	104	20	376
Ti6Al4V grade 5	4.43	830-924	900-993	114	14	500
Ti6Al4V ELI grade 23	4.43	760-827	830-896	114	15	n.a.
Tantalum	16.6	165-220	200-390	186	20-50	n.a.

Table 1.1: Literature values of the density and mechanical properties of standard annealed wrought titanium grades [1] and tantalum [2, 3]: The density (ρ_s), yield strength (σ_y), the ultimate tensile strength (UTS), Young's modulus (E) and the elongation (e). Fatigue strength ($S_{f,s}$) values were reported in [4].

One of the most used implant materials is Ti6Al4V since it has a very high strength to weight ratio. Tantalum is of interest because it has shown to be a very biocompatible implant material, and pure titanium came to the forefront after the first results of porous Ti6Al4V and tantalum implant performances that have led to new insights.

1.2. Scope and achievements of the research

Selective Laser Melting, or 3D printing in general, is often associated with prototyping although this technology is perfectly suited for serial production of functional parts or implants. The huge amount of unlocked possibilities and unknown processing variables do limit the industrial acceptance of SLM, but create on the other hand numerous opportunities for innovative implant designs.

This dissertation tries to take the next step towards industrialization of SLM for the production of porous titanium and tantalum implants by addressing the research questions that currently limit the industrial breakthrough of the technology:

- Almost endless possibilities may sound great, but it is important to know **the actual boundaries of what is possible**, before any further steps can be taken.
- Selective Laser Melting is subject to a number of processing variables. The **determining variables and their implication** on the final result should be identified and addressed properly.

To find the answers to these two questions, more specific aims and research questions can be identified:

- The porous implant design is where it all starts. The **porous implant architecture** (structure relative density and unit cell geometry) in combination with a certain **implant material** (titanium or tantalum) will influence the implant performance and need to be investigated from a mechanical and biological point of view.
- The characteristics of the SLM process define the design freedom, both in terms of achievable details and general accuracy. Clear understanding of these limitations and more specifically the **overall reproducibility** and the **influence of the build orientation**, can lead to improved porous implant designs and manufacturing with uniform properties.
- Post-processing operations can influence the implant performance significantly. A proper selection of post-processing operations like **heat treatments** or **bio-functionalizing surface treatments** and their mechanical and biological implications should be possible.
- Production cost will always be crucial, regardless of the industry or application. Increasing the productivity **by at least a factor 2** and lowering the associated cost should be achieved by investigating and optimizing the influencing factors.

The investigation of these research questions have led to some general achievements that haven't been reported before:

- **Highly porous (60-90%)** implants made from Ti6Al4V, tantalum and pure titanium, using several different geometries, have been successfully produced and mechanically evaluated. Both the structure relative density and the unit cell geometry alter the mechanical properties. Porous **tantalum** implants showed **excellent *in vivo* performance and a very high fatigue resistance** while porous **pure titanium** implants have a **higher fatigue strength** compared to the **statically stronger** porous **Ti6Al4V** implants.
- The **build orientation** during manufacturing is identified as an important variable and should be taken into account while preparing data for SLM manufacturing. If not taken into account, the **mechanical properties can decrease by up to 35%** by an improper selected build orientation.
- Post-processing **heat treatments** have an influence on the microstructure and mechanical properties and **bio-functionalizing surface treatments** can improve the bone regeneration performance of porous titanium implants. A **Hot Isostatic Pressing** (HIP) heat treatment slightly lowers the maximum strength but the **elongation at fracture increases significantly by up to 70%**.
- The new optimized production parameters **increase the productivity** of porous titanium implants by **1.6 to 4.2 times** compared to the current build rates.

1.3. Outline of the dissertation

The first chapter, Chapter 2, is a chapter that summarizes all previously published data on porous Ti6Al4V implants investigated in the framework of this dissertation. It is the largest collection of experimental data available in literature and takes into account geometrical, SLM related and post-processing influences on the static and dynamic properties and the bone regeneration performance.

Chapter 3 is based on the first publication that reports results of additively manufactured porous tantalum implants. A specific geometry of porous tantalum implants has been evaluated mechanically (both static and dynamic) and in an *in vivo* experiment in which critical size femur defects in rats were reconstructed by the new tantalum implants.

The findings of Chapter 3 gave new insights in different mechanisms influencing the implant performance by using ductile porous metals. This gave rise to an additional research question which is the subject of Chapter 4. In this chapter, the potential revival of pure titanium for dynamically loaded porous implants is discussed.

The last full chapter, Chapter 5, deals with the productivity improvements obtained for porous titanium implants. This is done by explaining the methodology and defined references and also by depicting the need for further standardization.

Finally, all results will be briefly summarized in Chapter 6, in which new material and process selection charts for porous metals are proposed. This chapter concludes with some suggestions for further research.

2. Porous Ti6Al4V Implants

This chapter is based on the following articles:

a) [5] Campoli G., Borleffs M.S., Amin Yavari S., **Wauthle R.**, Weinans H., Zadpoor A.A., *Mechanical properties of open-cell metallic biomaterials manufactured using additive manufacturing*. Materials & Design, 49, (2013), 957-965.

b) [6] Amin Yavari S., **Wauthle R.**, van der Stok J., Riemslag A., Janssen M., Mulier M., Kruth J.-P., Schrooten J., Weinans H., Zadpoor A.A., *Fatigue behavior of porous biomaterials manufactured using selective laser melting*. Materials Science and Engineering C, Materials for Biological Applications, 33, 8 (2013), 4849-4858.

c) [7] Ahmadi S., Campoli G., Amin Yavari S., Sajadi B., **Wauthle R.**, Schrooten J., Weinans H., Zadpoor A.A., *Mechanical behavior of regular open-cell porous biomaterials made of diamond lattice unit cells*. Journal of the Mechanical Behavior of Biomedical Materials, 34 (2014), 106-115.

d) [8] Amin Yavari S., van der Stok J., Chai Y., **Wauthle R.**, Birgani Z., Habibovic P., Mulier M., Schrooten J., Weinans H., Zadpoor A.A., *Bone regeneration performance of surface-treated porous titanium*. Biomaterials, 35, 24 (2014), 6172-6181.

e) [9] Amin Yavari S., Ahmadi S., van der Stok J., **Wauthle R.**, Riemslag A., Janssen M., Schrooten J., Weinans H., Zadpoor A.A., *Effects of bio-functionalizing surface treatments on the mechanical behavior of open porous titanium biomaterials*. Journal of the Mechanical Behavior of Biomedical Materials, 36 (2014), 109-119.

f) [10] **Wauthle R.**, Vrancken B., Beynaerts B., Jorissen K., Schrooten J., Kruth J.-P., Van Humbeeck J., *Effects of build orientation and heat treatment on the microstructure and mechanical properties of selective laser melted Ti6Al4V lattice structures*. Submitted, 2014.

g) [11] Ahmadi S.M., Amin Yavari S., **Wauthle R.**, Pouran B., Schrooten J., Weinans H., Zadpoor A.A., *Additively manufactured open-cell porous biomaterials*

made from six different space-filling unit cells: the mechanical and morphological properties, Submitted, 2014.

h) [12] Amin Yavari S., Ahmadi S.M., **Wauthle R.**, Pouran B., Schrooten J., Weinans H., Zadpoor A.A., *Relationship between unit cell type and porosity and the fatigue behavior of selective laser melted meta-biomaterials*, Submitted, 2014.

The author of this dissertation has contributed to these articles in the following manner:

a) Sample manufacturing, static compression testing and manuscript review.
b) Sample manufacturing, morphological analysis (dry weighing, Archimedes measurements, μ-CT measurements), static compression testing and manuscript review.
c) Sample manufacturing, morphological analysis (dry weighing, Archimedes measurements), static compression testing and manuscript review.
d) Sample manufacturing and manuscript review.
e) Sample manufacturing and manuscript review.
f) Sample manufacturing, morphological analysis (dry weighing, Archimedes measurements), static compression testing and writing of the manuscript.
g) Sample manufacturing, morphological analysis (dry weighing, Archimedes measurements) and manuscript review.
h) Sample manufacturing, morphological analysis (dry weighing, Archimedes measurements) and manuscript review.

2.1. Introduction

The most common material for porous implants in orthopedics is Ti6Al4V because it is a biocompatible material with a proven clinical track record and it has a very high strength to weight ratio [13]. New manufacturing techniques like AM that are used to produce these implants generate new opportunities, but they also raise additional questions and regulatory issues.

The more information about additively manufactured porous Ti6Al4V implants is available, the more likely the medical device industry is willing to consider using AM for serial production of the next generation implants.

The actual mechanisms of porous structures when loaded, in combination with the inherent process characteristics of SLM and potential post-processing operations result in a broad range of variables that can be changed in order to optimize implant performance. It also makes it difficult to predict implant outcomes when not all variables are taken into account.

Therefore, this chapter is written as a summary of all findings regarding the mechanical and biological performances of porous Ti6Al4V structures evaluated for this dissertation. It can be used as a handbook containing (design) guidelines for porous Ti6Al4V implants manufactured with SLM.

The first part will discuss the static mechanical properties of porous structures with different geometries, build orientations, heat treatments and bio-functionalizing surface treatments. The second part will deal with the dynamic mechanical properties. The third and last part will briefly discuss some results from *in vitro* and *in vivo* experiments. Each section will conclude with specific guidelines that should be kept in mind in early stages of new application developments.

2.2. Materials and methods

2.2.1. Materials and manufacturing

Porous cylindrical test samples (diameter 10 mm, height 15-17 mm) were manufactured using SLM (Layerwise NV, Leuven, Belgium). Spherical Ti6Al4V (grade 5) or Ti6Al4V ELI (grade 23) titanium powder (chemical composition according to ASTM F2924 and F3001) with particle size ranging from 10 μm to 45 μm was used. The production was performed in an inert atmosphere and the samples were built on top of a solid titanium substrate. Unless otherwise

specified, all cylindrical test samples were manufactured with the central axis parallel to the build direction. After production, the samples were removed from the substrate using wire electro discharge machining (EDM).

2.2.2. Heat treatment

Most of the test samples were evaluated without any additional heat treatment (as built condition, AB). However, the influence of two heat treatments, namely stress relieve heat treatment (SR) and hot isostatic pressing (HIP), on the static mechanical properties is discussed in in Section 2.3.3. The SR condition, with a heat treatment per ASTM F2924 class 1; and the HIP condition, with at heat treatment per ASTM F2924 class 2. These two heat treatments were chosen because stress relieve is often necessary after SLM, especially for parts containing large solid sections, and HIP treatment is sometimes applied for critical components used under a dynamic load.

2.2.3. Bio-functionalizing surface treatment

In Section 2.3.4 and 2.4.4, two bio-functionalizing surface treatments from the literature were used: the alkali-acid-heat treatment (AlAcH) and the acid-alkali treatment (AcAl). For the AlAcH treatment, specimens were first immersed in 5 M NaOH solution for 24 h at 60 °C and subsequently washed gently with distilled water. Thereafter, the samples underwent hot water treatment for 24 h at 40 °C followed by immersion in 0.5 mM HCl (24 h at 40 °C). Then, the specimens were dried in an oven at 40 °C for 24 h. After drying, the scaffolds were heated with a rate of 5 °C/min up to 600 °C and were kept for 1 h at this temperature. Finally, the specimens were cooled down to the room temperature in the furnace [14].

In the second technique, the AcAl treatment, samples first were immersed in a mixture of 18% HCl and 48% H_2SO_4 aqueous solutions at 70 °C for 1 h and subsequently in 6 M NaOH solution at 70 °C for 5 h. After washing gently in distilled water, the samples were dried in an oven at 40 °C for 24 h [15].

2.2.4. Archimedes measurements

Structure relative density was measured using the Archimedes method on 5 different samples of each series prior to being used for mechanical evaluation. Archimedes test results are calculated based on a combination of dry weighing and weighing in pure ethanol and on the theoretical density of 4.43 g/cm³ for Ti6Al4V [16]. The structure relative density was then calculated by dividing the measured structure volume by the theoretical macro volume of the cylindrical

test samples. All weighing measurements were performed on an OHAUS Pioneer balance.

2.2.5. Static mechanical testing

Static mechanical testing of 5 cylindrical samples of each of the presented series of porous structures in this chapter was carried out in accordance with the standard ISO 13314 [17]. All tests were done on an INSTRON 5985 mechanical testing machine (30 kN load cell) by applying a constant deformation rate of 1.8 mm/min. Each static compression test resulted in a stress-strain curve for which the following values were calculated: (i) the quasi-elastic gradient (E) as gradient of the straight line determined within the linear deformation region at the beginning of the compressive stress-strain curve, (ii) the yield strength (σ_y) as the compressive 0.2% offset stress, (iii) the maximum compressive strength (σ_{max}) and (iv) the strain at fracture (e_{frac}). In this context, the quasi-elastic gradient is closest to the concept of stiffness, which is used for solid materials. In order to facilitate understanding and comparison between the results of this study and those of similar studies on solid and porous materials, the quasi-elastic gradient will be referred to as stiffness. Nevertheless, the exact definitions presented above should be kept in mind when interpreting the data.

2.2.6. Dynamic mechanical testing

Compression–compression fatigue tests were carried out using a hydraulic test frame (MTS, Minneapolis, US) with a 25 kN load cell. The loading frequency was fixed at 15 Hz (sinusoidal wave shape) and a constant load ratio, R = 0.1, was used. Two specimens were tested for every stress level. The specimens were assumed to have failed once the stiffness of the specimen dropped by more than 90. The S–N curves of the tested porous structures were established by plotting both absolute and normalized values of stress versus number of cycles to failure for all tested specimens. In case of normalized S–N curves, a power law was fitted to all data points of the normalized S–N curves.

2.3. Static mechanical properties

Only a few years ago the first ISO standard was published for mechanical testing of cellular metals [17], regardless of the material or manufacturing method. Also, new ASTM standards have been established for solid Ti6Al4V processed using AM that specify the static mechanical properties [18, 19], but

no standards yet exist that specify evaluation methods or minimum requirements to what additively manufactured porous implants have to comply.

The broad range of influencing factors definitely complicates standardization, but the more the mechanical behavior of porous Ti6Al4V structures is known, the more it helps to set rules and regulations.

A relatively fast and easy way to assess and investigate the quality or behavior of porous structures used for implants is by doing compression tests. However, destructive testing of all possible variations is rather time consuming and costly.

In order to reduce the amount of experiments, finite element and analytical models have been developed that accurately can predict the mechanical properties of cellular structures made by AM [5, 7, 20], but still some amount of experimental data is necessary to 'calibrate' or validate these models. Also, these models cannot be used currently to evaluate actual processing characteristics or post-treatments. Nevertheless, these models are considered as potentially very valuable tools for porous implant performance simulations.

This part of the chapter on porous Ti6Al4V implants will give an overview of all investigated influences on the static mechanical properties. For a complete understanding of the mechanical behavior of porous Ti6Al4V structures, it is advised to take a look at Figure 4.2 B for a typical stress-strain curve of a porous Ti6Al4V structure under compression. It also graphically represents the calculated properties that will be used to compare different influences.

2.3.1. Influence of geometrical properties

The first selection that has to be made when designing and manufacturing a porous implant is the selection of the geometry by choosing a unit cell type and properties like the structure relative density or strut and pore size (see also **Error! Reference source not found.** for the manufacturing process flow). It is clear that this selection has a major impact on the mechanical properties of porous implants.

Many researchers have already studied in depth the mechanical properties of different porous structures made by SLM [6, 9, 21-27] and EBM [28-32], most of them made out of Ti6Al4V. The difficulty to compare all these data is that they either have been manufactured using different technologies, different machines or different processing parameters.

In this section, the static mechanical properties of the largest collection of different porous Ti6Al4V structures manufactured by the same company (LayerWise NV), using the same technology (SLM), the same machine (LayerWise machines) and the same processing parameters, are presented.

Six different unit cell geometries made out of Ti6Al4V ELI have been investigated and are visually represented in Figure 2.1. For the rhombic dodecahedron unit cell, the results were reported in [5] and [6] and the results for the diamond unit cell were taken from [7]. The static mechanical properties of the four other unit cells (cube, truncated cube, truncated cuboctahedron and rhombic cuboctahedron) are part of a manuscript in preparation and will be submitted soon [11].

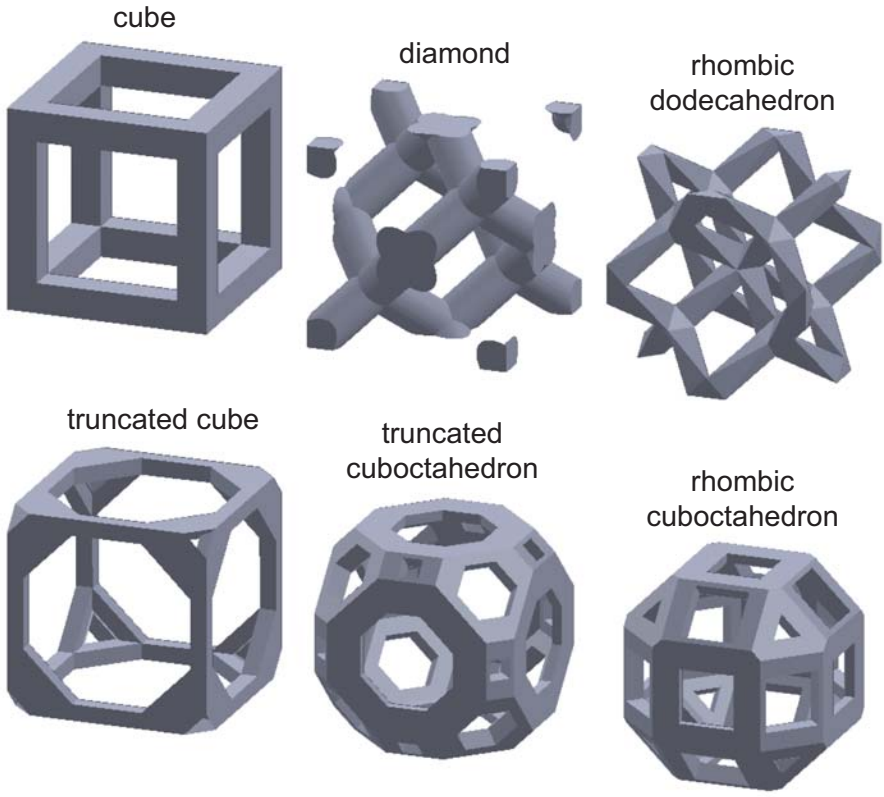

Figure 2.1: Overview of the different unit cell geometries that have been used to generate various porous structures made from Ti6Al4V.

The mechanical properties of the different porous geometries versus the structure relative densities are presented in the figures on the next pages. The yield strength and maximum compressive strength are shown in Figure 2.2 and Figure 2.3, whereas Figure 2.4 shows the obtained stiffness values. For easy comparison, only average reported values are displayed on the graphs.

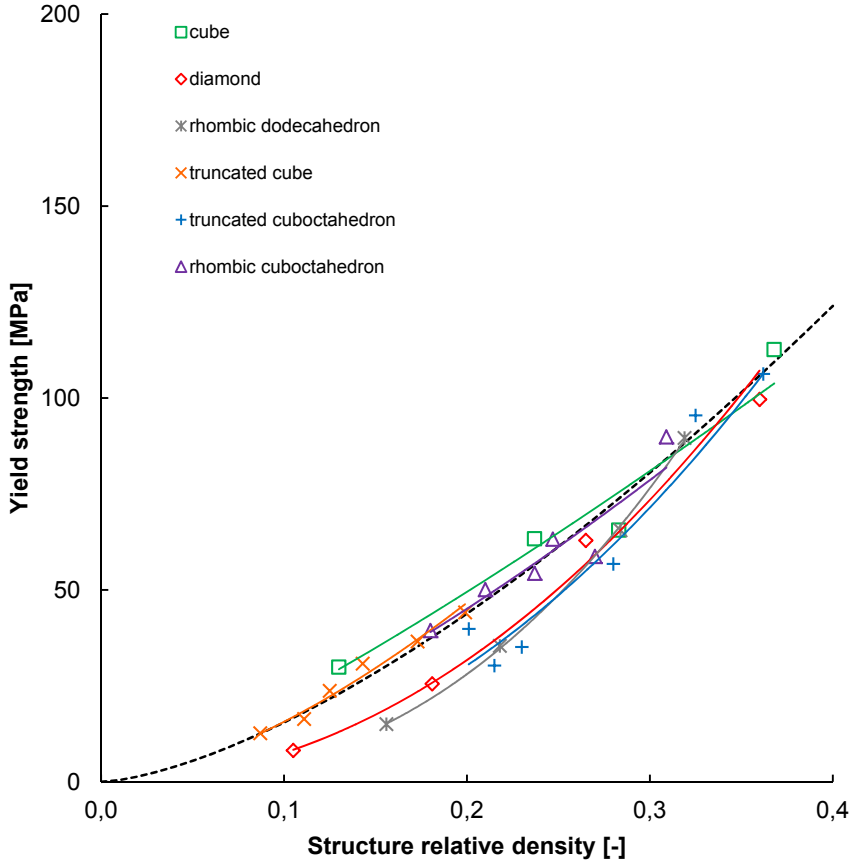

Figure 2.2: Yield strength (σ_y) of various SLM processed porous structures made from Ti6Al4V ELI with different unit cell geometries and different relative densities (ρ_{rel}).

Gibson and Ashby already found a general relation between the ratio of the plateau stress of the porous material and yield strength of the solid material versus the relative density [33]. Although Equation 2.1 is intended to be used for the plateau stress, in case there is a peak stress, as it is for Ti6Al4V (Figure 4.2 B), the maximum compressive strength should be used [34].

$$\frac{\sigma_{pl}}{\sigma_{y,s}} \approx C_5 \left(\frac{\rho}{\rho_s}\right)^{\frac{3}{2}} \tag{2.1}$$

In general $C_5 \approx 0.3$, but this value didn't resemble the results for the maximum compressive strength, nor the yield strength. In Figure 2.2 this relationship of Equation 2.1 is represented by the dashed line and a value of 0.5 for C_5, in Figure 2.3 the same relationship is shown but with a value of 0.8 for C_5.

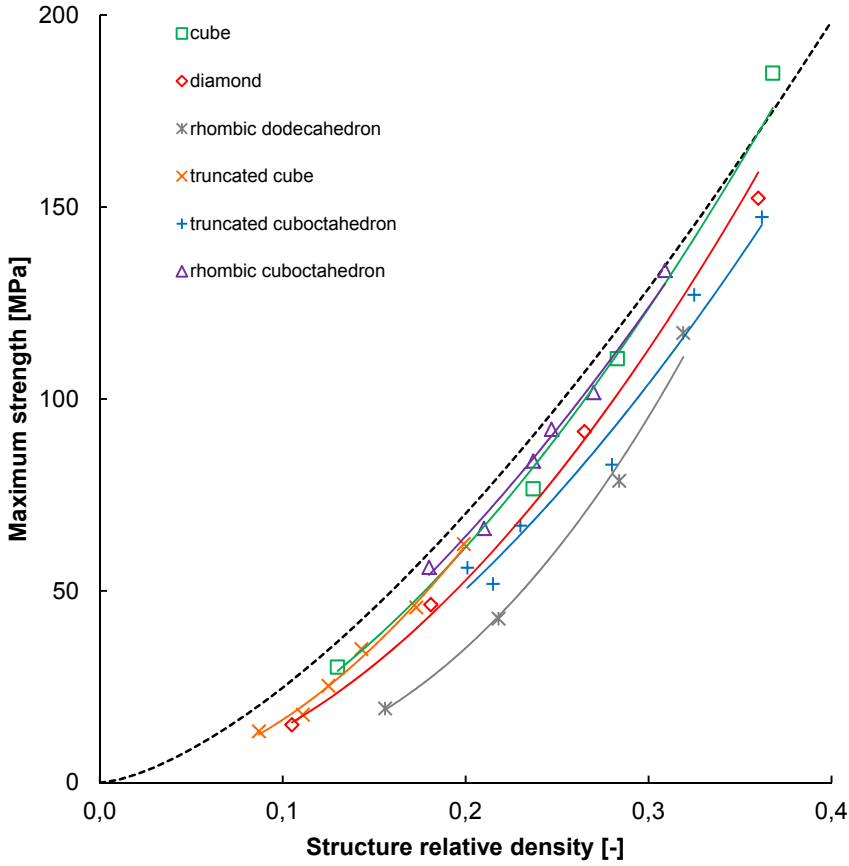

Figure 2.3: Maximum compressive strength (σ_{max}) of various SLM processed porous structures made from Ti6Al4V ELI with different unit cell geometries and different relative densities (ρ_{rel}).

For the yield strength this relationship seems to hold best for the cubic, truncated cube and rhombic cuboctahedron unit cell geometries. The diamond, rhombic dodecahedron and truncated cuboctahedron have a lower yield

strength that tends to follow a higher power relationship with regards to the structure relative density. The reason for this difference can be caused by the fact that these unit cell geometries have no or only very small struts that are vertically aligned and may influence the deformation behavior under a compressive load (Figure 2.1).

The relationship between the strength and the relative density from Equation 2.1 represents the results better for the maximum compressive strength (Figure 2.3). Again the cubic, truncated cube and rhombic cuboctahedron unit cells have the highest values, but the difference with the yield strength is that all unit cells now have a similar relationship towards the relative density. All curves of the different unit cell geometries could be fitted to the trend line by a linear translation.

For a full understanding of the static compressive strength, it should be noted that the mechanical evaluation was done by uniaxial compression tests. The load that porous implants have to withstand has in general multiple directions and therefore it is suggested to use isotropic unit cell designs like the diamond or rhombic dodecahedron, although they have slightly lower strength.

Also for the ratio of the structure stiffness and stiffness of the solid material versus the relative density, Gibson and Ashby found a relationship:

$$\frac{E}{E_s} \approx C_1 \left(\frac{\rho}{\rho_s}\right)^2 \tag{2.2}$$

For which C1 ≈ 1, but this was found not to be representative and overestimating the stiffness values of Figure 2.4. The dashed trend line in Figure 2.4 used Equation 2.2 but with a value of 0.25 for C_1, and it coincides almost perfectly with the stiffness values of the diamond unit cell and is very close to those of the rhombic dodecahedron unit cell. The four other unit cells tend to be more stiff and also have a more linear relationship between the stiffness and the relative density.

In order to explain all the different observations from the large datasets presented in Figure 2.2, Figure 2.3 and Figure 2.4, more detailed information is necessary. It is suggested to perform in-situ μ-CT measurements that can reveal the failure mechanisms of the different unit cells and structure relative densities in order to understand the different mechanical properties.

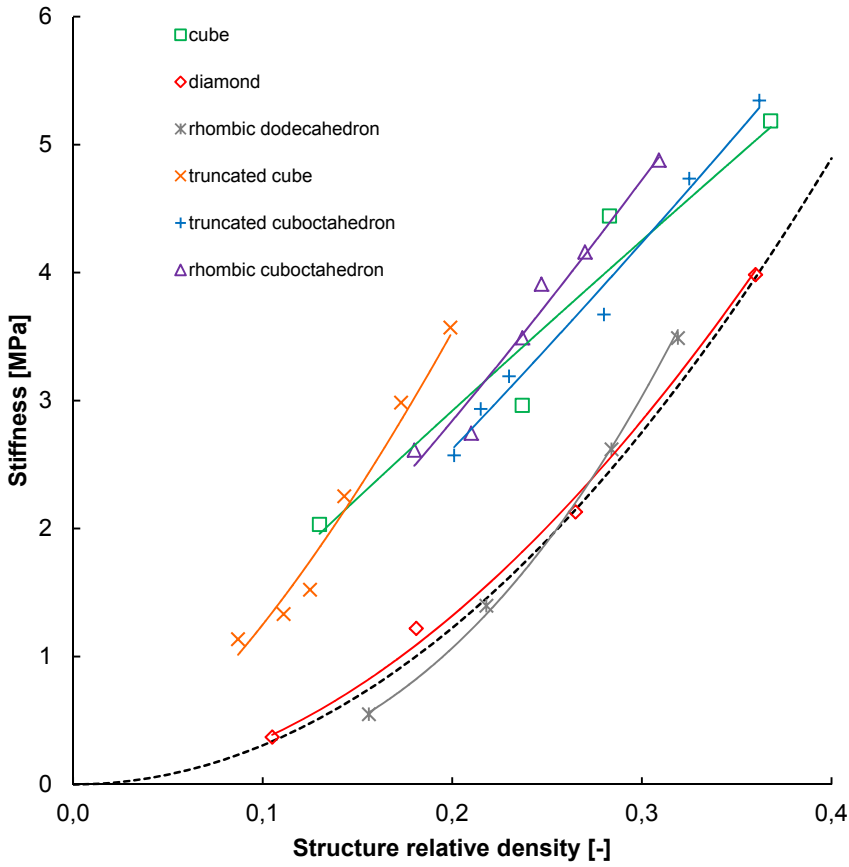

Figure 2.4: Stiffness (*E*) of various SLM processed porous structures made from Ti6Al4V ELI with different unit cell geometries and different relative densities (ρ_{rel}).

Nevertheless, the selection charts presented in this section can be a useful tool for porous implant design and manufacturing. The unit cell geometry has a certain influence and more specifically, unit cells with struts aligned with the direction of the load have a higher strength and stiffness. The structure relative density has even a more pronounced influence, meaning that the maximum compressive strength is defined by the relative density to the power of 3/2. The relationships defined by Gibson and Ashby can be used to predict the maximum strength and stiffness for some unit cell geometries, but should be used with care.

2.3.2. Influence of the build orientation

Many studies already investigated porous structures with different geometries and their influence on the mechanical properties, but little is known about the effect of specific processing characteristics that are inherent to metal additive manufacturing. Therefore this section investigates the effect of a crucial choice in the manufacturing process: the build orientation.

It has been reported before that due to the high temperature gradients that occur during the SLM process, specific microstructures can be present in the parts after processing, sometimes resulting in strong crystallographic textures that have a significant influence on the mechanical properties [3, 35, 36]. Since AM is a layer by layer process and since a crystallographic texture might be present in a certain direction if no heat treatment is applied, different build orientations can lead to significantly different mechanical properties [3, 37].

Therefore the aim of this section is to investigate the effects of the build orientation on the microstructure and mechanical properties of additively manufactured porous structures. The purpose is to verify if a crystallographic texture is also present in Ti6Al4V porous structures as it is for solid parts and if the microstructure and mechanical properties are influenced by changing the build orientation of the sample itself.

The materials and methods, results and discussion are described in detail in [10] and will be summarized here. Cylindrical porous samples based on the diamond unit cell were manufactured from Ti6Al4V (grade 5) in three different build orientations: the vertical (VER), diagonal (DIA) and horizontal build orientation, with a unit cell orientation that is fixed within the cylindrical sample (Figure 2.5).

The results show that the amount of enclosed pores increases with the inclination of the strut, meaning vertical struts have little or no pores present, whereas diagonal struts have more pores, and horizontal struts have lots of pores, as can be seen on Figure 2.5 C.

Because of the high temperature gradients that occur during the SLM process, the microstructure in the as built condition consists of a martensitic *a'*-phase (Figure 2.7 A) within prior β grains that are mostly aligned with the building or z direction, and sometimes aligned with the strut orientation.

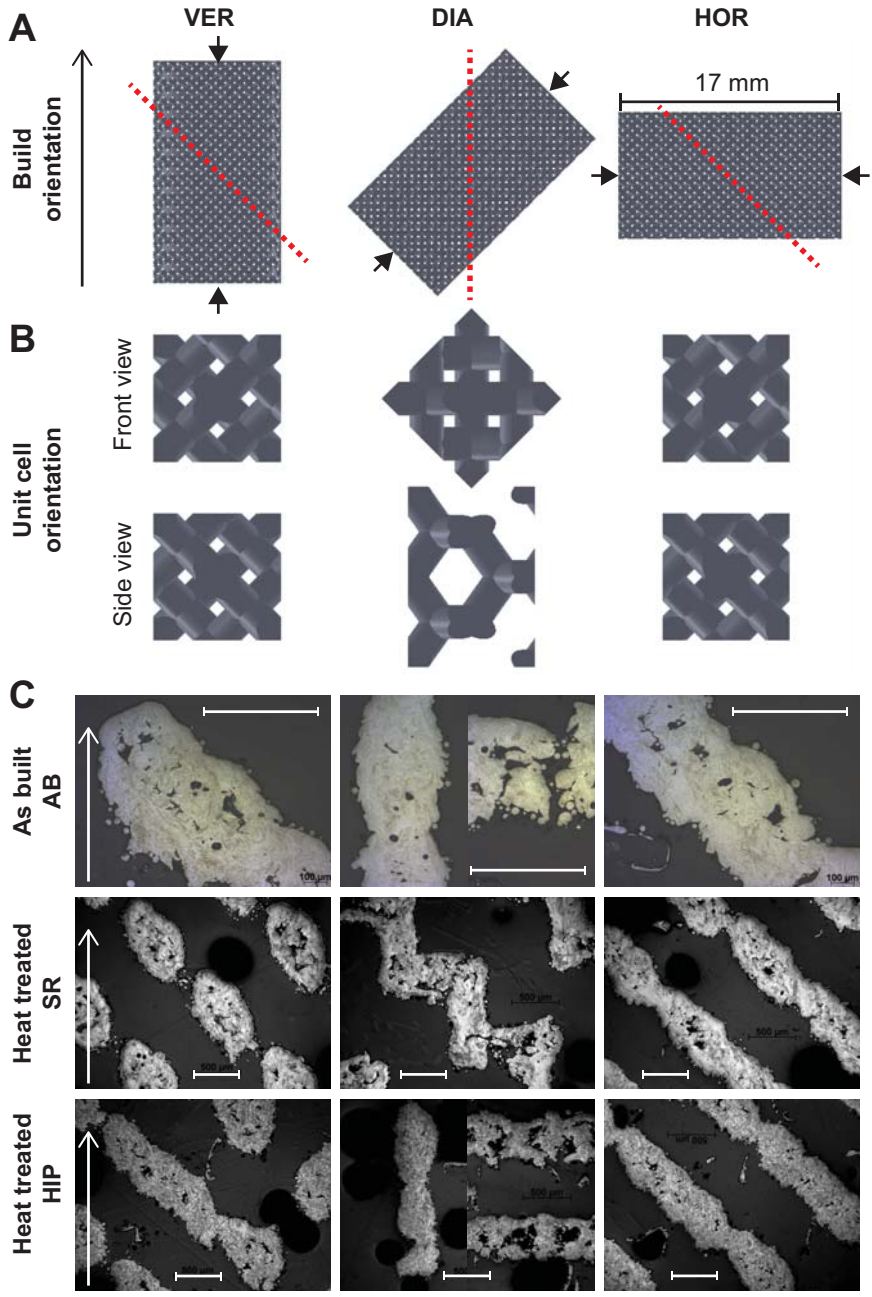

Figure 2.5: Test samples with different build orientation (VER, DIA and HOR), arrows indicating the axis of compression testing and the red dotted lines indicating the shear plane (A); the front and side view of the corresponding diamond unit cells (B) and the cross-sectional images of all 5 series in the three different conditions (AB, SR and HIP) (C). The scale bar indicates 500µm.

No consistent observations could be made on the grain alignment for all unit cell/build orientations. Solidification in Ti6Al4V processed via SLM occurs mainly through epitaxial growth, which means that the melt solidifies with the same crystal orientation as the solid substrate below. Furthermore, this happens in the direction of the maximum heat flux [35].

The build orientation has a significant influence on the mechanical properties as illustrated by Figure 2.6. The diagonal oriented sample is inferior to both the horizontal and vertical oriented samples that have near identical properties. Both the compressive strength (σ_y and σ_{max}) and the stiffness of the diagonal oriented sample are on average 35% lower compared to the vertical oriented sample, regardless of the heat treatment condition.

The horizontal build orientation has the same mechanical properties as the vertical orientation, because all struts are oriented identically. For the DIA sample the horizontal struts with bad quality are causing early failure of the structures, because the shear plane of fracture as clearly seen on Figure 2.8 B for the SR condition is now perpendicular to the horizontal oriented struts (the shear plane is in the vertical direction for the DIA sample and in the diagonal direction for all other orientations shown in Figure 2.5 A by the dashed red line).

In conclusion, it should be clear that horizontal oriented struts should be avoided for isotropic loaded porous structures (or in case the direction of loading is not known), unless the applied load can be properly supported by the other struts.

2.3.3. Influence of heat treatment

The microstructures obtained after SLM processing can, if required, be changed or optimized by applying a certain heat treatment, that also have an influence on the mechanical properties [38]. Some publications already reported about the microstructure of porous structures after SLM [39-42] and EBM [43-45].

It should be clear that both the build orientation and heat treatment have an influence on the microstructural and corresponding mechanical properties, but only little is known so far about the combination of those influences of solid parts made by AM. Some studies investigated the influence of an annealing treatment on Ti6Al4V porous structures [39, 40], but no studies have been

found that investigated other heat treatments. Therefore, the effect of different heat treatments on the mechanical properties is determined in this section.

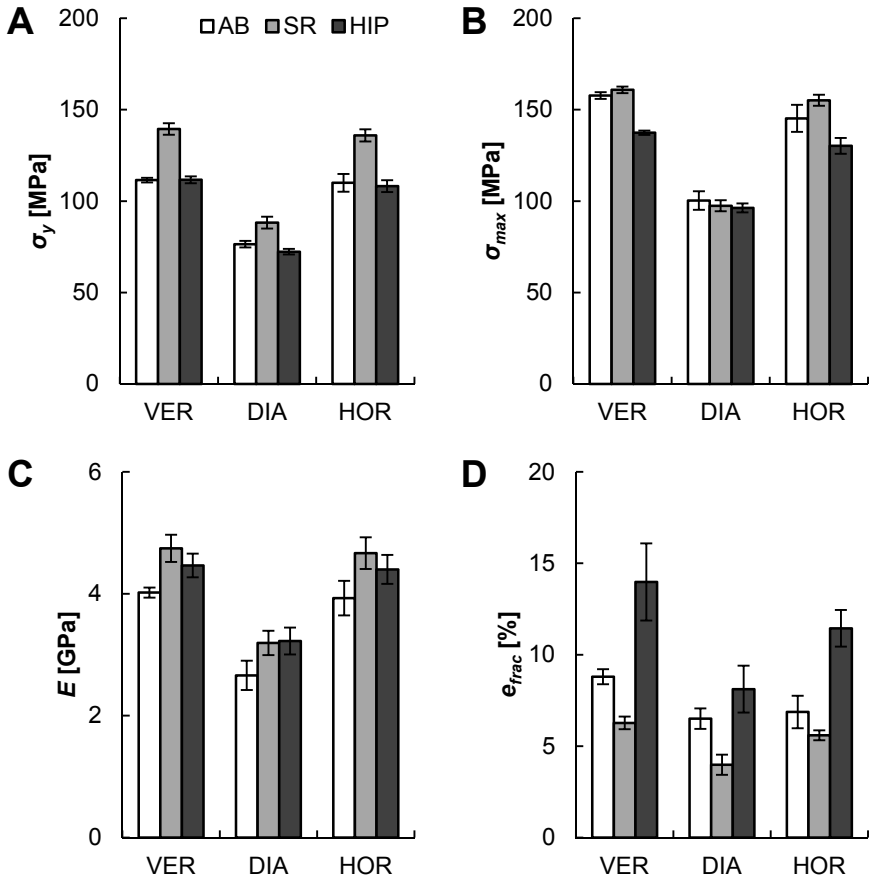

Figure 2.6: Comparison of the mechanical properties of the SLM processed porous structures for the three build orientations (VER, DIA and HOR) and the three heat treatment conditions (AB, SR and HIP): the yield strength, σ_y (A); the maximum strength, σ_{max} (B); the stiffness, E (C) and the strain at fracture, e_{frac} (D).

The materials and methods, results and discussion are described in detail in [10]. In short, cylindrical porous samples based on the diamond unit cell were manufactured from Ti6Al4V (grade 5) powder and heat treated with either a stress relieve (SR) or hot isostatic pressing (HIP) treatment, as described in Section 2.2.2.

Although an increase in strut density was expected after a HIP treatment, no significant differences could be observed (Figure 2.5 C). Figure 2.7 shows a representative microstructural detail at high magnification for the three heat treated conditions of the porous structures.

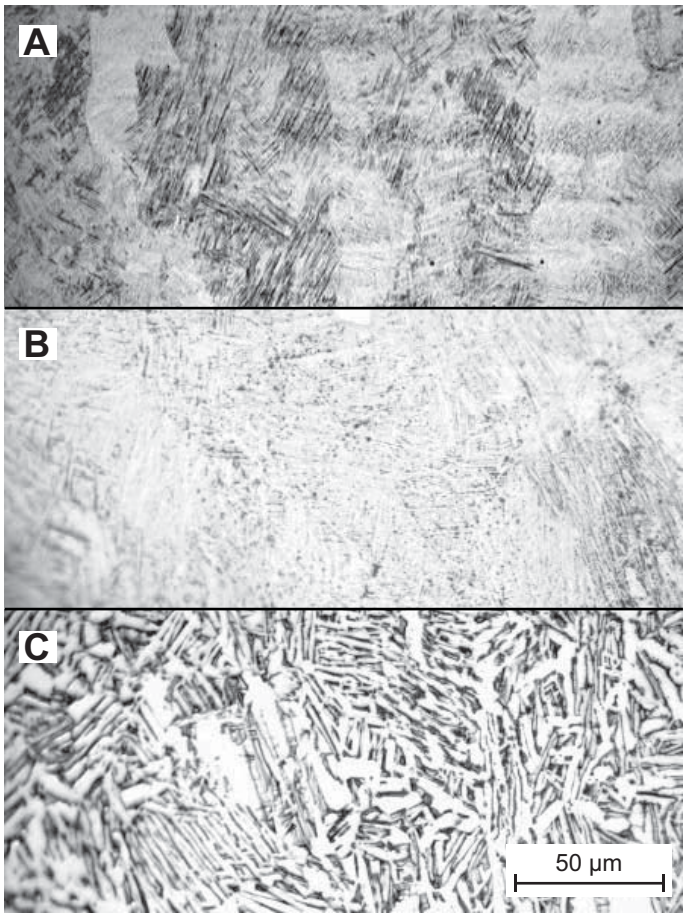

Figure 2.7: Microstructure of the SLM processed Ti6Al4V in the three tested conditions: the as built (AB) condition (A); after a stress relief (SR) heat treatment (B) and after a hot isostatic pressing (HIP) treatment (C).

After heat treating the porous structures by means of a SR cycle, a transformed *a'*-phase is visible that consists of fine *a* platelets (white) where in between the *β*-phase is present (Figure 2.7 B). The temperature during the SR was high enough to transform the *a'* martensitic phase, but no consistent observations

could be made on the grain orientation that could either align with the build direction or the strut orientation.

The microstructure after a HIP treatment consists of lamellar *a*- (white) and *β*-phase (black) (Figure 2.7 C). No preferential orientation of the grains could be observed after the HIP treatment, resulting in a rather isotropic microstructure regardless of the unit cell and build orientation. As none of these treatments cross the *β* transus, the original prior *β* grains can be distinguished after all heat treatments.

The three evaluated heat treatment conditions (AB vs. SR and HIP) have a clear influence on all measured mechanical properties, but in general, these trends are independent of the unit cell orientation or build orientation. The yield stress increases about 15 to 25% after a SR heat treatment, while a HIP treatment does not influence the yield stress compared to the AB condition (Figure 2.6 A). The maximum strength, on the other hand, is not influenced by the SR heat treatment, but the HIP treatment can decrease the maximum strength by almost 15% compared to the AB condition (Figure 2.6 B). The stiffness increases for both the SR heat treatment (15 to 20%) and the HIP treatment (10 to 20%) compared to the AB condition (Figure 2.6 C). And finally the strain at fracture decreases by 20 to 40% after the SR heat treatment whereas the HIP treatment increases the strain at fracture significantly by 25 to 70% (Figure 2.6 D).

Part of these effects and especially the low strain at fracture can be explained by the fact that after SR, the samples were oxidized, as can be seen on Figure 2.8 B, and this was also observed as an oxidation layer of a few μm on the metallographic cross sections of these samples. This can be avoided by applying the SR treatment under vacuum. The temperature during SR was just enough to transform the *a'* into a fine mixture of *a*+*β*.

After HIP, on the other hand, the lamellar *a*+*β* mixture is much coarser. This mainly results in a lower maximum strength, but a higher fracture strain, thanks to the more ductile or plastic deformation of the structure. This different deformation mechanism can clearly be recognized on Figure 2.8 A, where the samples after HIP reach the lower maximum stress at a higher strain, but continue to plastically deform after the point of maximum stress, instead of failing almost completely after reaching the maximum point like for the AB and SR conditions. This might be an interesting property for dynamically loaded

applications. An increased ductility is expected to increase the fatigue life of porous structures, but this still has to be confirmed by further research.

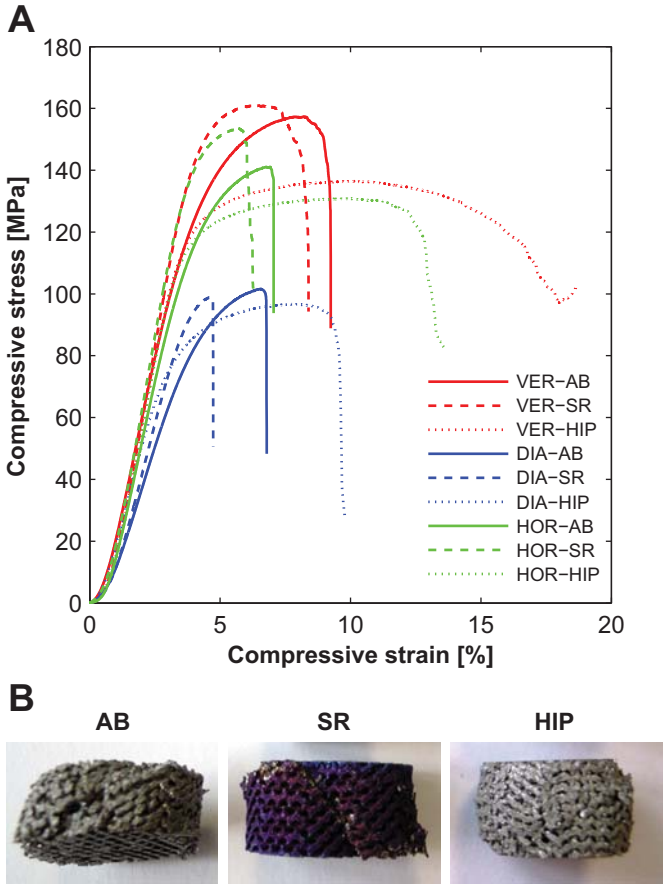

Figure 2.8: Representative stress-strain curves of the compression testing for each build orientation (VER, DIA and HOR) in each heat treatment condition (AB, SR and HIP) (A), and a picture of test samples after compression testing for each condition.

Proper selection of the heat treatment of porous structures is important and dependent on the actual application. In general, for statically loaded applications, the AB condition or the SR conditions are equally usable, whereas HIP treatment should be applied for cyclically loaded applications, since its high ductility is believed to have a beneficial influence on the fatigue strength.

2.3.4. Influence of bio-functionalizing surface treatments

Regardless of the chosen geometry, build orientation or heat treatment, there are still other possibilities to improve the performance of porous Ti6Al4V implants. Some of these options do not influence the mechanical properties at all since they use the functional geometry of the porous structure as a carrier for drug delivery media such as gels for controlled release of growth factors [46]. But other bio-functionalizing improvements do change the surface characteristics of the porous structure by removing or adding material from or to the structure surface.

Bio-functionalizing surface treatments that add material to the structure surface are mostly coating of hydroxyapatite (HA) or calcium phosphate (CaP) produced by e.g. plasma spraying or perfusion electrodepostion [47, 48]. Since it is believed that these surface coatings will not reduce the mechanical properties, this section will deal with bio-functionalizing surface treatments that change the actual surface topology.

Even though these surface modifications have shown to improve the interaction of the implant surface with the host tissue, they might also have consequences in terms of the mechanical properties, especially for open porous implants that have a completely different surface to volume ratio as compared to dense titanium implants. Since chemical surface treatment of open porous structures is often associated with strut erosion and creates micro-features on the surface, it is not clear how mechanical properties of the porous structure change after such modifications.

The materials and methods, results and discussion are described in detail in [9]. In short, cylindrical porous samples based on the rhombic dodecahedron unit cell with three different porosities (Ti 120-500, Ti 170-500 and Ti 230-500) were manufactured from Ti6Al4V ELI (grade 23). Two important chemical surface treatments, namely acid-alkali (AcAl) and alkali-acid-heat (AlAcH) treatments were applied after manufacturing and compared to the as built samples (AB).

In the AcAl treatment, the acidic treatment removes the passive oxide layer, while the alkali treatment creates an amorphous sodium titanate layer. In the AlAcH treatment, the alkali treatment creates a sodium titanate layer [15]. Then the acidic treatment removes sodium and contributes to the formation of an

amorphous titania. The subsequent heat treatment transforms the amorphous titania to crystalline titania (anatase and/or rutile) [14].

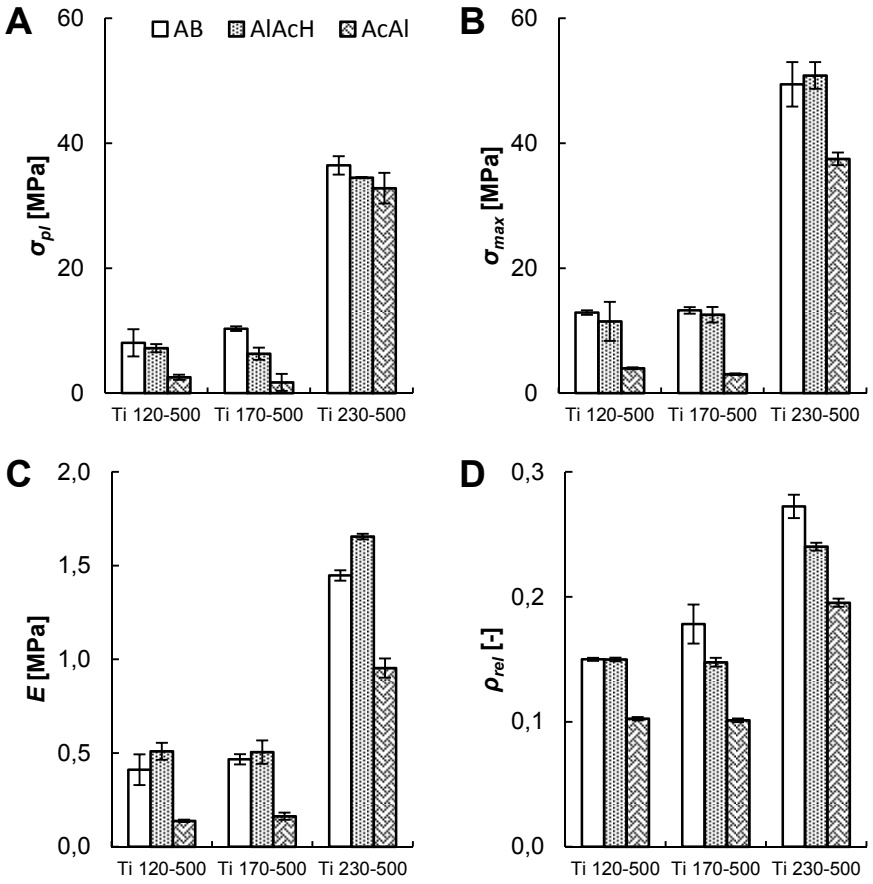

Figure 2.9: The static mechanical properties yield strength, maximum compressive strength and stiffness and structure relative density of three types of rhombic dodecahedron porous structures before (AB) and after bio-functionalizing surface treatments (AlAcH and AcAl).

In terms of absolute static mechanical properties, the AlAcH samples had similar strength compared to the AB samples except for the plateau stress of the Ti 170-500 structures that was significantly lower (Figure 2.9 A, B and C). The AcAl samples all had lower strength for the measured properties compared to the AB and AlAcH samples, except for the plateau stress of Ti 230-500 (Figure 2.9 A).

When comparing the relative densities shown in Figure 2.9 D, it is clear that one of the reasons for the different mechanical properties is due to different material volume. The relative density of all surface treated samples was lower for almost all samples, but the largest drop in volume was seen for the AcAl samples. A small change in structure relative density can have a significant influence on the mechanical properties, as was discussed before in section 2.3.1 and illustrated in Figure 2.2, Figure 2.3 and Figure 2.4 and is now confirmed by the decrease in mechanical properties of chemical etched porous structures after a AcAl surface treatment.

Although there was a significant decrease in structure density for two out of three AlAcH structures, the maximum compressive strength did not decrease and the stiffness increased slightly. The reason for this observation is the heat treatment after the alkali-acid treatment that was comparable to the stress relieve heat treatment discussed in section 2.3.3. Stress relieving porous Ti6Al4V structures increases the stiffness, without changing the maximum strength.

In conclusion, it can be stated that surface treatments which increase the biological performance of Ti6Al4V implants can have a significant influence on the static mechanical properties.

Porous implants have a large surface area, and chemical surface treatments like acid-alkali and alkali-acid-heat treatments may remove surface material and hence decrease the structure relative density. Small changes in relative density however, can have a significant influence on the static mechanical properties. Also, surface treatments at elevated temperatures may be considered as heat treatments that also influence the static mechanical properties. These observations should be kept in mind while designing porous implants that will be surface treated after SLM manufacturing.

2.4. Dynamic mechanical properties

Obtaining the static mechanical properties of porous Ti6Al4V implants can be done relatively easy and quick. Section 2.3 gives an overview of the most important variables that determine the static properties and should be taken into account during the early design stages.

Many of the porous implant applications can be found in orthopedics or spinal where the porous structure is either used to fill large bone defects or to create a

solid anchoring with the surrounding host bone. Either way, the implant is not merely subjected to a static load, but mainly to a dynamic load. For that reason it is important to have a better understanding of the fatigue behavior of these new porous implants.

Although it is believed that a basic knowledge about the fatigue behavior is important, very little or no information about the mechanical performance under a dynamic load of additively manufactured porous structures is available. Therefore, this part will summarize the first reported results on the fatigue behavior of porous Ti6Al4V implants.

2.4.1. Influence of geometrical properties

Section 2.3.1 showed a significant influence of both the unit cell geometry and the structure relative density on the static mechanical properties. There is no reason to believe that this is different for the dynamic properties, although it is expected that the relationships will be different.

In a first study the fatigue behavior of porous structures with four different relative densities using the rhombic dodecahedron unit cell was investigated. The same structures as used in section 2.3.1 were used for compression-compression fatigue tests. All details on the materials and methods, results and discussion can be found in [6].

The results are summarized in Figure 2.10, in which the normalized S-N curves are shown versus the cycles to failure. The absolute fatigue life of the four tested structures is quite different and the order of the S-N curves is similar to the order of yield stress values of the four structures (Figure 2.2). But if the stress values in the S-N curves are normalized with respect to the yield stress of the structures (Figure 2.10), all structures behave more or less the same. The power law fitted to all data points shows that the normalized S-N curves can be estimated by a power law with a very high coefficient of determination, $R^2 = 0.94$.

The fact that the normalized S-N curves are almost identical, can be used as a practical tool to estimate the S-N curves of porous Ti6Al4V structures with a rhombic dodecahedron unit cell, for which no fatigue test data is available. It is only required to obtain the yield stress of any similar porous structure using fast and easy static compression testing and translate the normalized S-N curve to a S-N curve with absolute stress values.

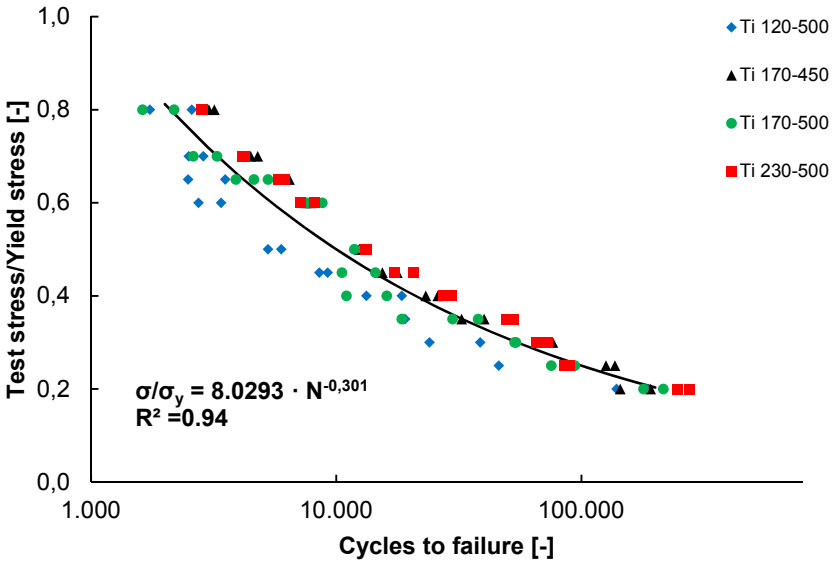

Figure 2.10: The S-N curves of four types of rhombic dodecahedron porous structures using normalized stress values. A power law is fitted to all data points.

According to the fitted power law, the allowed stress limit is $0.25\sigma_y$ for 10^5 loading cycles. If the power law is extrapolated to 10^6 loading cycles, the estimated allowed stress level is $0.12\sigma_y$. This is a rather low value compared to values found in literature for solid titanium (0.4-0.6) [4, 13, 16], but similar to the values reported for a study on the fatigue performance of porous structures made by EBM (0.1-0.2) [44]. There are mainly three reasons that explain the difference in fatigue strength with solid titanium: the high surface roughness that causes early crack initiation, in combination with the very low thickness of the struts (120-230 μm) and the microstructure after SLM manufacturing. It is believed that post-processing treatments that can reduce the surface roughness or change the microstructure will have a beneficial effect on the dynamic performance of porous Ti6Al4V implants.

Even though the power law provided in this section is based on extensive testing of four different relative densities, it is suggested to only use this law for porous structures with a rhombic dodecahedron unit cell and manufactured using SLM. Further extensive fatigue tests have already been carried out on some of the other unit cell geometries and relative densities of section 2.3.1, for which the results are summarized in Figure 2.11 from [12].

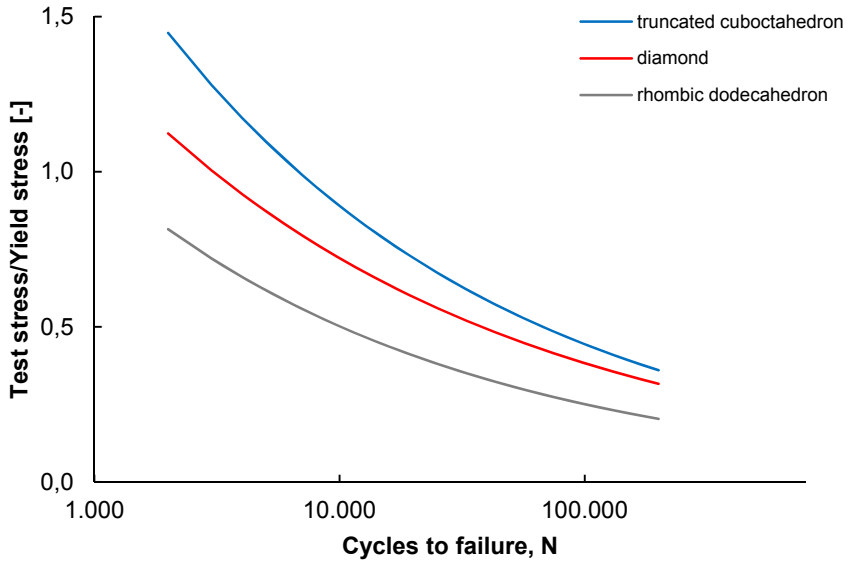

Figure 2.11: Comparison between the normalized S-N curves (fitted power laws) of the porous structures based on truncated cuboctahedron, diamond and rhombic dodecahedron unit cells.

It was observed that, in addition to static mechanical properties, the fatigue properties of the porous biomaterials are highly dependent on the type of unit cell as well as on structure relative density. None of the porous structures based on the cubic unit cell failed even when they were loaded for 80% of their yield stress for well over 10^6 loading cycles.

For both other unit cells, the absolute level of the S-N curves decreased as the structure relative density decreased. When normalized with respect to their yield stresses, the S-N data points of structures with different porosities very well ($R^2 > 0.8$) conformed to one single power law, specific to the type of the unit cell based on which the porous structures were made (Figure 2.11). The normalized S-N curve of the porous structure based on the truncated cuboctahedron unit cell was higher than that of the structures based on the diamond unit cell. Both normalized S-N curves were higher than that of the porous structures based on rhombic dodecahedron unit cell determined in a previous study [6].

These results are in accordance with the results reported for the static mechanical properties in Section 2.3, where the cubic unit cell geometry showed the highest strength and the rhombic dodecahedron unit cell the lowest

strength. The porous structures based on the cubic unit cell have perfectly manufactured struts aligned with the axis of loading, while porous structures based on e.g. the diamond unit cell, have struts that are not aligned with the axis of loading and have a higher surface roughness because of the non-vertical build orientation.

2.4.2. Influence of the build orientation

The influence of the build orientation during manufacturing on the dynamic behavior has not been investigated so far. But based on the findings in section 2.3.2 for the static mechanical properties, it can be stated that the same rules and guidelines are applicable. Horizontal struts during manufacturing should be avoided, since they can lower the static strength significantly and increase the surface roughness due to the dross formation. A higher surface roughness and incomplete struts will be detrimental for the dynamic properties. Future research could lead to more insights on this matter, but since porous implants with isotropic properties are preferred, the recommendations from section 2.3.2 should be followed for optimal orientation during manufacturing.

2.4.3. Influence of heat treatment

Parts made by SLM have a specific microstructure after processing, but can be changed by applying a certain heat treatment. As explained in section 2.3.3, these different microstructures have a significant influence on the static mechanical properties (Figure 2.6) and the deformation behavior (Figure 2.8). In general it is known that ductile materials perform better under a cyclic load due to the more plastic deformation that is possible before fracture occurs. Heat treating by means of a HIP treatment increased the ductility of porous Ti6Al4V implants significantly and is therefore believed to increase the fatigue life as well. No studies have been reported so far that confirm this assumption, so it is suggested for further research to investigate the influence of heat treatments on the dynamic performance of porous Ti6Al4V implants.

2.4.4. Influence of bio-functionalizing surface treatments

From the static mechanical properties discussed in section 2.3.4, it was already clear that bio-functionalizing surface treatments can significantly influence the results. In this section, compression-compression fatigue testing for two chosen stress levels ($0.35\sigma_{pl}$ and $0.5\sigma_{pl}$) on the same samples used in section 2.3.4, will be discussed. All details on the materials and methods, results and discussion can be found in [9].

The fatigue life of the AlAcH samples was generally not significantly different from that of the AB samples except for the high stress ($0.5\sigma_{pl}$) condition of the most porous structure, i.e. Ti 120-500, whereas the fatigue life of the AcAl samples was significantly lower than that of AB and AlAcH samples for both stress levels and all porosities (**Figure 2.12**).

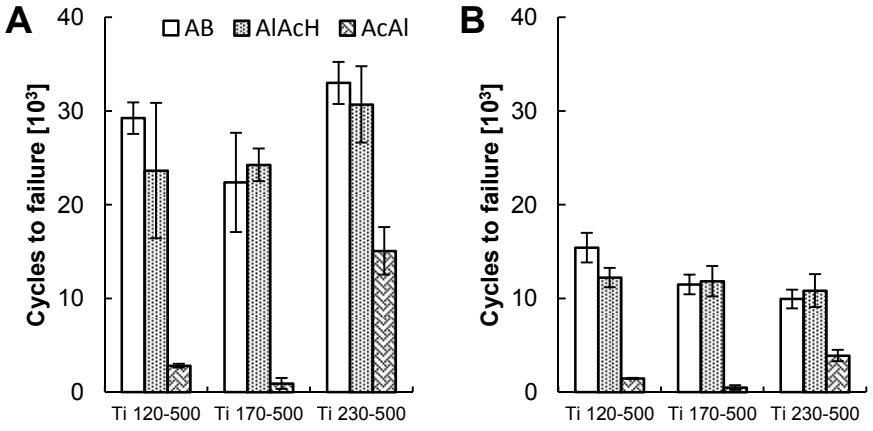

Figure 2.12: Fatigue life or cycles to failure of three types of rhombic dodecahedron porous structures before (AB) and after bio-functionalizing surface treatments (AlAcH and AcAl), tested under two different fatigue stress levels: $0.35\sigma_{pl}$ (A) and $0.50\sigma_{pl}$ (B).

Since for the AlAcH samples there was none or little difference in the static mechanical properties, it is reasonable to accept that the dynamic mechanical properties are also similar. In case of the AcAl samples, the substantial mass loss caused by the surface treatment results in even more significant loss of dynamic strength compared to the static properties. Where the static mechanical properties of AB samples were about 1.5-6 times higher compared to the AcAl samples, the fatigue strength of AB samples is up to 23 times that of AcAl samples.

2.5. *In vitro* and *in vivo* performance

New implants can be evaluated in several ways, but in the end the clinical performance is all that counts. Biocompatibility of the used material is often the first requirement, and since Ti6Al4V has a proven clinical track record of being a non-toxic biocompatible material, there is no reason to assume this would be different with SLM processed porous Ti6Al4V implants. This is confirmed by internal company records that have proven the non-cytotoxicity of porous parts

after SLM processing by LayerWise at an independent and accredited lab according to ISO 10993-5.

Second, the requirements in terms of mechanical strength are somewhat contradictive since they should avoid stress-shielding effects by a lower stiffness, but should be strong enough to withstand the load during the implant lifetime. It is obvious that this requirement still leads to a broad range of possible porous structures discussed in section 2.3 and 2.4. A proper selection based on the actual application and known loads on the implant should be made, using the results reported in these previous sections.

Regardless of the final choice, if the mechanical requirements are fulfilled for a biocompatible material like Ti6Al4V, bone will grow in eventually. But proper selection of the geometrical and mechanical properties of the porous implant, may lead to faster or more bone ingrowth and stronger implant-bone interfaces, as is illustrated by van der Stok in [49] using the same porous Ti6Al4V ELI implants with a rhombic dodecahedron unit cell geometry as presented in the previous sections to reconstruct a critical size femur defect in rats.

When all the basic requirements are fulfilled, other options that can improve the implant performance can be considered. The faster the bone gets triggered to grow inside the porous implant, the faster the initial fixation will be and the better the corresponding long-term outcome. Also the quality of the regenerated bone is of importance.

There are basically two potential ways to increase the bone regeneration performance of porous Ti6Al4V implants: by incorporating drugs or other stimulating factors in the open porosities so that the porous structure acts as a carrier or matrix, or by changing the surface properties. Both options are potential routes for the next generation additively manufactured porous implants, since they take the created opportunities of these novel manufacturing methods to a next level. Although these innovations seem promising, regulatory issues for drug delivery devices might be a hurdle for large scale clinical use in the near future.

Recently, the first promising results of porous Ti6Al4V implants with the same geometry as used in [49], incorporated with colloidal gelatin gels for time- and dose-controlled delivery of dual growth factors have been reported [46]. Gels with growth factors like BMP-2 and FGF-2 that can easily be embedded in the

porous Ti6Al4V implants, showed stimulatory effects for bone regeneration and an improved mechanical strength of the implant-host bone interface.

Another study, still using the same porous Ti6Al4V implants, compared the bio-functionalizing surface treatments acid-alkali (AcAl), alkali-acid-heat treatment (AlAcH) and anodizing-heat treatment (AnH) [8]. In brief, the applied surface treatments have considerable effects on apatite forming ability, cell attachment, cell proliferation, and bone ingrowth. The relationship between these properties and the bone-implant biomechanics is, however, not trivial.

Additively manufactured porous implants are relatively new and more *in vitro* and *in vivo* implant performance data will be available over time. This should give more insights in the mechanisms that can enhance the bone regeneration performance of porous Ti6Al4V implants. Until more data gets available, the improvements summarized in this section are considered as highly interesting.

2.6. Conclusions

Metal implants have been used for decades in orthopedics or other load-bearing applications. Still today, and although they are widely used, new insights in metal implant performance are under continuous investigation. This is not surprising, since almost endless variations have to be taken into account and influence the clinical outcome.

With the introduction of highly innovative AM techniques for the production of porous implants, new opportunities and applications are created, but also the number of possible variations that have to be considered, increased. A material that has been of great interest to process using metal AM and is commonly used for implant manufacturing is Ti6Al4V and is therefore the first material discussed in detail in this dissertation.

This chapter gives an overview of all the different studies that have been carried out on porous Ti6Al4V implants in the framework of this dissertation. It discusses all potential influences that have been identified so far and could influence the implant performance. This chapter can be used as a handbook for porous implants and as a starting point for further research.

3. Porous Tantalum Implants

This chapter is based on the following manuscript:

- [50] **Wauthle R.**, van der Stok J., Amin Yavari S., Van Humbeeck J., Kruth J.-P., Zadpoor A.A., Weinans H., Mulier M., Schrooten J.. *Additively manufactured porous tantalum implants*. Submitted, 2014.

In this article porous tantalum implants and test samples were manufactured by the main author, by first doing a SLM process parameter optimization. The full morphological evaluation and all static compression tests were carried out by the main author. Dynamic mechanical tests were done by S. Amin Yavari at TU Delft and the animal study was conducted by J. van der Stok at Erasmus Medical Centre in Rotterdam. Biomechanical torsion tests were carried out by S. Amin Yavari at TU Delft, the cytotoxicity test was done by Toxikon NV, and histological sample preparation was done at UZ Leuven by Dr. M. Maréchal and R. Kroes from the Prometheus research division. The manuscript was written by the main author and revised by all co-authors.

3.1. Introduction

Today, porous metal orthopedic implants are breaking new ground in skeletal reconstructive surgery and more specifically in total hip replacement, yet recently called 'The operation of the century' [51]. While total hip arthroplasty has become a routine treatment for hip osteoarthritis and as the number of surgical interventions increased from the seventies on, also the number of necessary revision operations has also increased.

The most common causes for revisions are mechanical loosening, infection and instability/dislocation [52]. A large portion of these failures are due to polyethylene wear and periprosthetic osteolysis and more recently metallosis [51, 53]. When this causes large bone defects and cavities in the bony structure and when the dimensions of these defects become too large, there is a chance of aseptic loosening of the implant.

These bone defects need to be reconstructed and filled during revision operations with new structures on which new prosthesis elements are attached. These new structures can be autografts, polymethylmethacrylate (PMMA, bone cement) or allografts.

In the case of large bone defects, the structural bone and compacted grafts are currently the best solution to create a mechanical stable reconstruction, which can withstand postoperative mechanical loads [54, 55].

Given the increased demand for allograft material and due its limited availability, more and more surgeons start to use artificial bone substitute materials. Preferably, these substitute materials should provide initial fixation and a long-term stability for surrounding prostheses.

Porous metals have the ability to allow for bone ingrowth and avoid stress-shielding by a lower stiffness without losing too much strength and thus are suitable to be used as bone substitute materials in load bearing applications. The first porous implants only had porous coatings of cobalt-chrome but were soon replaced by titanium (Ti), which is still today the most used material for porous biomaterials [51]. An alternative high potential biometal is tantalum (Ta).

Ta is a hard, ductile, highly chemically resistant material with good apposition to human bone [4]. It has been successfully used in clinical applications as a

biomaterial since the 1940s [4, 56], but because it is both expensive and difficult to machine [57], the use of Ta as a biomaterial has been limited.

The biocompatibility and non-toxic behavior of Ta in general has been reported previously [58, 59]. Tantalum's good attachment, proliferation and differentiation of human osteoblasts [60], even compared to the more commonly used surgical grade 5 Ti-6Al-4V [61, 62], are interesting properties.

More recently, surface modifications [63-69] or protein coatings [70] to enhance the biological performance of Ta have been investigated. Despite its promising biological properties, Ta is not considered as an appropriate material for large implants due to its high density and high price. The high density is on the other hand an advantage in case for high contrast applications such as bone markers for roentgen stereophotogrammetry (RSA) [71-75].

To avoid stress shielding, Ta is mostly limited to open porous structures in biomedical applications. Knowing that bulk Ta is difficult to process, and therefore commonly produced as a powder, it can also be applied as a coating on both solid [62, 76] and open porous implant surfaces [77, 78].

In the early 2000s, a new porous Ta biomaterial for acetabular cups was introduced (originally branded under the name *Hedrocel*™ by the company Implex, Allendale, NJ, USA and now known as *Trabecular Metal*™ *(TM)* by the company Zimmer, Warsaw, IN, USA). This highly innovative biomaterial is created by depositing a Ta coating upon open porous carbon matrices [78].

Ever since the introduction of TM, the use and range of applications has expanded. The increased interest in Ta, mainly thanks to TM, can clearly be illustrated by the number of publications on PubMed over the past 23 years shown in Figure 3.1. In the last ten years the number of publications on Ta has more than tripled.

Today, TM is the most commonly used biomaterial containing Ta in orthopedics [79-85]. Over 250 publications and 800,000 surgeries worldwide [86] illustrate its non-toxic and osteoconductive behavior, but without actual proof of outperforming other commonly used materials such as surgical grade 5 Ti-6Al-4V [87-91]. It has proven bone ingrowth both in animal studies [78, 92-94] and retrievals from clinical cases [95, 96], although some publications mention issues like implant failure and the brittle deformation behavior of TM

[97-99]. Moreover, the mechanical properties of TM are close to those of human bone [100-103]. Most uses of TM can be found in hip [104-111], knee [112-116], spinal [89, 117-119] and other orthopedic applications [120].

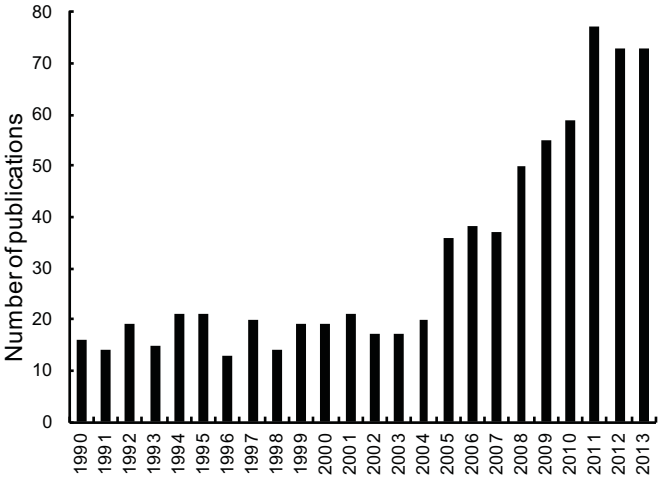

Figure 3.1: Resulting number of publications per year over the past 23 years on PubMed using search string "Tantalum"

Despite the clinical success of TM, no other implant manufacturers use Ta as raw material for orthopedic implants. Surgical grade 5 titanium and other titanium alloys are still the current standard for porous biomaterials used in orthopedics [85, 121]. Several manufacturing techniques like furnace sintering, plasma spraying, laser/electron beam melting, lost wax casting and vapor deposition techniques are used to manufacture porous Ti biomaterials [122-124].

Recently, new attempts have been made to produce both solid and porous Ta parts using novel manufacturing techniques such as Laser Engineered Net Shaping (LENS™) [125, 126], Spark Plasma Sintering (SPS) [127] and Selective Laser Melting (SLM) [3, 128].

Selective Laser Melting is an additive manufacturing technology in which a focused laser beam melts thin layers of metal powder together in order to create fully dense functional parts [129].

Some of the authors of this study were involved in previous research in which the first successful manufacturing of functional Ta parts by SLM was reported [3]. It is now possible to make nearly 100% dense parts fulfilling both the chemical and mechanical requirements according to ISO 13782 'Unalloyed Tantalum for Surgical Applications' [130].

Therefore, SLM manufacturing of porous Ta implants could lead to unexplored opportunities in orthopedics by tailoring mechanical properties and innovative implant designs with predictable mechanical properties.

The research presented in this work examines SLM as a new method to manufacture highly porous pure Ta bone replacement structures with controlled mechanical properties. Following morphological and mechanical characterization an *in vivo* assay in a load-bearing orthotopic animal model was conducted.

3.2. Materials and Methods

3.2.1. Materials and manufacturing

Porous Ta structures were manufactured from Ta powder using the selective laser melting technology (Layerwise NV, Leuven, Belgium). The unit cell used as the micro-architecture of these porous structures was a dodecahedron, with an average strut size of 150 μm and an average pore size of 500 μm, which resulted in an overall open porosity of ±80%.

This specific unit cell was chosen in order to compare the obtained results with those of previous studies that used identical dodecahedron structures made by SLM out of Ti6Al4V ELI powder [5, 6, 8, 46, 49].

In this work, the same spherical pure Ta powder (chemical composition according to ISO 13782 [131]) with particle size ranging from 13 μm to 26 μm as in [3] was used. The production was performed in an inert atmosphere and the samples were built on top of a solid Ti substrate. After production, the samples were removed from the substrate using wire electro discharge machining (EDM).

Porous structures in the shape of a rat femur defect with a maximum diameter of 4 mm and a height of 6 mm were manufactured for filling the segmental defect created in the animal model (Figure 3.2 A) [8, 46, 49]. Cylindrical porous

specimens with a diameter of 10 mm and height of 15 mm were manufactured for morphological analysis, static and dynamic mechanical testing and an *in vitro* cytotoxicity test (Figure 3.2 B).

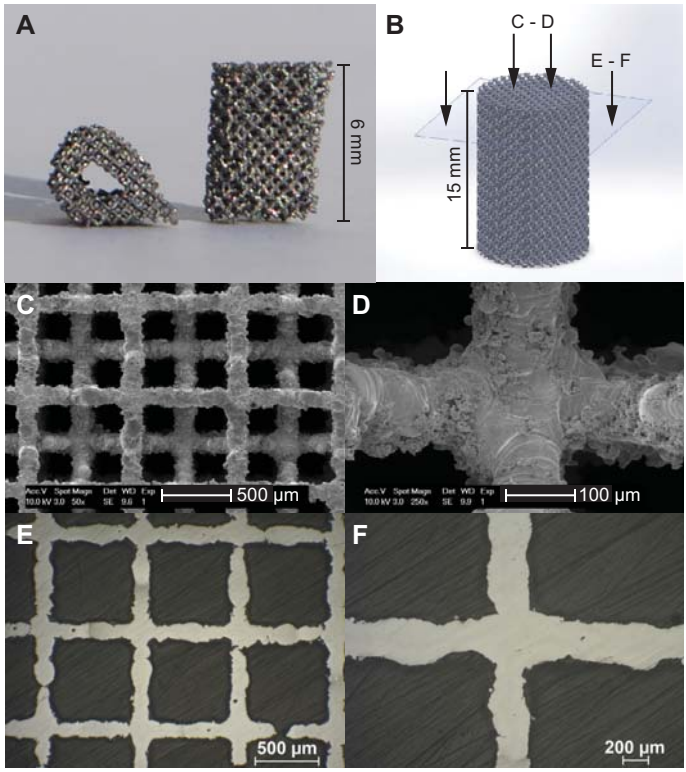

Figure 3.2: Morphological properties of open porous SLM processed Ta: Top and side view of the femur shaped porous Ta implant (A), 3D visual representation of the cylindrical test specimen (B), SEM pictures of the top view (C, D) and LOM pictures of a cross section (E, F)

3.2.2. Morphological analysis

Overall open porosity was measured using dry weighing and Archimedes measurements on 5 different cylindrical samples prior to their being used for mechanical evaluation.

Dry weighing occurred under normal atmosphere conditions and overall porosity was calculated by dividing actual weight by the theoretical weight of the macro volume using a theoretical density of 16.6 g/cm³ for pure Ta.

Archimedes measurements are based on a combination of dry weighing and weighing in pure ethanol. Overall porosity was then calculated by dividing the actual volume by the macro volume. All weighing measurements were performed on an OHAUS Pioneer balance.

The geometry and surface of the porous structures was viewed using secondary electrons in a PHILIPS SEM XL30 FEG equipped with a Schottky type of gun. A Leica DMILM 12V/100W Light Optical Microscope (LOM) was used to evaluate metallographic cross sections.

3.2.3. Mechanical testing

Static mechanical testing

Static mechanical testing of cylindrical porous samples was carried out in accordance with the standard ISO 13314 [17]. All tests were carried out using an INSTRON 5985 mechanical testing machine (30 kN load cell) by applying a constant deformation rate of 1.8 mm/min.

Each static compression test resulted in a stress-strain curve (Figure 3.3) for which the following values were calculated: plateau stress (σ_{pl}) as the arithmetic mean of the stresses between 20% and 30% compressive strain, plateau end stress (σ_{130}) and strain (ε_{ple}) as the point in the stress-strain curve at which the stress is 1.3 times the plateau stress, the quasi-elastic gradient (E) as gradient of the straight line determined within the linear deformation region at the beginning of the compressive stress-strain curve and the yield strength (σ_y) as the compressive 0.2% offset stress.

In this context, the quasi-elastic gradient is closest to the concept of stiffness, which is used for solid materials. In order to facilitate understanding and comparison between the results of this study and those of similar studies on solid and porous materials, the quasi-elastic gradient will be referred to as stiffness. Nevertheless, the exact definitions presented above should be kept in mind when interpreting the data.

Dynamic mechanical testing

Compression-compression fatigue tests were carried out on an identical set-up as reported before [6] using a hydraulic test frame (MTS, Minneapolis, US) with a 25 kN load cell. The loading frequency was fixed at 15 Hz (sinusoidal wave shape) and a constant load ratio, $R = 0.1$, was used.

Thirteen different values of maximum force were chosen, resulting in applied stress levels between 0.23 σ_{pl} and 0.9 σ_{pl}. The samples were considered to have failed once they lost +90% of their stiffness. The S-N curve of porous Ta was established by plotting the absolute values of stress versus the number of cycles to failure for all tested samples.

3.2.4. Biological evaluation

The biological and bone regeneration performance of porous Ta were evaluated through an *in vitro* cytotoxicity test, an *in vivo* segmental bone defect model and quantification of bone ingrowth by histological analysis.

Cytotoxicity test

Biocompatibility testing by means of an *in vitro* cytotoxicity test according to ISO 10993-5 [132] was performed (Toxikon Europe NV, Leuven, Belgium). The observed viability for the L929 mammalian cells exposed to the test sample at 41 hours observation is used as the test criterion and the tested biomaterial is considered non-cytotoxic if the percentage of viable cells is equal or greater than 70% of the untreated control.

Bone defect model

For the functional *in vivo* evaluation of the open porous Ta implants, load-bearing segmental bone defects were used as described earlier [8, 46, 49]. In brief, a critical-sized femoral bone defect was grafted with a porous Ta implant, in eight male Wistar rats. The Animal Ethics Committee of the Erasmus University approved the study and Dutch guidelines for care and use of laboratory animals were followed.

Prior to surgery, rats were administered one dose of antibiotics (enrofloxacin, 5 mg/kg body weight) through subcutaneous injection. Surgery was performed aseptically under general anaesthesia (1 - 3.5% isoflurane) as follows: first the right femur was exposed through a lateral skin incision and blunt division of underlying fascia.

Then, a 23 mm long Poly Ether Ether Ketone (PEEK) plate was fixated to the anterolateral plane using six bicortical titanium screws (0.8 x 6.5 Ø mm). Periosteum was removed over approximately 8 mm of the mid-diaphyseal region before a 6 mm cortical bone segment was removed with a wire saw and a tailor-made saw guide. The 6 mm femur-shaped implants were press-fit into the defect.

Finally, fascia and skin were sutured using Vicryl 5-0 and pain medication (buprenorphine, 0.05 mg/kg body weight) was administered through subcutaneous injection twice a day for 3 days. Rats were sacrificed after 12 weeks with overdose of pentobarbital (200 mg/kg body weight). Afterwards implant fixation was determined on explants using X-ray images acquired using a SkyScan 1076 (Bruker micro-CT NV, Kontich, Belgium).

Histological evaluation

Histology was performed on two specimens of the total group (n=8: 2x histological evaluation, 1x spare histological evaluation, 5x ex vivo testing) to qualitatively study the amount of bone ingrowth and to examine the bone-tantalum interface. The specimens were selected by two medically-trained co-authors as being representative of the whole group (the specimens with the least and most visible amount of bone formation were selected).

Specimens were first preserved and dehydrated and then embedded in methylmethacrylate. Serial sections of about 100 μm were made using a saw microtome (longitudinal cuts, anterior-posterior), which were polished to 50 μm and finally stained using Stevenel's blue and counterstained using von Gieson's picrofuchsine.

As a result bone stains red, fibrous tissue stains blue and cartilage stains purple. Stained sections were examined using a Leica M165 FC fluorescent stereo microscope. One additional specimen was kept as a spare part in case further histological examination was necessary, but was not ultimately used.

3.2.5. Biomechanical testing

The strength of the implant-bone connection was evaluated after explantation on the 5 remaining specimens by means of a torsion test as described earlier [133]. In brief, both ends of each femur were embedded in a cold-cured epoxy resin (Technovit 4071, Heraeus Kulzer, Germany), after removal of the PEEK fixation plate. On the upper clamping side, a Cardan joint was used to ensure the specimens were subjected to pure rotation without bending. The lower sides of the specimens were simply fixed. The tests were performed until failure with a rotation rate of 0.5° s^{-1} using a static mechanical testing machine (Zwick GmbH, Ulm, Germany). The torsional strength (maximum torque to failure, N.mm) and maximum rotation (degree) were determined and reported.

3.3. Results

3.3.1. Morphological properties

Dry weighing resulted in a mean overall open porosity of 79.9±0.2% and according to the Archimedes measurement the strut density was 99.0±0.2% and the overall porosity was 79.7±0.2%. Figure 3.2 C-D shows SEM pictures of the top view at different magnifications and Figure 3.2 E-F shows LOM pictures at a certain cross section of a prepared sample of the regular porous structure.

3.3.2. Mechanical properties

The results of the static compression tests are summarized in Table 3.1. Due to the ductile behavior of the porous Ta material, no maximum compressive stress (σ_{max}) and strain at maximum compressive stress (e_{max}) could be registered.

	Symbol	Units	Mean	St. Dev.
yield stress	σ_y	[MPa]	12.7	0.6
plateau stress	σ_{pl}	[MPa]	21.8	0.9
plateau end stress	σ_{130}	[MPa]	28.3	1.2
plateau end strain	e_{ple}	[%]	36.1	0.4
stiffness	E	[GPa]	1.22	0.07

Table 3.1: Results of the static compression tests of open porous SLM processed Ta according to ISO 13314

Figure 3.3 A shows a representative stress-strain curve and the ductile behavior of the porous Ta structure during static compression testing. The repeatability of the mechanical properties of the porous Ta is illustrated by Figure 3.3 B, in which the stress-strain curves for 0-20% strain of all tested samples are shown.

The dynamic compression test results are shown in Figure 3.4 through an S-N curve consisting of 13 data points obtained by compression-compression fatigue testing. The horizontal line at the level of the yield strength differentiates between low cycle fatigue strength (above σ_y and mainly plastic deformation) and high cycle fatigue strength (below σ_y and mainly elastic deformation). Since three samples did not fail at 10^6 cycles, the highest of these three values (7.35 MPa) is considered as an indication of the fatigue limit, S_f, of the porous Ta biomaterial.

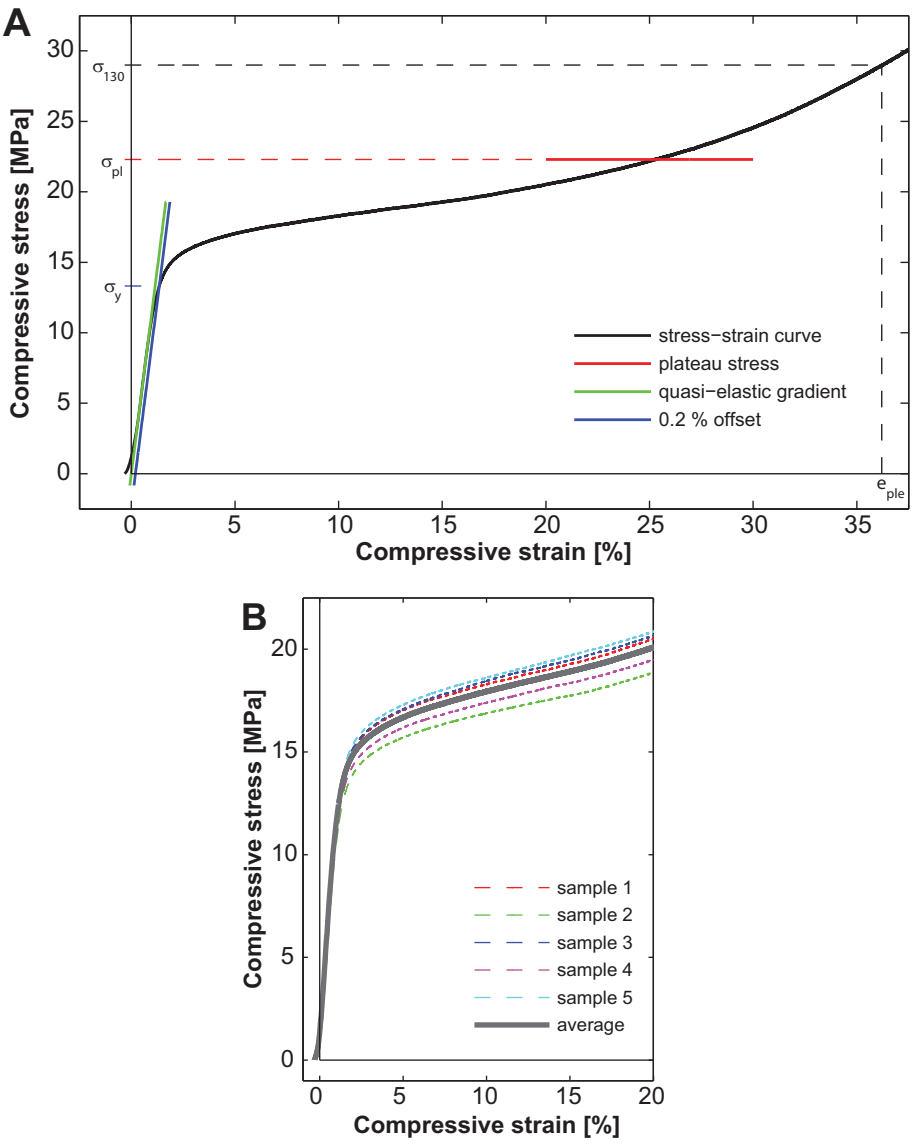

Figure 3.3: Static mechanical properties of open porous SLM processed Ta: representative compressive stress-strain curve and graphical representation of the calculated values σ_y, σ_{pl}, σ_{130} and E (A) and overview of the individual and average stress-strain curves of all 5 tested specimens (B)

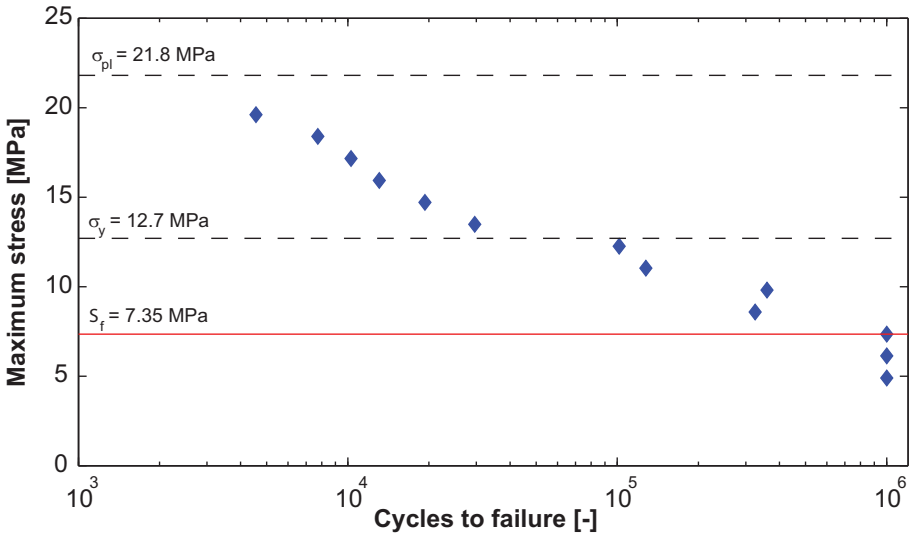

Figure 3.4: Dynamic mechanical properties of open porous SLM processed Ta: S-N curve obtained by compression-compression fatigue testing with indication of the plateau stress (σ_{pl}), the yield stress (σ_y) and the fatigue limit (S_f)

3.3.3. Biological properties

Cytocompatibility of SLM produced Ta implants was determined *in vitro* using a cytotoxicity test. For this test, 82% viability was observed and the cellular response obtained from the positive control extract (4% viability) and the negative control extract (108% viability) confirmed the suitability of the test system. The test sample is considered non cytotoxic and meets the requirements of ISO 10993-5, thus showing that SLM produced Ta is cytocompatible.

Figure 3.5 shows X-ray images and histology images of the two implants that were processed for histology after 12 weeks *in vivo*. On the X-ray images (Figure 3.5 A, G) the porous Ta implant can clearly be recognized thanks to the high contrast caused by the high specific weight and atomic number of the Ta material. However, this X-ray absorbing property makes it difficult or impossible to draw any conclusions on bone formation and bone ingrowth into the porous Ta implant based on radiological images.

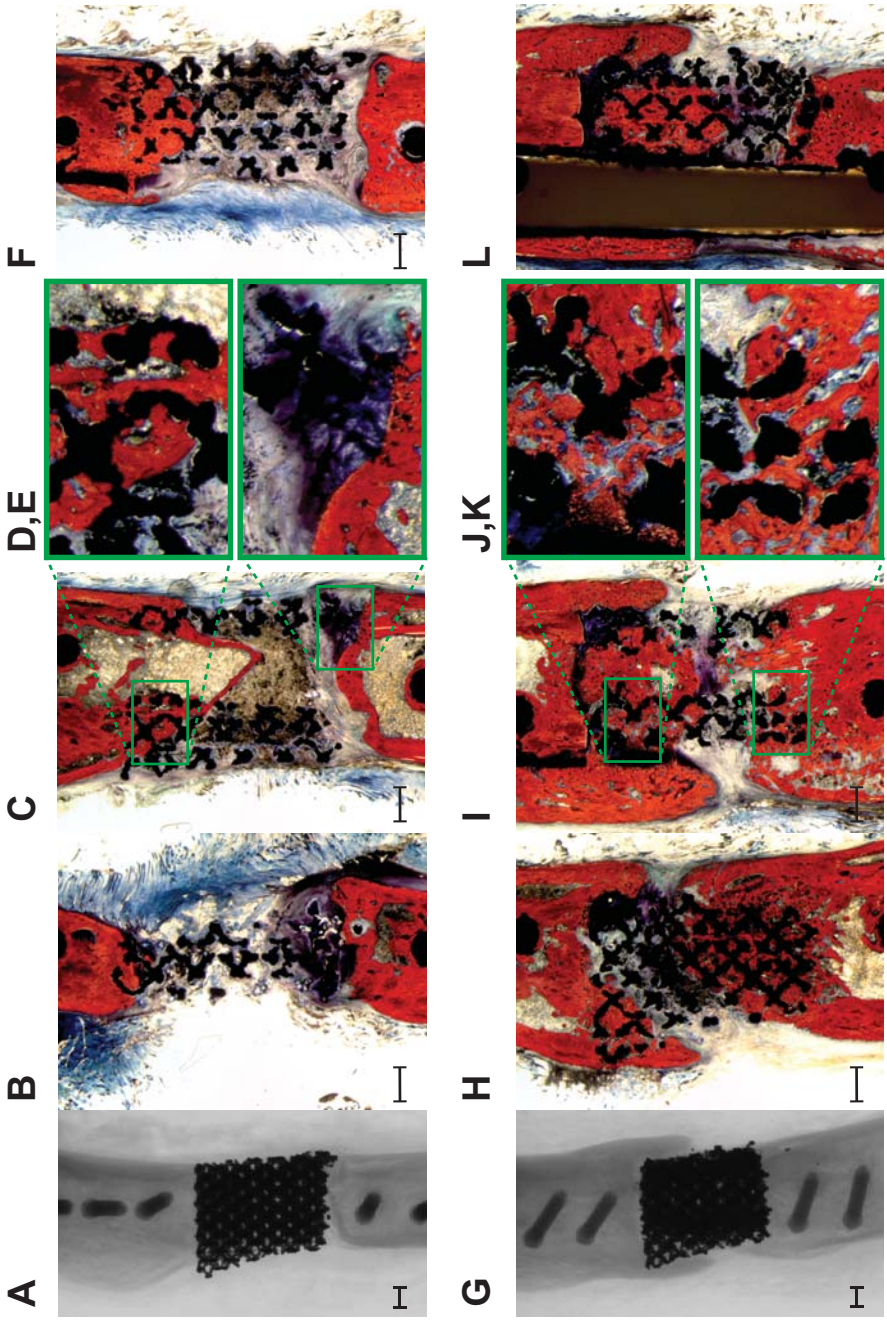

Figure 3.5: X-Ray and histological images of open porous SLM processed Ta: explant specimen 1 (A-F) and explant specimen 2 (G-L), including detailed interface view (D,E) for specimen 1 and (J,K) for specimen 2. The scale bar indicates 1 mm.

The only observation that could be made is that on Figure 3.5 A there is a radiolucent line visible, indicating a weak implant-bone connection at the bottom, probably resulting in no bone ingrowth (or very little), whilst at the connection at the top no radiolucent line is visible. Also for Figure 3.5 G no radiolucent lines are present at the implant-bone interface and in this case the bone has clearly grown around the implant.

Two explant specimens were selected for histological analysis as being representative for the whole group. Three images of cross-sections at different locations including two detail images are shown in Figure 3.5 B-F and Figure 3.5 H-L respectively. All cross-sections show some amount of bone ingrowth inside the porous Ta implant.

On Figure 3.5 B, C, F the X-ray observation of bad implant-bone connection at the bottom is confirmed by no visible bone ingrowth, but the purple staining indicates the presence of cartilage-like tissue at these locations (Figure 3.5 B, C, E). Furthermore, a thorough bone ingrowth from the top with restoration of the femur canal can be seen on Figure 3.5 C and soft tissue is observed on Figure 3.5 B and F.

For the second specimen (Figure 3.5 H, I, L), the bone has not only grown around the implant, but also deep inside the pores of the implant resulting in an almost full bridging of the defect at all cross-sections. At some locations only small gaps are in between, and the presence of cartilage can be noticed. As shown by the detail images in Figure 3.5 D, J, K, a good implant-bone interface is established since the bone has grown closely to the Ta surface.

3.3.4. Biomechanical properties

5 explant specimens were biomechanically evaluated using torsion testing for which the results can be found in Table 3.2. Two specimens did not fail at the maximum torque (450 Nmm) of the test setup, whereas three samples did fail at an average maximum torque of 331.3 Nmm and an average rotation of 59.1 °. Two of the failed specimens showed a fracture at the implant-bone interface and one specimen had a fracture in the bone.

3.4. Discussion

It has been shown previously that it is possible to produce solid bulky Ta parts by SLM that meet both the requirements in terms of chemical composition and mechanical properties [3, 130, 131]. In this study, the SLM technology was used

to produce for the first time porous structures consisting of a dodecahedron unit cell with an overall porosity of 80%, a strut size of 150 μm and a pore size of 500 μm. Morphological analysis revealed the regular dodecahedral architecture of the porous structure with a highly repeatable overall porosity. The small difference between the dry weighing and Archimedes method can be explained by the small amount of enclosed pores inside the struts (Figure 3.2 E). Other strut defects are caused by the strut surface roughness and the imperfect alignment of the cross-sectional plane

Specimen	Max. torque [Nmm]	Rotation at max. torque [°]	Fracture location
1	>450.0	/	not broken
2	324.6	54.6	implant-bone interface
3	324.4	65.7	bone
4	345.0	56.9	implant-bone interface
5	>450.0	/	not broken
Average	331.3*	59.1*	/

Table 3.2: Torsion test results of 5 open porous SLM processed Ta explants after 12 weeks. *specimen 1 and 5 not included

Therefore it can be concluded that the SLM technology is able to produce very fine porous Ta structures with high reproducibility. This quality is also noticeable in the mechanical properties and is important if this technology is considered to be used for serial manufacturing of implants.

The actual static mechanical properties like yield strength (12.7±0.6 MPa) and stiffness (1.22±0.07 GPa) are in the range of human cancellous bone and are hence favorable in lowering stress shielding effects although it should be noted that the elastic modulus of the porous Ta implants evaluated here is below the stiffness of most human cortical bone [4]. Compared to similar porous structures in Ti6Al4V ELI made by SLM [5-7], the stress-strain curve of porous Ta does not reach a first local maximum due to the intrinsic ductile behavior of the Ta material (comparative data not shown) [3, 130, 134, 135].

Instead of failure at the local maximum, now continuous (plastic) deformation occurs. This different deformation behavior is expected since conventionally processed pure tantalum has a higher ductility compared to Ti-6Al-4V ELI [4].

As already postulated by the morphological properties, the reproducibility of the process is confirmed by the static mechanical properties since all calculated values – except for the stiffness – have standard deviations lower than 5% of the nominal values.

The fatigue behavior has been evaluated at thirteen different stress levels of which six are above and seven are below the yield strength. Despite the fact that tests at these stress levels were only performed once per level, a shift in the trend can be noticed when passing the yield strength.

This observation and the indication of the fatigue limit S_f should be interpreted with care, since further tests have to be done in order to confirm the results. Normalizing the fatigue limit by the yield strength results in an endurance limit of 0.58 σ_y, which is much higher when compared to identical porous structures in Ti6Al4V ELI which have an estimated endurance limit of 0.12 σ_y for an open porosity range from 66% to 84%. Even for absolute values, porous Ta (7.35 Mpa) apparently has higher fatigue strength than porous Ti-6Al-4V ELI (4.18 MPa) [6].

The reason for the good fatigue behavior of porous Ta can be explained by its high ductility which lowers crack initiation and propagation by softening the material when loaded [136]. Yet again, since no statistics can be done, further tests have to be conducted in order to confirm the observed trends.

The cytotoxicity test confirmed the non-cytotoxicity of the porous Ta biomaterial, also after SLM processing, but to evaluate the *in vivo* functionality of the new biomaterial an animal experiment was done. In this experiment, eight rats have been implanted with a 6 mm porous Ta implant to reconstruct a critical-sized femoral bone defect.

Since Ta has a high atomic weight, it highly absorbs X-rays and it is therefore difficult to use standard evaluation techniques like radiographic or 3D CT follow-up as was performed in previous studies [8, 46, 49]. Nevertheless, implant fixation can still be observed from the presence of radiolucent lines, but no conclusions on the amount of bone ingrowth can be done based on the radiographic images.

Histological analysis of two explant specimens confirmed the observation of fixation based on X-rays by the presence of bone inside the porous Ta implant

at the sides with no radiolucent lines (top of Figure 3.5 A vs. B, C and F and top and bottom of Figure 3.5 G vs. H, I and L).

The depth of bone ingrowth varied between the cross-sections within one specimen, but was at least for one cross-section of each specimen more than 50% of the total length of the defect, resulting in an almost 100% bridging of the defect for the second specimen.

The regenerated bone grows closely to the Ta surface and proofs the good apposition of Ta to bone and enables a continuous load transfer. The lack of bone ingrowth in the first specimen (at the bottom of Figure 3.5 B, C, F) could be explained by less initial fixation during surgery. However this mechanical instability is a fairly reasonable cause, but other factors may have influenced the bone regeneration.

Nevertheless, the inter-implant differences are not considered to have an influence since the differences in morphological and mechanical properties are very small. Despite the mechanical instability, a stimulating biological effect is noticeable by means of cartilage formation (Figure 3.5 B, C, E). In a biological preferential environment, micro-motions lead to bone generation through a phase of cartilage formation [137, 138].

A good implant-bone interface connection is also visible in the biomechanical torsion test results. Two out of 5 explant specimens did not fail. One specimen failed due to a fracture in the host bone and two specimens failed at the implant-bone interface.

The maximum torque for the three failed specimens did not differ significantly, indicating that the implant-bone interface was at least as strong as the host bone. This assumption is in agreement with previous reported maximum torque values of 146.7±19.1 Nmm of intact femurs in a comparable study in which the same animal model was used [139].

Based on the radiographical and histological analysis and biomechanical evaluation of these porous Ta implants after 12 weeks *in vivo* it can be concluded that this new biomaterial functions well in a biomechanically loaded environment. The bone regenerates and grows inside the porous biomaterial, except for one side of a histologically examined specimen, resulting in a very stable and strong reconstruction.

The favorable biological properties of the Ta material that facilitate cell attachment and proliferation [58-62] and the preferential mechanical properties of the porous structure that likely avoid stress-shielding effects by transferring loads in a stimulating way [140], are considered to be the main reasons for the excellent implant performance. To progress from the first promising results of this new porous Ta biomaterial, further more extensive tests should be carried out on large animal models to confirm the findings of this study. Also, the potential risk for infection deep inside the pores of large porous implants and the effects and optimization of the microporosity are important to take into consideration when translating this porous tantalum biomaterial to human implants.

This work has illustrated for the first time that SLM technology can become a robust method to manufacture porous Ta implants, allowing for almost full design freedom to create any interconnected porous structure with controllable mechanical properties and personalized outer geometries.

Also no additional surface modification treatment (e.g. etching, anodizing, HA plasma sprayed coating, etc.) was applied yet to improve implant-host interaction, whereas this is more common for Ti implant surfaces. Still, the high cost of the material and the difficult radiological interpretations are currently major disadvantages to be well considered before clinical use of this new type of implants.

Given both the advantages and disadvantages, SLM processed porous Ta result new window of opportunities for new and innovative implant designs, both for standard and patient-specific orthopedic implants. Small implant types (e.g. dental implants, spinal implants, small joints and extremities, examples see Figure 3.6) will benefit of less material consumption, whereas highly porous structures can be applied as a thin layer on top of a solid substrate for larger load bearing applications for which a fast and solid anchoring of the implant is required.

Compared to identical Ti porous structures, SLM produced Ta shows excellent osteoconductive properties even without any surface treatments, has a higher normalized fatigue strength and allows for a higher formability due to its excellent ductile properties. The latter can lead to unexplored applications by easier surgical handling and intraoperative manipulation of the implant to obtain an optimal implant-bone fit.

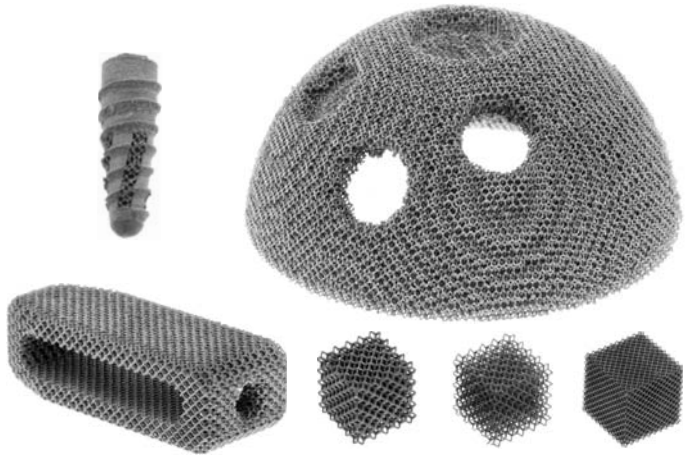

Figure 3.6: Examples of additively manufactured porous tantalum implants: A dental implant with integrated helix-shaped porous structure (upper left corner); A porous acetabular shell (upper right corner); a porous spinal fusion cage (lower left corner); and cubic test samples illustrating different possible porous structures.

Further research on this topic could investigate the optimization of the geometric and mechanical properties for optimal load transfer and bone ingrowth for different applications and the enhancement of cell attachment and proliferation by modifying the surface characteristics.

3.5. Conclusions

In this study the additive manufacturing technology selective laser melting was used to manufacture a highly open porous (80%) pure Ta implant. The morphological and mechanical evaluation of this biomaterial demonstrated the high repeatability of the SLM process. With a yield strength of 12.7 MPa, a stiffness of 1.22 GPa and a ductile deformation mechanism, the porous Ta exhibits mechanical properties that are in the range of cancellous bone and appear to allow for bone ingrowth. Moreover, with a fatigue limit of 7.35 MPa, the investigated material has relatively high resistance to cyclic loading. A cytotoxicity test as part of the biological evaluation raised no concerns over biocompatibility of the SLM processed material and an *in vivo* rat segmental bone defect model was used to investigate the osteoconductive and biomechanical performance of the porous material. Substantial bone ingrowth after 12 weeks was shown by histological analysis with almost full bridging of the created defect in isolated cases. Torsion testing of the explants indicated a strong implant-bone interface connection and a high strength of the repaired

bone defect. Altogether, it can be concluded that based on this initial study, selective laser melting can be used to manufacture highly porous, pure Ta orthopedic implants with interesting mechanical properties and promising *in vivo* performance for the used animal model.

4. Porous Pure Titanium Implants

This chapter is based on the following manuscript:

- [141] Wauthle R., Ahmadi S.M., Amin Yavari S., Mulier M., Zadpoor A.A., Weinans H., Van Humbeeck J., Kruth J.-P., Schrooten J.. *Revival of pure titanium for dynamically loaded porous implants using additive manufacturing*. Submitted, 2014.

In this article porous pure titanium test samples were manufactured by the main author. The full morphological evaluation and all static compression tests were carried out by the main author. Dynamic mechanical tests were done by S.M. Ahmadi and S. Amin Yavari at TU Delft. The manuscript was written by the main author and revised by all co-authors.

4.1. Introduction

Porous metal structures in orthopedics were first reported in the late sixties, and ever since then the interest has only increased [4, 85, 121]. The reasons for this trend in reconstructive surgery are obvious: coming from solid metal implants with high strength and stiffness, porous metals are optimal for uncemented use since they allow for bone ingrowth through the open porosities, have an improved fixation thanks to the high roughness and corresponding coefficient of friction and have in addition a lower stiffness and thus avoid stress-shielding [142].

Today, one of the most well-known porous metal bone replacement structures is *Trabecular Metal*™ (Zimmer, Warsaw, IN, USA), which is a highly porous carbon matrix coated with tantalum (Ta) [4, 78, 82, 83, 100, 101]. But due to the high density and high cost of Ta and its difficulty to process, most orthopedic device manufacturers choose to use porous biomaterials based on titanium or titanium alloys [85, 121, 143]. These titanium porous structures are usually manufactured using conventional techniques such as furnace sintering, plasma spraying, lost wax casting and vapor deposition [28, 122, 123, 143].

Recently, additive manufacturing (AM) techniques such as selective laser melting (SLM, [129]) and electron beam melting (EBM) are breaking new ground in implant manufacturing and more specifically in the manufacturing of porous metal bone replacement structures. AM allows for almost full design freedom, giving the possibility to manufacture regular open porous structures with high repeatability and thus full control over both geometrical and mechanical properties.

The design freedom and reproducibility are important features when there is a need for implant performance simulations and outcome predictions [5, 7]. Also, using AM has the advantage to manufacture implants with both porous and solid sections in one step (monolithic design), with less material consumption since the non-used powder can be recycled for future use. Finally, materials like Ta that are difficult to process conventionally, could be also processed using AM, creating a whole range of new opportunities [50].

In the current study, the SLM technology was used to manufacture porous structures from commercially pure (CP) grade 1 titanium. Previous studies mostly dealt with porous structures in Ti6Al4V (grade 5 or grade 23), either

using SLM [5-8, 21, 24, 26, 39, 40, 46, 49, 124, 144-146] or EBM [28, 29, 31, 32, 44, 45, 147]. This biocompatible titanium alloy is the material of choice for load-bearing applications since it has a high strength to weight ratio.

Commercially pure titanium, on the other hand, has a lower strength and therefore its use is often limited to non-load bearing applications like cranio-maxillo-facial implants [13]. A general overview of these mechanical properties of different grades of titanium and tantalum can be found in Table 1.1.

Also, only few publications about additively manufactured CP titanium are available, all of them covering SLM of CP grade 2 titanium [148-152] and none were found that deal with CP grade 1 titanium. Nevertheless, the use of CP titanium has some major advantages over alloyed titanium that can potentially bring additively manufactured CP titanium back in the scope of medical device manufacturers.

First of all, pure titanium has the advantage of having no potential hazardous or toxic alloying components such as V or Al [4]. Secondly, the high ductility that provides CP titanium with the sometimes necessary deformability in certain applications like e.g. bone plates, could be an interesting property of porous metals that could be deformed intra operatively to the patient specific bone defect. And finally, in a previous study on porous Ta structures, the ductile behavior of the Ta material led to a very high fatigue strength compared to similar Ti6Al4V ELI structures and a preferential load transfer and bone ingrowth in an animal study [50]. It was proposed that the mechanical behavior of the porous Ta including its high ductility was partly responsible for the excellent *in vivo* performance of Ta.

Therefore, the aim of this study is to investigate whether pure titanium can have a revival in orthopedics as a raw material for SLM processed porous implants. This is the first study that presents and discusses the mechanical properties of additively manufactured porous structures made of CP grade 1 titanium and compares them with those of additively manufactured Ti6Al4V ELI and Ta structures. This could be useful for facilitating proper selection of the most appropriate material for the envisioned implant application.

4.2. Materials and Methods

The materials and methods section describes the details of the new porous CP grade 1 Ti samples, manufactured and analyzed in the current study. The

properties of identical porous structures made from Ti6Al4V ELI and Ta to which the CP titanium samples are compared, were published elsewhere unless otherwise implied [6, 50].

4.2.1. Materials and manufacturing

Porous CP Ti structures were manufactured from CP Ti powder using the selective laser melting technology (Layerwise NV, Leuven, Belgium). The details of the laser processing method were similar to the ones presented in previous studies [6, 124, 145, 146].

The unit cell used as the micro-architecture of these porous structures was in all cases dodecahedron, in four different porosities. This specific unit cell, pore and strut sizes were chosen in order to compare the results with those of a previous study that used identical dodecahedron structures made by SLM out of Ti6Al4V ELI powder [6].

In this work, spherical commercially pure grade 1 Ti powder (chemical composition according to ASTM F67, further referred to as CP Ti) with particle size ranging from 10 μm to 45 μm was used. The production was performed in an inert atmosphere and the samples were built on top of a solid Ti substrate. After production, the samples were removed from the substrate using wire electro discharge machining (EDM). Cylindrical porous specimens with a diameter of 10 mm and height of 15 mm were manufactured for morphological analysis, static and dynamic mechanical testing (Figure 4.1).

4.2.2. Morphological analysis

Overall open porosity was measured using dry weighing and Archimedes measurements on 5 different cylindrical samples prior to mechanical testing. Dry weighing occurred under normal atmosphere conditions and overall porosity was calculated by dividing the actual weight by the theoretical weight of the macro volume using a theoretical density of 4.507 g/cm³ for pure Ti [2].

Archimedes measurements are based on a combination of dry weighing and weighing in pure ethanol. Overall porosity was then calculated by dividing the actual volume by the macro volume. All weighing measurements were performed on an OHAUS Pioneer balance.

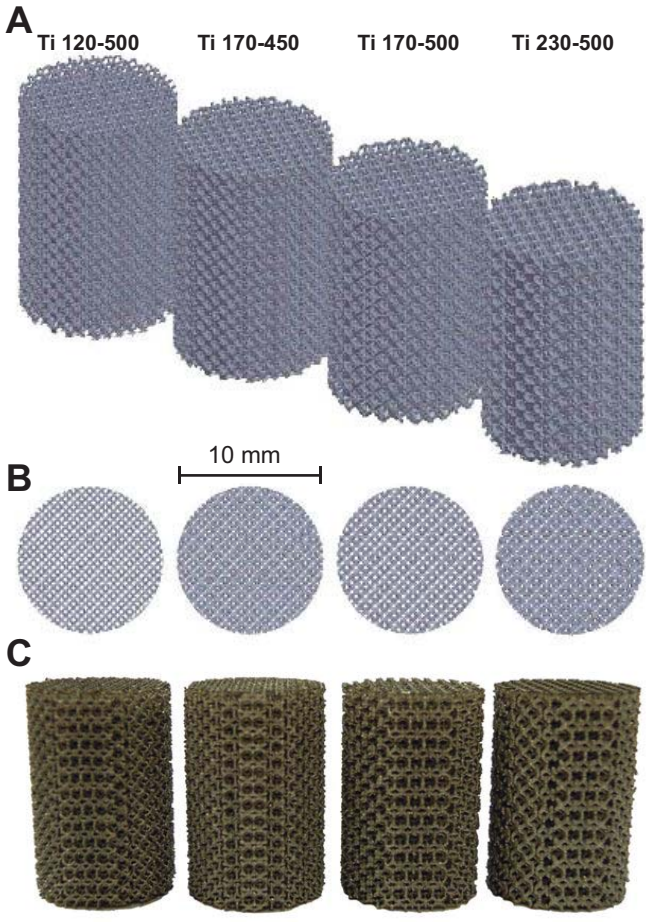

Figure 4.1: Additively manufactured porous CP Ti structures: 3D CAD visual representation of the four different structures in isometric (A) and top (B) view and a picture of actual samples after manufacturing (C).

4.2.3. Mechanical testing

Static mechanical testing

Static mechanical testing of 5 cylindrical samples of each of the four series of porous structures was carried out in accordance with the standard ISO 13314 [17]. All tests were done using an INSTRON 5985 mechanical testing machine (30 kN load cell) by applying a constant deformation rate of 1.8 mm/min.

Each static compression test resulted in a stress-strain curve (Figure 4.2) for which the following values were calculated: plateau stress (σ_{pl}) as the arithmetical mean of the stresses between 20% and 40% compressive strain, plateau end stress (σ_{130}) and strain (e_{ple}) as the point in the stress-strain curve at which the stress is 1.3 times the plateau stress, the quasi-elastic gradient (E) as gradient of the straight line determined within the linear deformation region at the beginning of the compressive stress-strain curve and the yield strength (σ_y) as the compressive 0.2% offset stress.

In this context, the quasi-elastic gradient is closest to the concept of stiffness, which is used for solid materials. In order to facilitate understanding and comparison between the results of this study and those of similar studies on solid and porous materials, the quasi-elastic gradient will be referred to as stiffness. Nevertheless, the exact definitions presented above should be kept in mind when interpreting the data.

In the previous study on Ti6Al4V ELI porous structures, it was assumed that the plateau stress was close to the concept of yield stress [6], and this is confirmed by re-calculating the yield stress according the 0.2% offset stress explained above (solid and dashed grey lines in Figure 4.3 A). For three out of four data points, there is no significant difference between the yield stress and the plateau stress for Ti6Al4V ELI porous structures, meaning that the assumptions were valid. However, for CP Ti porous structures, there is a significant difference between the yield stress and the plateau stress, and therefore both values were calculated and analyzed separately.

Dynamic mechanical testing

Compression-compression fatigue tests were carried out on an identical set-up as reported before [6] using a hydraulic test frame (MTS, Minneapolis, US) with a 25 kN load cell. The loading frequency was fixed at 15 Hz (sinusoidal wave shape) and a constant load ratio, $R = 0.1$, was used.

Ten different values of maximum force were chosen for every porous structure (except one, for which only 7 values were tested), resulting in applied stress levels between 0.45 σ_y and 0.8 σ_y. Two samples were tested for each stress level with 20 samples in total for series Ti 120-500, Ti170-500 and Ti 230-500 and 14 samples for series Ti 170-450 (see Figure 4.1 and Table 4.1. for details on the series nomenclature)

The samples were considered to have failed once they lost +90% of their stiffness. The S-N curves of the four tested porous structures were established by plotting both absolute and normalized values of stress versus number of cycles to failure for all tested samples. In case of normalized S-N curves, a power law was fitted to all data points of the normalized S-N curves.

4.3. Results

4.3.1. Morphological properties

The measured values for the overall porosity by dry weighing and Archimedes measurements are summarized in Table 4.1. A high repeatability in terms of overall porosity (< 1%) and a high density of the struts (> 98%) was achieved, which is of importance for reproducibility of the mechanical properties.

Series	**Ti 120-500**	**Ti 170-450**	**Ti 170-500**	**Ti 230-500**
Porosity, dry weighing [%]	81.7 ± 0.2	71.4 ± 0.6	78.5 ± 0.3	66.7 ± 0.4
Porosity, Archimedes [%]	81.6 ± 0.2	71.1 ± 0.6	78.4 ± 0.4	66.0 ± 0.6
Strut density, Archimedes [%]	99.8 ± 0.2	99.2 ± 0.1	99.5 ± 0.3	98.0 ± 1.1
Pore size, nominal [µm]	500	450	500	500
Strut size, nominal [µm]	120	170	170	230

Table 4.1: The geometrical/physical properties of the four different series of porous CP Ti samples tested in the current study.

4.3.2. Mechanical properties

The results of the static compression tests are summarized in Table 4.2. Due to the ductile behavior of the porous CP Ti material, no maximum compressive stress (σ_{max}) and strain at maximum compressive stress (ε_{max}) could be registered. Figure 4.2 A shows a representative stress-strain curve and the ductile behavior of the porous CP Ti Ti 120-500 structure during static compression testing, including a graphical representation of all calculated properties.

The actual values of the static mechanical properties are summarized in Table 4.2 and are visually presented and compared to Ti6Al4V ELI and Ta in Figure

4.3 A and B, in which the actual open porosity of each porous structure is taken into account. For the Ta values, σ_{pl} was recalculated for the 20-40% strain interval instead of the previously reported 20-30% strain interval.

Series	σ_y [MPa]	σ_{pl} [MPa]	σ_{130} [Mpa]	e_{ple} [%]	E [GPa]
Ti 120-500	8.6 ± 0.3	14.3 ± 0.2	18.6 ± 0.3	46.3 ± 0.4	0.58 ± 0.02
Ti 170-450	29.2 ± 2.3	63.2 ± 3.8	82.3 ± 5.2	40.3 ± 0.5	2.08 ± 0.14
Ti 170-500	13.7 ± 0.4	27.6 ± 2.2	36.3 ± 3.4	41.4 ± 2.3	0.96 ± 0.05
Ti 230-500	36.5 ± 0.4	62.7 ± 1.4	81.5 ± 1.9	42.4 ± 0.5	2.61 ± 0.05

Table 4.2: The static mechanical properties of the four different series of porous CP Ti samples tested according to ISO 13314.

The dynamic compression test results are shown through S-N curves in Figure 4.4 A for absolute and in Figure 4.4 B for normalized stress values obtained by compression-compression fatigue testing, including the power law for the normalized S-N curves of Ti6Al4V ELI and Ta structures as reported previously [6, 50].

Power laws were fitted to the normalized data points of all four series and to all series together and are presented in Table 4.3. The coefficient of determination was very high for all fitted power laws, but it should be noted that the series Ti 170-450 and the combined data have a lower coefficient of determination. When multiplying these power laws by the yield strength of each series for both materials, this results in power laws for the absolute stress values as shown in Figure 4.5 A. The point where the same series in the two materials intersect is marked with an 'X'. It should be noted that Figure 4.5 A assumes that each of the four series in CP Ti are completely identical to the corresponding series in Ti6Al4V ELI, while in fact there are minor differences in overall open porosities between them, which should be kept in mind while interpreting this figure.

In conclusion, Figure 4.5 B shows the fatigue strength S_f after 10^6 cycles, for CP Ti based on an extrapolation of the fitted power laws in Table 4.3, for Ti6Al4V ELI based on the estimated fatigue strength of $0.12\sigma_y$ in [6], taking into account the actual overall porosity for both materials and for all four series, and finally for Ta based on the determined fatigue strength of 7.35 MPa (or $0.57\sigma_y$) for only one porosity mentioned in [50].

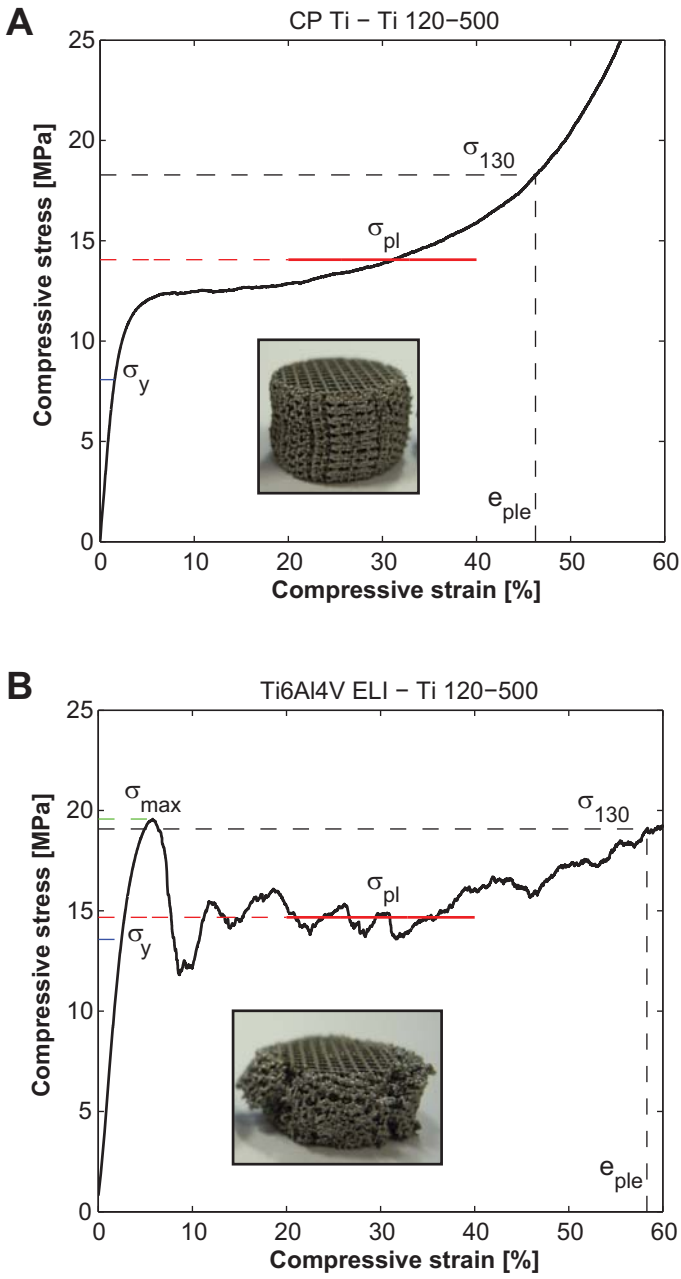

Figure 4.2: Static mechanical properties of open porous SLM processed titanium structures: representative compressive stress-strain curve and graphical representation of the calculated values σ_y, σ_{pl}, σ_{130}, e_{ple} for a Ti 120-500 structure in CP Ti (A) and Ti6Al4V ELI (B), both including a picture of a sample after compression testing.

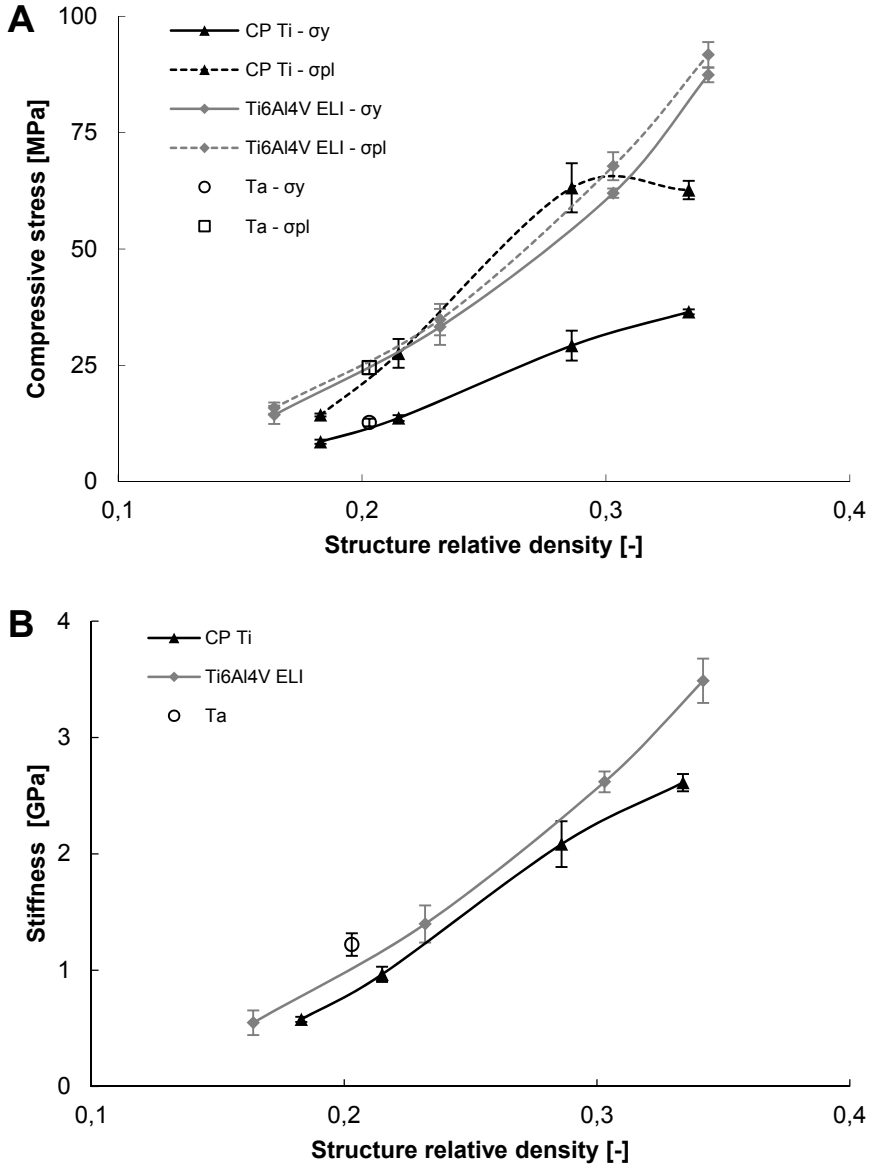

Figure 4.3: Static mechanical properties of open porous SLM processed titanium and tantalum structures: A comparison between the yield strength and plateau stress (A) and stiffness (B) for all three materials versus the actual measured open porosity of each structure.

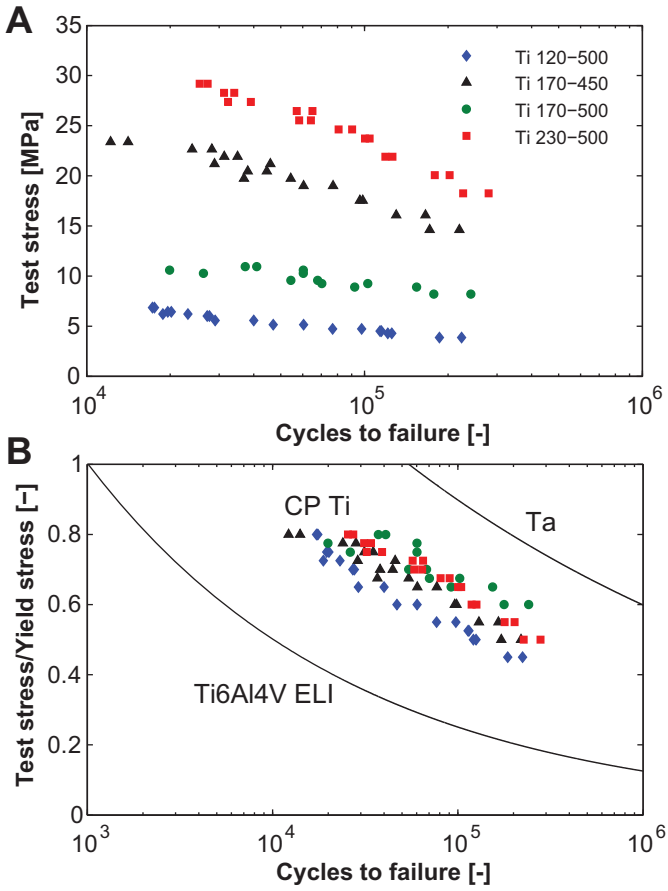

Figure 4.4: Dynamic mechanical properties of open porous SLM processed titanium and tantalum structures: S-N curves obtained by compression-compression fatigue testing of all CP Ti samples using absolute (A) and normalized (B) stress values and a power law representing the results of Ti6Al4V ELI and tantalum structures from previous studies (B) [6, 50];

4.4. Discussion

Recently, it has been shown that selective laser melted porous structures made from Ti6Al4V ELI and Ta can be clinically used as implant materials [46, 50]. Although Ti6Al4V ELI is the current standard for load-bearing implant applications, Ta showed excellent *in vivo* performance and bone ingrowth. The ductile mechanical behavior and the high fatigue strength are believed to be one of the key factors for the performance of porous Ta implants, but due to high material cost, the use of Ta in large orthopedic implants is expected to remain relatively limited. In this study, the SLM technology was used to manufacture

porous CP Ti structures based on dodecahedron unit cells with overall porosities ranging from 66% to 82% in order to compare them with previously published data of Ti6Al4V ELI and Ta structures with the same geometrical architecture.

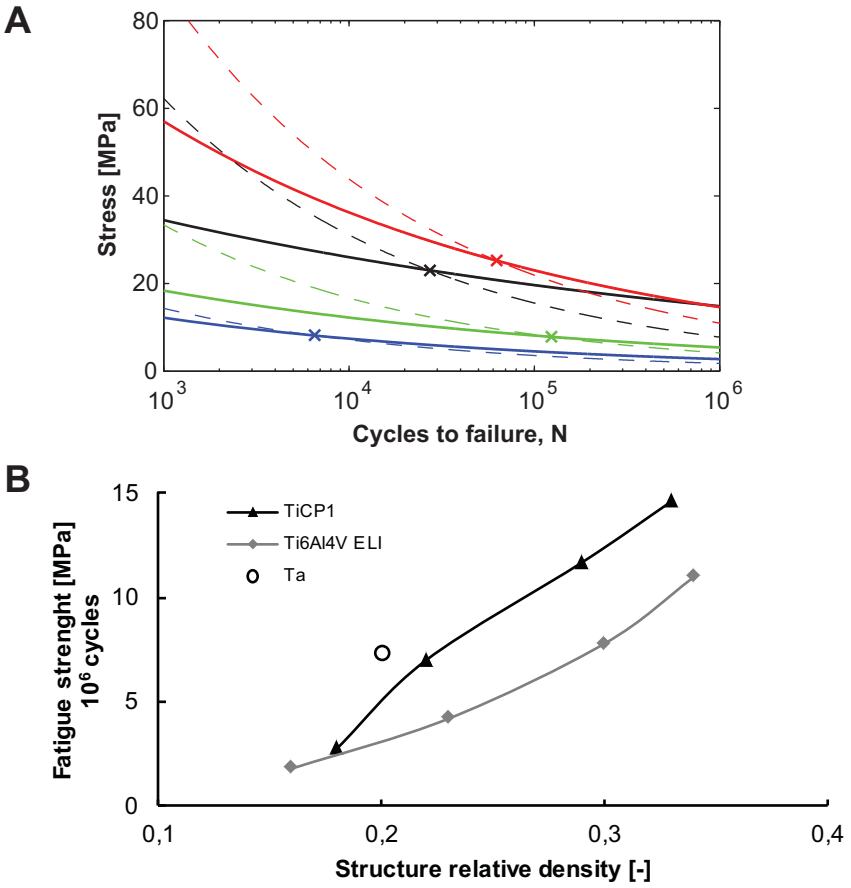

Figure 4.5: Dynamic mechanical properties of open porous SLM processed titanium and tantalum structures: An overview of all fitted power laws for all four porous structures in both titanium materials using absolute stress values, including the structure intersection points marked by 'X' (A); an extrapolation of the fitted power laws to 10^6 cycles for all four porous structures in both titanium materials and the actual fatigue limit of the tantalum structure versus the actual measured open porosity of each structure (B).

A first part investigates whether CP Ti porous structures have similar static and dynamic mechanical properties as compared to pure Ta structures. It was observed that CP Ti porous structures continuously deform under increased

compressive load, without reaching a first local maximum (Figure 4.2 A). This ductile mechanical behavior of CP Ti porous structures is very similar to what was previously reported for pure Ta [50].

Series	Fitted power law	R^2 value	Stress level at 10^6 cycles
Ti 120-500	$\sigma_y \cdot 6.266 \cdot N^{-0.215}$	0.98	$0.32\sigma_y$
Ti 170-450	$\sigma_y \cdot 2.742 \cdot N^{-0.122}$	0.77	$0.51\sigma_y$
Ti 170-500	$\sigma_y \cdot 4.465 \cdot N^{-0.177}$	0.93	$0.39\sigma_y$
Ti 230-500	$\sigma_y \cdot 6.095 \cdot N^{-0.197}$	0.95	$0.40\sigma_y$
All series	$\sigma_y \cdot 4.154 \cdot N^{-0.167}$	0.72	$0.41\sigma_y$

Table 4.3: The power laws fitted to the data points of the normalized S-N curves for all four different series of porous CP Ti samples tested. When multiplied by the corresponding value of the yield strength, the power law of the absolute values is obtained. Also the extrapolated values at $N = 10^6$ cycles are listed.

In order to compare the actual measurable static mechanical properties, it is important to take the overall porosity into account. It was concluded that for both the yield strength and the plateau stress, there is no significant difference between the values of porous Ta and the trend lines of porous CP Ti obtained in this study (Figure 4.3 A and B).

To explain this resemblance, the properties of the solid pure metals Ta and CP Ti should be compared. Both metals are single phase metals, but they do have a different crystal structure; Ta has a cubic BCC structure and Ti has a close packed hexagonal HCP structure [2]. In terms of yield strength both Ta and CP Ti have similar bulk properties (Table 1.1). Since both metals are single phase ductile materials with similar yield strength, the resembling mechanical behavior of Ta and CP Ti as a porous structure can be explained.

The stiffness of porous Ta however appears to be different from the trend line of porous CP Ti stiffness values (Figure 4.3). This difference can be explained by the fact that the stiffness of pure Ta is higher than that of CP Ti (Table 1.1).

Regarding the dynamic mechanical properties it was observed that porous Ta has a higher relative fatigue strength (0.58 σ_y vs. 0.41 σ_y) and since there is no significant difference in yield strength, this resulted in a slightly higher absolute fatigue strength for porous Ta compared to CP Ti (Figure 4.5).

In conclusion it can be stated that porous CP Ti has a comparable mechanical behavior compared to porous Ta, except that CP Ti has a slightly lower stiffness and absolute fatigue strength after 10^6 cycles. This is a very interesting finding, since in a previous study it was shown that the mechanical behavior of porous Ta was likely responsible for the excellent *in vivo* performance, which could now be replaced by the much cheaper, more commonly available and easier to process CP Ti. Therefore the authors suggest for future research to evaluate porous CP Ti implants in an *in vivo* animal study and compare the results with those obtained for porous Ta.

In the second part, identical porous structures in CP Ti and Ti6Al4V ELI have to be compared in order to understand their differences in static and dynamic mechanical properties. To do so, the researchers aimed to manufacture porous CP Ti structures with nearly identical geometrical properties as reported before for Ti6Al4V ELI [6].

The results show that the morphological properties of the CP Ti structures are very close to those of Ti6Al4V ELI, but nevertheless the small differences should be taken into account wherever possible because small changes in overall porosity can have significant influence on the mechanical properties.

Firstly, comparing the mechanical behavior during compression testing already reveals a significant difference between both materials. While porous CP Ti continuously deforms during compression without fracture, Ti6Al4V ELI reaches a maximum compression point, after which the structure starts to fail locally. Due to the geometry of the Ti6Al4V ELI structure, non-failed parts of the structure continue to deform until they fail. This compressive failure behavior continues until a plateau is reached and full compression occurs.

The difference in mechanical deformation or failure can also be seen on the test sample images after compression. The porous CP Ti sample is completely deformed (Figure 4.2 A), whereas the Ti6Al4V ELI structure failed during compression testing (Figure 4.2 B).

This also explains the difference between the values of the plateau end ε_{plE}, which occurs between 40 and 47 % strain for CP Ti and between 56 and 76% strain for Ti6Al4V ELI [6]. Because of the pure deformation of CP Ti structures, full or final compression occurs at lower strains. The yield strength is lower for CP Ti compared to Ti6Al4V ELI. This is also expected since the

yield strength of wrought Ti6Al4V ELI is about four times the strength of CP Ti (Table 1.1). However, for the porous structures compared in this study, the Ti6Al4V ELI structures have a yield strength that is only 1.7 to 2.4 times more than that of CP Ti, as would be expected for standard grade 3 or 4 titanium.

The lower difference can be explained by the fact that the reference values for solid material were processed conventionally (wrought titanium). If strength values of as-manufactured selective laser melted solid Ti6Al4V ELI (1110 MPa [38]) and CP Ti (555 MPa [153]) are used, it should be noted that SLM Ti6Al4V ELI is 40% and CP Ti is 170% stronger compared to their conventionally processed counterparts. In that case, a yield strength difference of 2.0 is obtained, which is in the difference range that actually was observed for both porous materials.

The plateau stress is not significantly different in the range of 70-80% overall porosity, but it tends to be lower for CP Ti outside this interval. Also a strange curve in the trend line for CP Ti is noticeable for the Ti 170-450 series data point. Since this is the only series with smaller pore size compared to the others (450 μm vs. 500 μm) and since porous CP Ti continuously deforms as a whole instead of failing by local fracturing, it is assumed that these two factors are the reason for the particular curve in the trend line of the plateau stress of porous CP Ti.

Given the ductile deformation behavior and the sensitivity of the plateau stress to the pore size, it is important to careful interpret and compare plateau stress for CP Ti, since the calculated values do not represent an actual plateau as is reached with Ti6Al4V ELI. The authors therefore suggest including the deformation mechanism for pure and ductile metals and corresponding definitions of representative values in a next revision of the ISO 13314 standard.

The stiffness of porous CP Ti structures appears to be lower, but not significantly different for porosities >70%, compared to Ti6Al4 ELI. Since solid CP Ti has a lower stiffness compared to Ti6Al4V ELI (Table 1.1), and since both overall porosity and deformation mechanism influence the stiffness of a cellular metal [33, 34], the small differences for the porous structures in Figure 4.3 B are justified.

Summarizing the differences in static mechanical properties between porous CP Ti and Ti6Al4V ELI structures, it can be stated that selective laser melted porous CP Ti has about half the yield strength and a more ductile deformation mechanism compared to Ti6Al4V ELI, while the stiffness remains the same.

When the normalized stress levels of the dynamic properties are compared, it can be concluded that CP Ti has a higher normalized fatigue strength, and an overall normalized fatigue strength after 10^6 cycles of 0.41 σ_y, which is 3.4 times higher than the normalized fatigue strength of Ti6Al4V ELI (Figure 4.4 B, Table 4.3 and [6]).

The S-N curves obtained by fitting power laws through all data series for absolute stress levels, reveal that the S-N curves of CP Ti and Ti6Al4V ELI for each separate series intersect at some point (Figure 4.5 A). Keeping in mind that the porosities were not exactly the same for both materials, which will cause a shift in the intersection point of Ti 120-500 to the right and of Ti 170-500 to the left, it can be reasonably stated that all intersection points lie in the interval 10^4 – 10^5 cycles.

Hence the general observation and conclusion is that Ti6Al4V ELI porous structures are mechanically stronger for static or low cycle fatigue (< 10^4 cycles) applications, whereas commercially pure CP Ti titanium structures are mechanically superior for high cycle fatigue (> 10^5 cycles) applications. This statement is ratified by the extrapolated values at 10^6 cycles for both materials and for the full range of tested porosities, which show superior fatigue strength for porous CP Ti structures compared to Ti6Al4V ELI (Figure 4.5 B).

In general, titanium is known to have a very good fatigue resistance, and properties like crack initiation and crack propagation or growth are often used to explain or predict the fatigue behavior of a material. But for porous structures the situation is more complex, since it is a combination of actual material properties and the architectural properties and surface condition of the structure itself.

Assuming the structures do have identical geometrical morphology, it is reasonable to say that the ductile deformation behavior of porous CP Ti is likely to be the reason for the excellent high cycle fatigue performance, because ductile materials have a lower crack initiation and propagation by softening the material when loaded [136].

This, however, remains a remarkable observation since the wrought titanium alloys generally have a superior fatigue strength compared to commercially pure titanium grades (Table 1.1). Since little is known about the fatigue mechanism for porous metals in general and given that fatigue properties of additively manufactured solid Ti6Al4V ELI reported elsewhere are non-consistent [154-156], the authors consider it as future research to further investigate more in detail the fatigue behavior mechanism of porous metals manufactured by AM and how post process heat treatments can influence these results.

4.5. Conclusions

In this study the additive manufacturing technology selective laser melting was used to manufacture highly open porous (66-82%) CP grade 1 titanium structures. After a morphological characterization, both static and dynamic compression tests were done on four series of porous structures based on the dodecahedron unit cell architecture. The results were compared to previously reported data on identical porous structures in Ta [50] and Ti6Al4V ELI [6].

Based on the experimental results obtained in this study and the comparison with the other two already established orthopedic porous metals (Ti6Al4V ELI and Ta), it can be concluded that CP Ti is an excellent material for dynamically loaded porous implants. At first, it has almost identical mechanical behavior and properties compared to porous Ta, which has proven excellent in vivo performance, likely thanks to these properties. Secondly, for high cycle fatigue strength ($> 10^5$ cycles), CP Ti outperforms Ti6Al4V ELI, but for statically loaded or low cycle fatigue applications ($<10^4$ cycles), Ti6Al4V ELI remains the preferred material.

These conclusions can have a potential huge impact on the medical device industry, because it brings CP Ti back in the scope of implant designers, has a lower cost compared to tantalum and has the advantage of no potential hazardous or toxic alloying components like the presently applied titanium alloys. However, no comparative in vitro and in vivo data between additively manufactured CP Ti and Ti6Al4V ELI is available and the authors suggest to investigate this in future research.

5. CONFIDENTIAL: SLM Productivity Improvements

5.1. Summary

The results presented and discussed in this chapter are confidential and not publically available. In brief, the productivity of porous implants made by SLM has been investigated. Significant productivity improvements have been achieved with build rates up to 4.2 times the previous 'default' build rates for porous implants. Build rates up to 2.7 faster result in porous Ti6Al4V implants with the same mechanical properties as with the previous processing parameters. Higher build rates result in lower mechanical properties and are part of future work to increase the strength. Figure 5.1 and Figure 5.2 below summarize the most important findings.

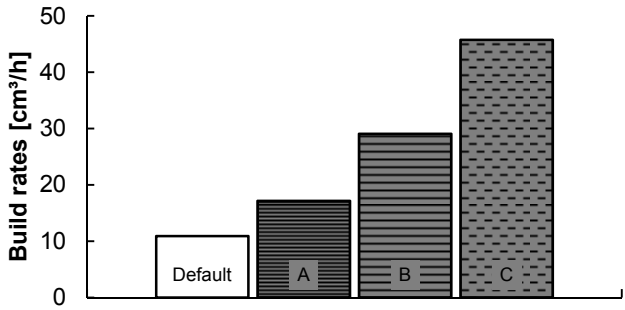

Figure 5.1: Comparison of the build rates of three (A, B, C) optimized processing parameter sets with the current Default processing parameter set.

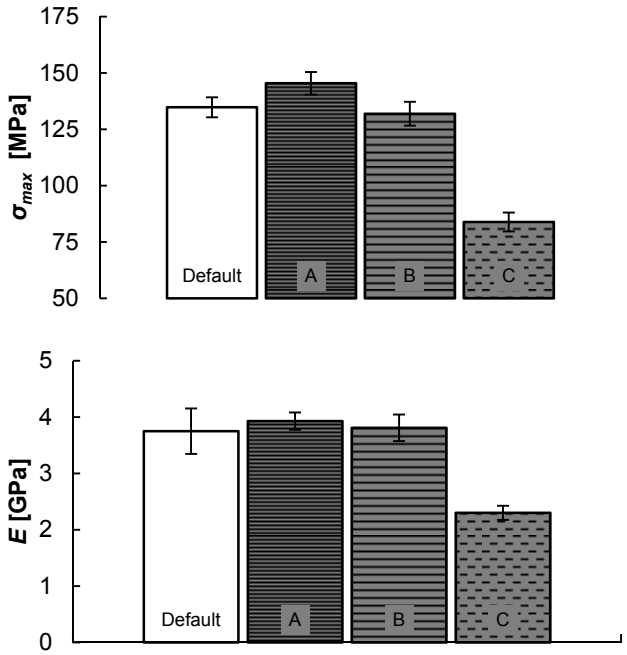

Figure 5.2: Comparison of the mechanical properties of three (A, B, C) optimized processing parameter sets with the current 'Default' processing parameter set. There is no significant difference in the compressive strength (top) and stiffness (bottom) of set A and B, but set C results in significantly lower strength.

6. Conclusions and future research

Metal additive manufacturing is here to stay and will definitely change the future of implant manufacturing. One of the greatest advantages is the almost unlimited design freedom that allows to create regular open porous structures that can be used as functional implants.

Porous metal implants have been of interest for many years now because they avoid stress-shielding effects by a lower stiffness, but still providing sufficient mechanical strength. On top of that, they ensure a good initial fixation by the high coefficient of friction and a long-term stability by the ability of bone ingrowth into the open porosity.

This dissertation investigated porous titanium and tantalum implants manufactured by the Selective Laser Melting technology. Chapter 2 discussed the largest set of experimental data available for porous Ti6Al4V implants, while Chapter 3 reported the first promising results of additively manufactured tantalum implants. The potential revival of pure titanium in orthopedics is predicted in Chapter 4 and finally, significant productivity improvements were achieved in Chapter 5.

In this final chapter, the most important achievements of this dissertation and their implications will be discussed. Since this research was done within the framework of a Baekeland mandate, the connection with the valorization accomplishments will be made. Finally, suggestions for future research will be given.

6.1. Conclusions

Titanium and tantalum are both biocompatible metals that can be used as implant materials. The mechanical properties of these metals, however, do change when they are used as the base material for porous structures. The mechanical strength and stiffness change with a certain amount related to the structure relative density. This is illustrated by Figure 6.1 and Figure 6.2 in

which the traditional material selection charts for the strength and the Young's modulus versus the density have been updated with all experimental results of porous titanium and tantalum reported in this dissertation.

It is clear from these figures that **the application range** of these metals has been extended by new regions that have been defined by these porous metals. For the strength, this new region ranges from the traditional foams to the solid metals fully overlapping the polymer application range (Figure 6.1). The new stiffness values start from the foams and partly overlap with the polymers, but are still an order of magnitude lower compared to the solid metals (Figure 6.2).

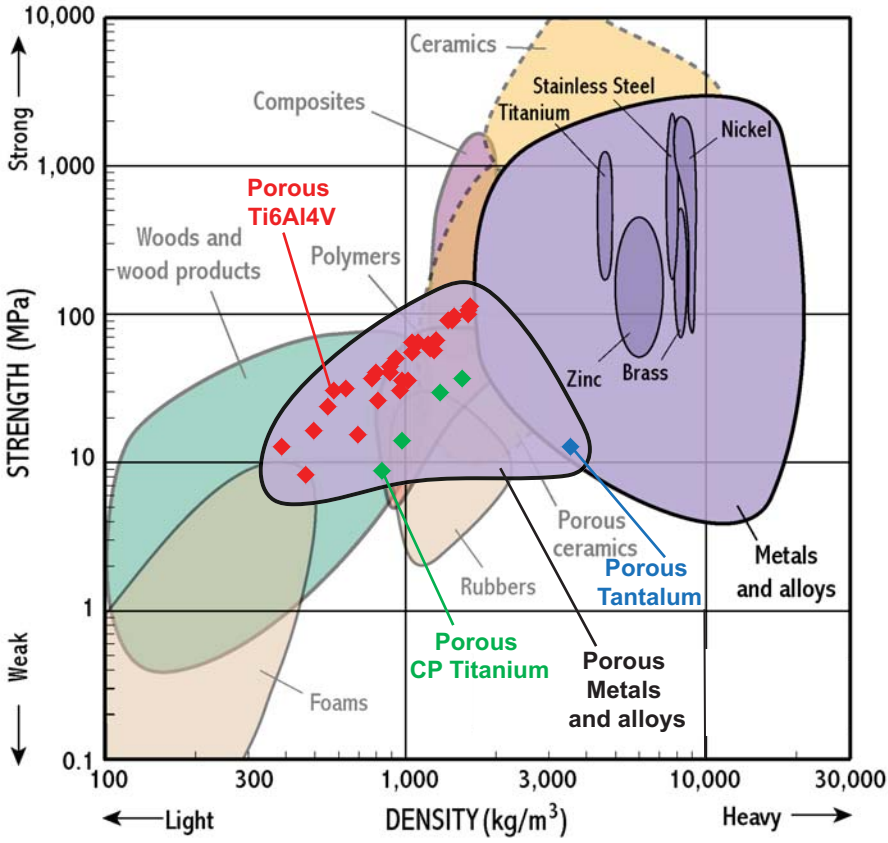

Figure 6.1: Material selection chart for the combination of strength and density. All reported results in this dissertation for the yield strength of porous metallic implants are displayed as red (porous Ti6Al4V), green (CP Titanium) and blue (Tantalum) diamond markers. Chart obtained and modified from [157].

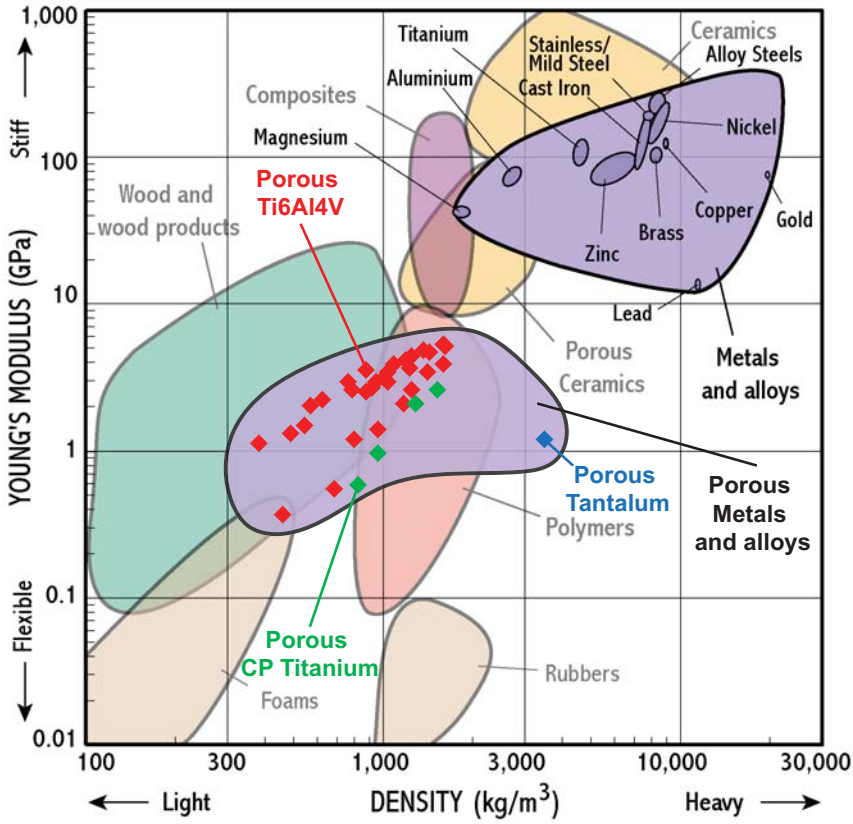

Figure 6.2: Material selection chart for the combination of Young's modulus and density. All reported results in this dissertation for the stiffness of porous metallic implants are displayed as red (porous Ti6Al4V), green (CP Titanium) and blue (Tantalum) diamond markers. Chart obtained and modified from [157].

These updated material selection graphs that summarize part of the results of this dissertation can be useful tools in selecting the right material and density for a certain implant application. But regardless of the mechanical design requirements, there are a lot of other conditions that should be considered while choosing the right porous implant:

The porous implant design

It all starts with designing a porous implant. Additive manufacturing techniques like SLM allow for almost full design freedom, but changing the porous implant

architecture in combination with a certain material, will affect the mechanical properties and bone regeneration performance:

- Increasing the **structure relative density** of porous Ti6Al4V implants between 0.1 and 0.4 increases the static mechanical properties like the yield strength (10 – 110 MPa), maximum strength (15 – 185 MPa) and stiffness (0.5 – 5.5 GPa) by a more than linear relationship. The fatigue strength also increases with an increasing structure relative density, and this is linearly related to the static mechanical properties.
- Porous implants based on a cubic-like **unit cell design** or unit cells with struts parallel to the axis of loading are stronger (both statically and dynamically) and have a higher stiffness compared to more uniform unit cell designs like a diamond or rhombic dodecahedron unit cell.
- The selected **implant material** influences both the mechanical and biological performance. For statically loaded applications, porous Ti6Al4V is still the material of choice, but since both tantalum and pure titanium have a purely ductile deformation behavior, these metals exhibit an excellent fatigue behavior. Porous tantalum showed excellent *in vivo* performance compared to Ti6Al4V, but no results for pure titanium are available yet.

The characteristics of the SLM process

Every manufacturing technique has its limitations and proper knowledge about the characteristics of the SLM process allows to manufacture porous implants with reproducible and uniform mechanical properties:

- Regardless of the structure relative density, the unit cell design, the material and the build orientation, SLM is able to manufacture porous implants with high **reproducibility** of the mechanical properties. In most cases, the standard deviation is less than 5% of the mean value.
- Horizontal struts should be avoided during SLM manufacturing. Improper selection of the **build orientation** can result in inferior mechanical properties (up to 30% less strength).

Post-processing operations

Once a porous implant is manufactured using SLM, many post-processing operations can be applied in order to change or optimize the mechanical or bone regeneration properties:

- **Heat treatments** change the microstructure and the corresponding mechanical properties of porous Ti6Al4V implants. A stress relieve heat treatment increases the yield strength (15 to 25%), while a HIP treatment lowers the maximum strength slightly (up to 15%) and increases the elongation at fraction by up to 70%.
- If certain conditions are met, bone will grow into porous implants made out of a biocompatible metal. **Bio-functionalizing surface treatments or growth factors** can speed up the process of bone regeneration and implant fixation.

Production cost

Eventually, at some point the material and manufacturing cost needs to be taken into account when considering serial manufacturing of porous implants made by SLM:

- Titanium and titanium alloys are relatively **cheap materials** and are easy to (post-)process. Tantalum, on the other hand, is up to 20 times more expensive for the same volume and is difficult to post-machine. Therefore, the use of tantalum for porous implants will be mostly limited to small sized applications.
- The manufacturing cost of porous implants can be reduced significantly by defining **faster processing parameters** (1.6 to 4.2 times faster), but at a certain point, the improved productivity is at the expense of the implant quality.

The obtained productivity improvements are very important for the valorization and industrialization of selective laser melted porous metallic implants. The associated manufacturing cost reductions are absolutely necessary for further establishment of Selective Laser Melting as a fast and reliable method for implant manufacturing. Figure 6.3 shows a comparison of reported build rates of commercial available SLM and EBM machines versus the theoretical build rates achieved for this dissertation. It is recommended to interpret this comparison with care since no details were available on how the

reported build rates were calculated. Nevertheless, two conclusions can be made based on this figure: Although EBM is often associated with being a much faster metal AM process compared to SLM, the productivity gap between the two technologies is disappearing, while SLM keeps a number of advantages over EBM (better surface finish and resolution and easier powder handling). And it should be clear that the productivity improvements lead to a competitive advantage over manufacturers that only use commercial SLM machines.

In conclusion, new insights in additively manufactured porous titanium and tantalum implants have been discussed and can be used as a handbook for design and manufacturing of new generation porous metallic implants. Moreover, significant productivity improvements should pave the path for further industrialization and acceptance of Selective Laser Melting as an established method for producing porous metal implants.

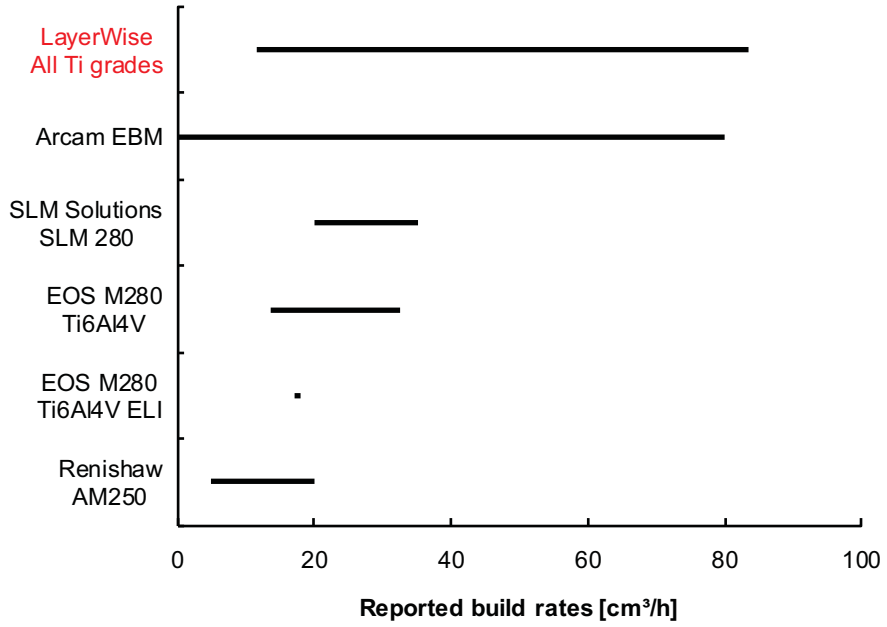

Figure 6.3: Reported build rates for commercial SLM [158-160] and EBM [161] machines compared with the theoretical build rates achieved in this dissertation. The theoretical build rate is determined by multiplying the scan speed, *v* with the hatch spacing, *h* and layer thickness, *t*.

6.2. Suggestions for future research

Using a relatively new technology for new applications in medicine raises a lot of questions, which cannot be answered by only one dissertation. The human body is a complex system and its interactions with implantable devices can be hard to predict and long term clinical outcome results are still the gold standard for measuring actual implant performance. The increased possibilities created by metal additive manufacturing of porous implants make it rather impossible and very costly to do long term evaluations of all possible variations. Therefore this final section provided some suggestions for future research in order to properly use the results of this dissertation for fast and innovative implant advancements.

Many attempts have already been made to create **implant performance simulation software tools**, but only few have tried to incorporate process related aspects of metal additive manufacturing. The results presented in this dissertation can be used to further optimize these models for all processing conditions and different mechanical deformation mechanisms. A few static compression tests can be done in order to 'calibrate' the models and make realistic implant performance predictions.

New manufacturing technologies used for medical device manufacturing will be subjected to the need for more **standardization**. The actual processing steps and parameters during additive manufacturing of porous implants can have a significant influence on the implant properties as illustrated by this dissertation. Proper standards should be developed that take into account all these variables and list minimum requirements in terms of mechanical properties.

Ductile porous metals like tantalum and pure titanium are of interest since they can be deformed intra-operatively to fit to the patient-specific host bone anatomy. Also in the case of tantalum the specific ductile deformation behavior is believed to be partly responsible for the excellent bone regeneration performance and the excellent fatigue life. Therefore it is strongly suggested to further explore these possibilities for pure titanium by initial *in vivo* experiments.

Bibliography

[1] Lampman S. Wrought Titanium and Titanium Alloys. Properties and Selection: Nonferrous Alloys and Special-Purpose Materials, ASM Handbook: ASM International; 1990. p. 592–633.

[2] Lyman WS. Properties of Pure Metals. Properties and Selection: Nonferrous Alloys and Special-Purpose Materials, ASM Handbook: ASM International; 1990. p. 1099–1201.

[3] Thijs L, Montero Sistiaga ML, Wauthle R, Xie Q, Kruth J-P, Van Humbeeck J. Strong morphological and crystallographic texture and resulting yield strength anisotropy in selective laser melted tantalum. Acta Materialia. 2013;61:4657-4668.

[4] Helsen JA, Missirlis Y. Biomaterials - A Tantalus Experience: Springer; 2010.

[5] Campoli G, Borleffs MS, Amin Yavari S, Wauthle R, Weinans H, Zadpoor AA. Mechanical properties of open-cell metallic biomaterials manufactured using additive manufacturing. Materials & Design. 2013;49:957-965.

[6] Amin Yavari S, Wauthle R, van der Stok J, Riemslag AC, Janssen M, Mulier M, et al. Fatigue behavior of porous biomaterials manufactured using selective laser melting. Materials science & engineering C, Materials for biological applications. 2013;33:4849-4858.

[7] Ahmadi SM, Campoli G, Amin Yavari S, Sajadi B, Wauthle R, Schrooten J, et al. Mechanical behavior of regular open-cell porous biomaterials made of diamond lattice unit cells. Journal of the mechanical behavior of biomedical materials. 2014;34C:106-115.

[8] Amin Yavari S, van der Stok J, Chai YC, Wauthle R, Tahmasebi Birgani Z, Habibovic P, et al. Bone regeneration performance of surface-treated porous titanium. Biomaterials. 2014;35:6172-6181.

[9] Amin Yavari S, Ahmadi SM, van der Stok J, Wauthle R, Riemslag AC, Janssen M, et al. Effects of bio-functionalizing surface treatments on the mechanical behavior of open porous titanium biomaterials. Journal of the mechanical behavior of biomedical materials. 2014;36:109-119.

[10] Wauthle R, Vrancken B, Beynaerts B, Jorissen K, Schrooten J, Kruth J-P, et al. Effects of build orientation and heat treatment on the microstructure and mechanical properties of selective laser melted Ti6Al4V lattice structures. Submitted. 2014.

[11] Ahmadi SM, Amin Yavari S, Wauthle R, Pouran B, Schrooten J, Weinans H, et al. Additively manufactured open-cell porous biomaterials made from six different space-filling unit cells: the mechanical and morphological properties. Submitted. 2014.

[12] Amin Yavari S, Ahmadi SM, Wauthle R, Pouran B, Schrooten J, Weinans H, et al. Relationship between unit cell type and porosity and the fatigue behavior of selective laser melted meta-biomaterials. Submitted. 2014.

[13] Brunette DM, Tengvall P, Textos M, Thomsen P. Titanium in Medicine: Springer Berlin Heidelberg; 2001.

[14] Takemoto M, Fujibayashi S, Neo M, Suzuki J, Matsushita T, Kokubo T, et al. Osteoinductive porous titanium implants: effect of sodium removal by dilute HCl treatment. Biomaterials. 2006;27:2682-2691.

[15] Zhao CY, Zhu XD, Yuan T, Fan HS, Zhang XD. Fabrication of biomimetic apatite coating on porous titanium and their osteointegration in femurs of dogs. Materials Science and Engineering: C. 2010;30:98-104.

[16] Materials Properties Handbook: Titanium Alloys: ASM International; 1994.

[17] ISO. 13314: Mechanical testing of metals – Ductility testing – Compression test for porous and cellular metals. 2011.

[18] ASTM. F2924: Standard Specification for Additive Manufacturing Titanium-6 Aluminum-4 Vanadium with Powder Bed Fusion. 2014.

[19] ASTM. F3001: Standard Specification for Additive Manufacturing Titanium-6 Aluminum-4 Vanadium ELI (Extra Low Interstitial) with Powder Bed Fusion. 2014.

[20] Smith M, Guan Z, Cantwell WJ. Finite element modelling of the compressive response of lattice structures manufactured using the selective laser melting technique. International Journal of Mechanical Sciences. 2013;67:28-41.

[21] Wieding J, Jonitz A, Bader R. The Effect of Structural Design on Mechanical Properties and Cellular Response of Additive Manufactured Titanium Scaffolds. Materials. 2012;5:1336-1347.

[22] Yan C, Hao L, Hussein A, Raymont D. Evaluations of cellular lattice structures manufactured using selective laser melting. International Journal of Machine Tools and Manufacture. 2012;62:32-38.

[23] Yang L, Cormier D, West H, Harrysson O, Knowlson K. Non-stochastic Ti–6Al–4V foam structures with negative Poisson's ratio. Materials Science and Engineering: A. 2012;558:579-585.

[24] Sun J, Yang Y, Wang D. Mechanical properties of a Ti6Al4V porous structure produced by selective laser melting. Materials & Design. 2013;49:545-552.

[25] Abele E, Stoffregen HA, Kniepkamp M, Lang S, Hampe M. Selective Laser Melting for Manufacturing of Thin-walled Porous Elements. Journal of Materials Processing Technology. 2014.

[26] Challis VJ, Xu X, Zhang LC, Roberts AP, Grotowski JF, Sercombe TB. High Specific Strength And Stiffness Structures Produced Using Selective Laser Melting. Materials & Design. 2014.

[27] Campanelli SL, Contuzzi N, Ludovico AD, Caiazzo F, Cardaropoli F, Sergi V. Manufacturing and Characterization of Ti6Al4V Lattice Components Manufactured by Selective Laser Melting. Materials. 2014;7:4803-4822.

[28] Heinl P, Muller L, Korner C, Singer RF, Muller FA. Cellular Ti-6Al-4V structures with interconnected macro porosity for bone implants fabricated by selective electron beam melting. Acta biomaterialia. 2008;4:1536-1544.

[29] Parthasarathy J, Starly B, Raman S, Christensen A. Mechanical evaluation of porous titanium (Ti6Al4V) structures with electron beam melting (EBM). Journal of the mechanical behavior of biomedical materials. 2010;3:249-259.

[30] Parthasarathy J, Starly B, Raman S. A design for the additive manufacture of functionally graded porous structures with tailored mechanical properties for biomedical applications. Journal of Manufacturing Processes. 2011;13:160-170.

[31] Horn TJ, Harrysson OLA, Marcellin-Little DJ, West HA, Lascelles BDX, Aman R. Flexural properties of ti6al4v rhombic dodecahedron open cellular structures fabricated with electron beam melting. Additive Manufacturing. 2014.

[32] Li SJ, Xu QS, Wang Z, Hou WT, Hao YL, Yang R, et al. Influence of cell shape on mechanical properties of Ti-6Al-4V meshes fabricated by electron beam melting method. Acta biomaterialia. 2014.

[33] Gibson LJ, Ashby MF. Cellular Solids - Structure and Properties: Cambridge University Press; 1999.

[34] Degischer H-P, Kriszt B. Handbook of Cellular Metals: Production, Processing, Applications: Wiley-VCH Verlag GmbH & Co. KGaA; 2002.

[35] Thijs L, Verhaeghe F, Craeghs T, Humbeeck JV, Kruth J-P. A study of the microstructural evolution during selective laser melting of Ti–6Al–4V. Acta Materialia. 2010;58:3303-3312.

[36] Thijs L, Kempen K, Kruth J-P, Van Humbeeck J. Fine-structured aluminium products with controllable texture by selective laser melting of pre-alloyed AlSi10Mg powder. Acta Materialia. 2013;61:1809-1819.

[37] Tolosa I, Garciandía F, Zubiri F, Zapirain F, Esnaola A. Study of mechanical properties of AISI 316 stainless steel processed by "selective laser melting", following different manufacturing strategies. The International Journal of Advanced Manufacturing Technology. 2010;51:639-647.

[38] Vrancken B, Thijs L, Kruth J-P, Van Humbeeck J. Heat treatment of Ti6Al4V produced by Selective Laser Melting: Microstructure and mechanical properties. Journal of Alloys and Compounds. 2012;541:177-185.

[39] Brenne F, Niendorf T, Maier HJ. Additively manufactured cellular structures: Impact of microstructure and local strains on the monotonic and cyclic behavior under uniaxial and bending load. Journal of Materials Processing Technology. 2013;213:1558-1564.

[40] Sallica-Leva E, Jardini AL, Fogagnolo JB. Microstructure and mechanical behavior of porous Ti-6Al-4V parts obtained by selective laser melting. Journal of the mechanical behavior of biomedical materials. 2013;26:98-108.

[41] Zhang S, Wei Q, Cheng L, Li S, Shi Y. Effects of scan line spacing on pore characteristics and mechanical properties of porous Ti6Al4V implants fabricated by selective laser melting. Materials & Design. 2014;63:185-193.

[42] Speirs M, Humbeeck JV, Schrooten J, Luyten J, Kruth JP. The Effect of Pore Geometry on the Mechanical Properties of Selective Laser Melted Ti-13Nb-13Zr Scaffolds. Procedia CIRP. 2013;5:79-82.

[43] Murr LE, Gaytan SM, Medina F, Martinez E, Martinez JL, Hernandez DH, et al. Characterization of Ti–6Al–4V open cellular foams fabricated by additive manufacturing using electron beam melting. Materials Science and Engineering: A. 2010;527:1861-1868.

[44] Li SJ, Murr LE, Cheng XY, Zhang ZB, Hao YL, Yang R, et al. Compression fatigue behavior of Ti–6Al–4V mesh arrays fabricated by electron beam melting. Acta Materialia. 2012;60:793-802.

[45] Cheng XY, Li SJ, Murr LE, Zhang ZB, Hao YL, Yang R, et al. Compression deformation behavior of Ti-6Al-4V alloy with cellular structures fabricated by electron beam melting. Journal of the mechanical behavior of biomedical materials. 2012;16:153-162.

[46] van der Stok J, Wang H, Amin Yavari S, Siebelt M, Sandker M, Waarsing JH, et al. Enhanced bone regeneration of cortical segmental bone defects using porous titanium scaffolds incorporated with colloidal gelatin gels for time- and dose-controlled delivery of dual growth factors. Tissue engineering Part A. 2013;19:2605-2614.

[47] Chai YC, Truscello S, Bael SV, Luyten FP, Vleugels J, Schrooten J. Perfusion electrodeposition of calcium phosphate on additive manufactured titanium scaffolds for bone engineering. Acta biomaterialia. 2011;7:2310-2319.

[48] Chai YC, Kerckhofs G, Roberts SJ, Van Bael S, Schepers E, Vleugels J, et al. Ectopic bone formation by 3D porous calcium phosphate-Ti6Al4V hybrids produced by perfusion electrodeposition. Biomaterials. 2012;33:4044-4058.

[49] Van der Stok J, Van der Jagt OP, Amin Yavari S, De Haas MF, Waarsing JH, Jahr H, et al. Selective laser melting-produced porous titanium scaffolds regenerate bone in critical size cortical bone defects. Journal of orthopaedic research : official publication of the Orthopaedic Research Society. 2013;31:792-799.

[50] Wauthle R, van der Stok J, Amin Yavari S, Van Humbeeck J, Kruth JP, Zadpoor AA, et al. Additively manufactured porous tantalum implants. Submitted. 2014.

[51] Learmonth ID, Young C, Rorabeck C. The operation of the century: total hip replacement. The Lancet. 2007;370:1508-1519.

[52] Bozic KJ, Kurtz SM, Lau E, Ong K, Vail TP, Berry DJ. The epidemiology of revision total hip arthroplasty in the United States. The Journal of bone and joint surgery American volume. 2009;91:128-133.

[53] Sundfeldt M, Carlsson LV, Johansson CB, Thomsen P, Gretzer C. Aseptic loosening, not only a question of wear: a review of different theories. Acta orthopaedica. 2006;77:177-197.

[54] Villanueva M, Rios-Luna A, Pereiro De Lamo J, Fahandez-Saddi H, Bostrom MP. A review of the treatment of pelvic discontinuity. HSS journal : the musculoskeletal journal of Hospital for Special Surgery. 2008;4:128-137.

[55] Brubaker SM, Brown TE, Manaswi A, Mihalko WM, Cui Q, Saleh KJ. Treatment options and allograft use in revision total hip arthroplasty the acetabulum. The Journal of arthroplasty. 2007;22:52-56.

[56] Black J. Biological performance of tantalum. Clin Mater. 1994;16:167-173.

[57] Balla VK, Bose S, Davies NM, Bandyopadhyay A. Tantalum—A bioactive metal for implants. Jom. 2010;62:61-64.

[58] Matsuno H, Yokoyama A, Watari F, Uo M, Kawasaki T. Biocompatibility and osteogenesis of refractory metal implants, titanium, hafnium, niobium, tantalum and rhenium. Biomaterials. 2001;22:1253-1262.

[59] Johansson CB, Hansson HA, Albrektsson T. Qualitative interfacial study between bone and tantalum, niobium or commercially pure titanium. Biomaterials. 1990;11:277-280.

[60] Findlay DM, Welldon K, Atkins GJ, Howie DW, Zannettino ACW, Bobyn D. The proliferation and phenotypic expression of human osteoblasts on tantalum metal. Biomaterials. 2004;25:2215-2227.

[61] Stiehler M, Lind M, Mygind T, Baatrup A, Dolatshahi-Pirouz A, Li H, et al. Morphology, proliferation, and osteogenic differentiation of mesenchymal stem cells cultured on titanium, tantalum, and chromium surfaces. Journal of biomedical materials research Part A. 2008;86:448-458.

[62] Tang Z, Xie Y, Yang F, Huang Y, Wang C, Dai K, et al. Porous tantalum coatings prepared by vacuum plasma spraying enhance bmscs osteogenic differentiation and bone regeneration in vitro and in vivo. PloS one. 2013;8:e66263.

[63] Miyazaki T, Kim H-M, Kokubo T, Ohtsuki C, Kato H, Nakamura T. Mechanism of bonelike apatite formation on bioactive tantalum metal in a simulated body fluid. Biomaterials. 2002;23:827-832.

[64] Garbuz DS, Hu Y, Kim WY, Duan K, Masri BA, Oxland TR, et al. Enhanced gap filling and osteoconduction associated with alendronate-calcium phosphate-coated porous tantalum. The Journal of bone and joint surgery American volume. 2008;90:1090-1100.

[65] Justesen J, Lorentzen M, Andersen LK, Hansen O, Chevallier J, Modin C, et al. Spatial and temporal changes in the morphology of preosteoblastic cells seeded on microstructured tantalum surfaces. Journal of biomedical materials research Part A. 2009;89:885-894.

[66] Wang N, Li H, Wang J, Chen S, Ma Y, Zhang Z. Study on the anticorrosion, biocompatibility, and osteoinductivity of tantalum decorated with tantalum oxide nanotube array films. ACS applied materials & interfaces. 2012;4:4516-4523.

[67] Paganias CG, Tsakotos GA, Koutsostathis SD, Macheras GA. Osseous integration in porous tantalum implants. Indian journal of orthopaedics. 2012;46:505-513.

[68] Miyazaki T, Kim HM, Kokubo T, Miyaji F, Kato H, Nakamura T. Effect of thermal treatment on apatite-forming ability of NaOH-treated tantalum metal. Journal of materials science Materials in medicine. 2001;12:683-687.

[69] Miyazaki T, Kim HM, Miyaji F, Kokubo T, Kato H, Nakamura T. Bioactive tantalum metal prepared by NaOH treatment. Journal of biomedical materials research. 2000;50:35-42.

[70] Lord MS, Modin C, Foss M, Duch M, Simmons A, Pedersen FS, et al. Monitoring cell adhesion on tantalum and oxidised polystyrene using a quartz crystal microbalance with dissipation. Biomaterials. 2006;27:4529-4537.

[71] Karrholm J, Gill RH, Valstar ER. The history and future of radiostereometric analysis. Clinical orthopaedics and related research. 2006;448:10-21.

[72] Karrholm J, Herberts P, Hultmark P, Malchau H, Nivbrant B, Thanner J. Radiostereometry of hip prostheses. Review of methodology and clinical results. Clinical orthopaedics and related research. 1997:94-110.

[73] Valstar ER, de Jong FW, Vrooman HA, Rozing PM, Reiber JH. Model-based Roentgen stereophotogrammetry of orthopaedic implants. Journal of biomechanics. 2001;34:715-722.

[74] Valstar ER, Gill R, Ryd L, Flivik G, Borlin N, Karrholm J. Guidelines for standardization of radiostereometry (RSA) of implants. Acta orthopaedica. 2005;76:563-572.

[75] Valstar ER, Nelissen RGHH, Reiber JHC, Rozing PM. The use of roentgen stereophotogrammetry to study micromotion of orthopaedic implants. Journal of Photogrammetry & Remote Sensing. 2002;56:376-389.

[76] Duan Y, Liu L, Wang L, Guo F, Li H, Shi L, et al. Preliminary study of the biomechanical behavior and physical characteristics of tantalum (Ta)-coated prostheses. Journal of orthopaedic science : official journal of the Japanese Orthopaedic Association. 2012;17:173-185.

[77] Li X, Wang L, Yu X, Feng Y, Wang C, Yang K, et al. Tantalum coating on porous Ti6Al4V scaffold using chemical vapor deposition and preliminary biological evaluation. Materials science & engineering C, Materials for biological applications. 2013;33:2987-2994.

[78] Bobyn JD, Stackpool GJ, Hacking SA, Tanzer M, Krygier JJ. Characteristics of bone ingrowth and interface mechanics of a new porous tantalum biomaterial. The Journal of bone and joint surgery British volume. 1999;81:907-914.

[79] Gulotta LV, Wiznia D, Cunningham M, Fortier L, Maher S, Rodeo SA. What's new in orthopaedic research. The Journal of bone and joint surgery American volume. 2011;93:2136-2141.

[80] Mantripragada VP, Lecka-Czernik B, Ebraheim NA, Jayasuriya AC. An overview of recent advances in designing orthopedic and craniofacial implants. Journal of biomedical materials research Part A. 2013;101:3349-3364.

[81] Russell RD, Estrera KA, Pivec R, Mont MA, Huo MH. What's new in total hip arthroplasty. The Journal of bone and joint surgery American volume. 2013;95:1719-1725.

[82] Levine B, Della Valle CJ, Jacobs JJ. Applications of porous tantalum in total hip arthroplasty. J Am Acad Orthop Surg. 2006;14:646-655.

[83] Levine BR, Sporer S, Poggie RA, Della Valle CJ, Jacobs JJ. Experimental and clinical performance of porous tantalum in orthopedic surgery. Biomaterials. 2006;27:4671-4681.

[84] Bobyn JD, Poggie RA, Krygier JJ, Lewallen DG, Hanssen AD, Lewis RJ, et al. Clinical validation of a structural porous tantalum biomaterial for adult reconstruction. The Journal of bone and joint surgery American volume. 2004;86-A Suppl 2:123-129.

[85] Levine B. A New Era in Porous Metals: Applications in Orthopaedics. Advanced Engineering Materials. 2008;10:788-792.

[86] ZIMMER HOLDINGS, INC. annual report 2012.

[87] Welldon KJ, Atkins GJ, Howie DW, Findlay DM. Primary human osteoblasts grow into porous tantalum and maintain an osteoblastic phenotype. Journal of biomedical materials research Part A. 2008;84:691-701.

[88] Sagomonyants KB, Hakim-Zargar M, Jhaveri A, Aronow MS, Gronowicz G. Porous tantalum stimulates the proliferation and osteogenesis of osteoblasts from elderly female patients. Journal of orthopaedic research : official publication of the Orthopaedic Research Society. 2011;29:609-616.

[89] Blanco JF, Sanchez-Guijo FM, Carrancio S, Muntion S, Garcia-Brinon J, del Canizo MC. Titanium and tantalum as mesenchymal stem cell scaffolds for spinal fusion: an in vitro comparative study. European spine journal : official publication of the European Spine Society, the European Spinal Deformity Society, and the European Section of the Cervical Spine Research Society. 2011;20 Suppl 3:353-360.

[90] Jonitz A, Lochner K, Lindner T, Hansmann D, Marrot A, Bader R. Oxygen consumption, acidification and migration capacity of human primary osteoblasts within a three-dimensional tantalum scaffold. Journal of materials science Materials in medicine. 2011;22:2089-2095.

[91] Schildhauer TA, Peter E, Muhr G, Koller M. Activation of human leukocytes on tantalum trabecular metal in comparison to commonly used orthopedic metal implant materials. Journal of biomedical materials research Part A. 2009;88:332-341.

[92] Hacking SA, Bobyn JD, Toh K, Tanzer M, Krygier JJ. Fibrous tissue ingrowth and attachment to porous tantalum. Journal of biomedical materials research. 2000;52:631-638.

[93] Reach JS, Jr., Dickey ID, Zobitz ME, Adams JE, Scully SP, Lewallen DG. Direct tendon attachment and healing to porous tantalum: an experimental animal study. The Journal of bone and joint surgery American volume. 2007;89:1000-1009.

[94] Deglurkar M, Davy DT, Stewart M, Goldberg VM, Welter JF. Evaluation of machining methods for trabecular metal implants in a rabbit intramedullary osseointegration model. Journal of biomedical materials research Part B, Applied biomaterials. 2007;80:528-540.

[95] Sambaziotis C, Lovy AJ, Koller KE, Bloebaum RD, Hirsh DM, Kim SJ. Histologic retrieval analysis of a porous tantalum metal implant in an infected primary total knee arthroplasty. The Journal of arthroplasty. 2012;27:1413 e1415-1419.

[96] Hanzlik JA, Day JS, Acknowledged Contributors: Ingrowth Retrieval Study G. Bone ingrowth in well-fixed retrieved porous tantalum implants. The Journal of arthroplasty. 2013;28:922-927.

[97] Kasliwal MK, Baskin DS, Traynelis VC. Failure of porous tantalum cervical interbody fusion devices: two-year results from a prospective, randomized, multicenter clinical study. Journal of spinal disorders & techniques. 2013;26:239-245.

[98] Kwong Y, Desai VV. The use of a tantalum-based Augmentation Patella in patients with a previous patellectomy. The Knee. 2008;15:91-94.

[99] Nebosky PS, Schmid SR, Pasang T. Formability of porous tantalum sheet-metal. IOP Conference Series: Materials Science and Engineering. 2009;4:012018.

[100] Zardiackas LD, Parsell DE, Dillon LD, Mitchell DW, Nunnery LA, Poggie R. Structure, metallurgy, and mechanical properties of a porous tantalum foam. Journal of biomedical materials research. 2001;58:180-187.

[101] Shimko DA, Shimko VF, Sander EA, Dickson KF, Nauman EA. Effect of porosity on the fluid flow characteristics and mechanical properties of tantalum scaffolds. Journal of biomedical materials research Part B, Applied biomaterials. 2005;73:315-324.

[102] Vivanco J, Fang Z, Levine D, Ploeg HL. Evaluation of the mechanical behavior of a direct compression molded porous tantalum-UHMWPE construct: a microstructural model. Journal of applied biomaterials & biomechanics : JABB. 2009;7:34-42.

[103] Niinomi M, Nakai M, Hieda J. Development of new metallic alloys for biomedical applications. Acta biomaterialia. 2012;8:3888-3903.

[104] Kosashvili Y, Backstein D, Safir O, Lakstein D, Gross AE. Acetabular revision using an anti-protrusion (ilio-ischial) cage and trabecular metal acetabular component for severe acetabular bone loss associated with pelvic discontinuity. The Journal of bone and joint surgery British volume. 2009;91-B:870-876.

[105] Deirmengian GK, Zmistowski B, O'Neil JT, Hozack WJ. Management of acetabular bone loss in revision total hip arthroplasty. The Journal of bone and joint surgery American volume. 2011;93:1842-1852.

[106] Issack PS. Use of porous tantalum for acetabular reconstruction in revision hip arthroplasty. The Journal of bone and joint surgery American volume. 2013;95:1981-1987.

[107] Veillette CJ, Mehdian H, Schemitsch EH, McKee MD. Survivorship analysis and radiographic outcome following tantalum rod insertion for osteonecrosis of the femoral head. The Journal of bone and joint surgery American volume. 2006;88 Suppl 3:48-55.

[108] Macheras GA, Kateros K, Koutsostathis SD, Tsakotos G, Galanakos S, Papadakis SA. The Trabecular Metal Monoblock acetabular component in patients with high congenital hip dislocation: a prospective study. The Journal of bone and joint surgery British volume. 2010;92:624-628.

[109] Macheras GA, Papagelopoulos PJ, Kateros K, Kostakos AT, Baltas D, Karachalios TS. Radiological evaluation of the metal-bone interface of a porous tantalum monoblock acetabular component. The Journal of bone and joint surgery British volume. 2006;88:304-309.

[110] Mulier M, Rys B, Moke L. Hedrocel trabecular metal monoblock acetabular cups: mid-term results. Acta orthopaedica Belgica. 2006;72:326-331.

[111] Simon JP, Bellemans J. Clinical and radiological evaluation of modular trabecular metal acetabular cups. Short-term results in 64 hips. Acta orthopaedica Belgica. 2009;75:623-630.

[112] Dunbar MJ, Wilson DA, Hennigar AW, Amirault JD, Gross M, Reardon GP. Fixation of a trabecular metal knee arthroplasty component. A prospective randomized study. The Journal of bone and joint surgery American volume. 2009;91:1578-1586.

[113] Meneghini RM, Lewallen DG, Hanssen AD. Use of porous tantalum metaphyseal cones for severe tibial bone loss during revision total knee replacement. The Journal of bone and joint surgery American volume. 2008;90:78-84.

[114] Howard JL, Kudera J, Lewallen DG, Hanssen AD. Early results of the use of tantalum femoral cones for revision total knee arthroplasty. The Journal of bone and joint surgery American volume. 2011;93:478-484.

[115] Minoda Y, Kobayashi A, Iwaki H, Ikebuchi M, Inori F, Takaoka K. Comparison of bone mineral density between porous tantalum and cemented tibial total knee arthroplasty components. The Journal of bone and joint surgery American volume. 2010;92:700-706.

[116] Hayakawa K, Date H, Tsujimura S, Nojiri S, Yamada H, Nakagawa K. Mid-term results of total knee arthroplasty with a porous tantalum monoblock tibial component. The Knee. 2014;21:199-203.

[117] Fernandez-Fairen M, Sala P, Dufoo M, Jr., Ballester J, Murcia A, Merzthal L. Anterior cervical fusion with tantalum implant: a prospective randomized controlled study. Spine. 2008;33:465-472.

[118] Lofgren H, Engquist M, Hoffmann P, Sigstedt B, Vavruch L. Clinical and radiological evaluation of Trabecular Metal and the Smith-Robinson technique in anterior cervical fusion for degenerative disease: a prospective, randomized, controlled study with 2-year follow-up. European spine journal : official publication of the European Spine Society, the European Spinal Deformity Society, and the European Section of the Cervical Spine Research Society. 2010;19:464-473.

[119] Sinclair SK, Konz GJ, Dawson JM, Epperson RT, Bloebaum RD. Host bone response to polyetheretherketone versus porous tantalum implants for cervical spinal fusion in a goat model. Spine. 2012;37:E571-580.

[120] Frigg A, Dougall H, Boyd S, Nigg B. Can porous tantalum be used to achieve ankle and subtalar arthrodesis?: a pilot study. Clinical orthopaedics and related research. 2010;468:209-216.

[121] Levine BR, Fabi DW. Porous metals in orthopedic applications - A review. Poröse Metalle in orthopädischen Anwendungen - Eine Übersicht. Materialwissenschaft und Werkstofftechnik. 2010;41:1001-1010.

[122] Marin E, Fedrizzi L, Zagra L. Porous metallic structures for orthopaedic applications: a short review of materials and technologies. European Orthopaedics and Traumatology. 2010;1:103-109.

[123] Vandenbroucke B, Kruth J-P. Selective laser melting of biocompatible metals for rapid manufacturing of medical parts. Rapid Prototyping Journal. 2007;13:196-203.

[124] Van Bael S, Chai YC, Truscello S, Moesen M, Kerckhofs G, Van Oosterwyck H, et al. The effect of pore geometry on the in vitro biological behavior of human periosteum-derived cells seeded on selective laser-melted Ti6Al4V bone scaffolds. Acta biomaterialia. 2012;8:2824-2834.

[125] Balla VK, Banerjee S, Bose S, Bandyopadhyay A. Direct laser processing of a tantalum coating on titanium for bone replacement structures. Acta biomaterialia. 2010;6:2329-2334.

[126] Balla VK, Bodhak S, Bose S, Bandyopadhyay A. Porous tantalum structures for bone implants: fabrication, mechanical and in vitro biological properties. Acta biomaterialia. 2010;6:3349-3359.

[127] Zhang YS, Zhang XM, Wang G, Bai XF, Tan P, Li ZK, et al. High strength bulk tantalum with novel gradient structure within a particle fabricated by spark plasma sintering. Materials Science and Engineering: A. 2011;528:8332-8336.

[128] Fox P, Pogson S, Sutcliffe CJ, Jones E. Interface interactions between porous titanium/tantalum coatings, produced by Selective Laser Melting (SLM), on a cobalt–chromium alloy. Surface and Coatings Technology. 2008;202:5001-5007.

[129] Kruth JP, Levy G, Klocke F, Childs THC. Consolidation phenomena in laser and powder-bed based layered manufacturing. CIRP Annals - Manufacturing Technology. 2007;56:730-759.

[130] Wauthle R, Kruth J-P, Montero M, Thijs L, Van Humbeeck J. New opportunities for using tantalum for implants with Additive Manufacturing. European cells & materials. 2013;26:15.

[131] ISO. 13782: Implants for surgery – Metallic materials – Unalloyed tantalum for surgical implant applications. 1996.

[132] ISO. 10993-5: Biological Evaluation of Medical Devices – Part 5: Tests for In Vitro Cytotoxicity. 2009.

[133] Amin Yavari S, van der Stok J, Ahmadi SM, Wauthle R, Schrooten J, Weinans H, et al. Mechanical analysis of a rodent segmental bone defect model: The effects of internal fixation and implant stiffness on load transfer. Journal of biomechanics. 2014;In Press, Corrected Proof.

[134] Köck W, Paschen P. Tantalum—processing, properties and applications. JOM. 1989;41:33-39.

[135] Schussler M, Droegkamp RE. ASM Handbook: ASM International; 1990.

[136] Ritchie RO. Mechanisms of fatigue-crack propagation in ductile and brittle solids. International Journal of Fracture. 1999;100:55-83.

[137] Goodship AE, Kenwright J. The influence of induced micromovement upon the healing of experimental tibial fractures. The Journal of bone and joint surgery British volume. 1985;67:650-655.

[138] Morgan EF, Gleason RE, Hayward LN, Leong PL, Palomares KT. Mechanotransduction and fracture repair. The Journal of bone and joint surgery American volume. 2008;90 Suppl 1:25-30.

[139] Van der Stok J, et a. Osteostatin-coated porous titanium implants improve early bone regeneration in cortical bone defects in rats. Submitted. 2014.

[140] Huiskes R, Ruimerman R, van Lenthe GH, Janssen JD. Effects of mechanical forces on maintenance and adaptation of form in trabecular bone. Nature. 2000;405:704-706.

[141] Wauthle R, Ahmadi SM, Amin Yavari S, Mulier M, Zadpoor AA, Weinans H, et al. Revival of pure titanium for dynamically loaded porous implants using additive manufacturing. Submitted. 2014.

[142] Andani MT, Moghaddam NS, Haberland C, Dean D, Miller MJ, Elahinia M. Metals for bone implants. Part 1. Powder metallurgy and implant rendering. Acta biomaterialia. 2014.

[143] Lewis G. Properties of open-cell porous metals and alloys for orthopaedic applications. Journal of materials science Materials in medicine. 2013;24:2293-2325.

[144] Emmelmann C, Scheinemann P, Munsch M, Seyda V. Laser Additive Manufacturing of Modified Implant Surfaces with Osseointegrative Characteristics. Physics Procedia. 2011;12:375-384.

[145] Van Bael S, Kerckhofs G, Moesen M, Pyka G, Schrooten J, Kruth JP. Micro-CT-based improvement of geometrical and mechanical controllability of selective laser melted Ti6Al4V porous structures. Materials Science and Engineering: A. 2011;528:7423-7431.

[146] Pyka G, Burakowski A, Kerckhofs G, Moesen M, Van Bael S, Schrooten J, et al. Surface Modification of Ti6Al4V Open Porous Structures Produced by Additive Manufacturing. Advanced Engineering Materials. 2012;14:363-370.

[147] Murr LE, Gaytan SM, Medina F, Lopez MI, Martinez E, Wicker RB. Additive Layered Manufacturing of Reticulated Ti-6Al-4V Biomedical Mesh Structures by Electron Beam Melting. In: McGoron A, Li C-Z, Lin W-C, editors. 25th Southern Biomedical Engineering Conference 2009, 15 – 17 May 2009, Miami, Florida, USA: Springer Berlin Heidelberg; 2009. p. 23-28.

[148] Mullen L, Stamp RC, Brooks WK, Jones E, Sutcliffe CJ. Selective Laser Melting: a regular unit cell approach for the manufacture of porous, titanium, bone in-growth constructs, suitable for orthopedic applications. Journal of biomedical materials research Part B, Applied biomaterials. 2009;89:325-334.

[149] Mullen L, Stamp RC, Fox P, Jones E, Ngo C, Sutcliffe CJ. Selective laser melting: a unit cell approach for the manufacture of porous, titanium, bone in-growth constructs, suitable for orthopedic applications. II. Randomized structures. Journal of biomedical materials research Part B, Applied biomaterials. 2010;92:178-188.

[150] Barbas A, Bonnet AS, Lipinski P, Pesci R, Dubois G. Development and mechanical characterization of porous titanium bone substitutes. Journal of the mechanical behavior of biomedical materials. 2012;9:34-44.

[151] de Wild M, Schumacher R, Mayer K, Schkommodau E, Thoma D, Bredell M, et al. Bone regeneration by the osteoconductivity of porous titanium implants manufactured by selective laser melting: a histological and micro computed tomography study in the rabbit. Tissue engineering Part A. 2013;19:2645-2654.

[152] Lipinski P, Barbas A, Bonnet AS. Fatigue behavior of thin-walled grade 2 titanium samples processed by selective laser melting. Application to life prediction of porous titanium implants. Journal of the mechanical behavior of biomedical materials. 2013;28:274-290.

[153] Attar H, Calin M, Zhang LC, Scudino S, Eckert J. Manufacture by selective laser melting and mechanical behavior of commercially pure titanium. Materials Science and Engineering: A. 2014;593:170-177.

[154] Chan KS, Koike M, Mason RL, Okabe T. Fatigue Life of Titanium Alloys Fabricated by Additive Layer Manufacturing Techniques for Dental Implants. Metallurgical and Materials Transactions A. 2012;44:1010-1022.

[155] Leuders S, Thöne M, Riemer A, Niendorf T, Tröster T, Richard HA, et al. On the mechanical behaviour of titanium alloy TiAl6V4 manufactured by selective laser melting: Fatigue resistance and crack growth performance. International Journal of Fatigue. 2013;48:300-307.

[156] Edwards P, Ramulu M. Fatigue performance evaluation of selective laser melted Ti–6Al–4V. Materials Science and Engineering: A. 2014;598:327-337.

[157] University of Cambridge - Department of Engineering - Materials Group. http://www-materials.eng.cam.ac.uk/mpsite/interactive_charts/ August, 2014

[158] SLM Solutions GmbH. http://stage.slm-solutions.com/index.php?index_de July, 2014

[159] EOS GmbH. http://www.eos.info/en July, 2014

[160] Renishaw plc. http://www.renishaw.com/en/renishaw-enhancing-efficiency-in-manufacturing-and-healthcare--1030 July, 2014

[161] Arcam AB. http://www.arcam.com/ July, 2014

Curriculum Vitae

Personal Data

Name	Ruben Wauthle
Date of birth	12 March 1986
Place of birth	Hasselt, Belgium
E-mail	ruben.wauthle@gmail.com
Phone	+32 498 30 28 94

Education

2010-2014: PhD Student
Department of Mechanical Engineering, KU Leuven, Belgium

2007-2009: MSc Degree in Mechanical Engineering – Production and Design
KU Leuven, Belgium
Master Thesis: *"Reducing thermal stresses for Selective Laser Melting"*

2004-2007: BSc Degree in Mechanical Engineering – Industrial Management
KU Leuven, Belgium

1998-2004: Secondary School (Science-Mathematics)
VIA Tienen, Belgium

Work Experience

2010-2014: Medical Application Engineer
LayerWise NV, Belgium

2010: Research Engineer Hip Reconstructive Surgery
UZ Leuven, Belgium

2009-2010: Research Engineer Vibration Assisted Turning of Ceramics
KU Leuven, Belgium

List of Publications

Articles in internationally reviewed journals

- Kruth J.-P., Deckers J., Yasa E., **Wauthle R.**, *Assessing and comparing influencing factors of residual stresses in Selective Laser Melting using a novel analysis method*. Proceedings of the Institution of Mechanical Engineers B, Journal of Engineering Manufacture, 226, 6 (2012), 980-991.
- Thijs L., Montero Sistiaga M., **Wauthle R.**, Xie Q., Kruth J.-P., Van Humbeeck J., *Strong morphological and crystallographic texture and resulting yield strength anisotropy in Selective Laser Melted tantalum*. Acta Materialia, 61, 12 (2013), 4657-4668.
- Campoli G., Borleffs M.S., Amin Yavari S., **Wauthle R.**, Weinans H., Zadpoor A.A., *Mechanical properties of open-cell metallic biomaterials manufactured using additive manufacturing*. Materials & Design, 49, (2013), 957-965.
- Amin Yavari S., **Wauthle R.**, van der Stok J., Riemslag A., Janssen M., Mulier M., Kruth J.-P., Schrooten J., Weinans H., Zadpoor A.A., *Fatigue behavior of porous biomaterials manufactured using selective laser melting*. Materials Science and Engineering C, Materials for Biological Applications, 33, 8 (2013), 4849-4858.
- Amin Yavari S., **Wauthle R.**, Böttger A., Schrooten J., Weinans H., Zadpoor, A.A., *Crystal structure and nanotopographical features on the surface of heat-treaded and anodized porous titanium biomaterials produced using selective laser melting*. Applied Surface Science, 290 (2014), 287-294.
- Ahmadi S., Campoli G., Amin Yavari S., Sajadi B., **Wauthle R.**, Schrooten J., Weinans H., Zadpoor A.A., *Mechanical behavior of regular open-cell porous biomaterials made of diamond lattice unit cells*. Journal of the Mechanical Behavior of Biomedical Materials, 34 (2014), 106-115.
- Amin Yavari S., Ahmadi S., van der Stok J., **Wauthle R.**, Riemslag A., Janssen M., Schrooten J., Weinans H., Zadpoor A.A., *Effects of bio-functionalizing surface treatments on the mechanical behavior of open porous titanium*

biomaterials. Journal of the Mechanical Behavior of Biomedical Materials, 36 (2014), 109-119.

- Amin Yavari S., van der Stok J., Chai Y., **Wauthle R.**, Birgani Z., Habibovic P., Mulier M., Schrooten J., Weinans H., Zadpoor A.A., *Bone regeneration performance of surface-treated porous titanium*. Biomaterials, 35, 24 (2014), 6172-6181.
- Amin Yavari S., van der Stok J., Ahmadi S., **Wauthle R.**, Schrooten J., Weinans H., Zadpoor A.A., *Mechanical analysis of a rodent segmental bone defect model: The effects of internal fixation and implant stiffness on load transfer*. Journal of Biomechanics, 47, 11 (2014), 2700-2708.
- **Wauthle R.**, van der Stok J., Amin Yavari S., Van Humbeeck J., Kruth J.-P., Zadpoor A.A., Weinans H., Mulier M., Schrooten J.. *Additively manufactured porous tantalum implants*. Submitted, 2014.
- **Wauthle R.**, Ahmadi S.M., Amin Yavari S., Mulier M., Zadpoor A.A., Weinans H., Van Humbeeck J., Kruth J.-P., Schrooten J.. *Revival of pure titanium for dynamically loaded porous implants using additive manufacturing*. Submitted, 2014.
- **Wauthle R.**, Vrancken B., Beynaerts B., Jorissen K., Schrooten J., Kruth J.-P., Van Humbeeck J.. *Effects of build orientation and heat treatments on the microstructure and mechanical properties of selective laser melted Ti6Al4V lattice structures*. Submitted, 2014.
- Ahmadi S.M., Amin Yavari S., **Wauthle R.**, Pouran B., Schrooten J., Weinans H., Zadpoor A.A., *Additively manufactured open-cell porous biomaterials made from six different space-filling unit cells: the mechanical and morphological properties*, Submitted, 2014.
- Amin Yavari S., Ahmadi S.M., **Wauthle R.**, Pouran B., Schrooten J., Weinans H., Zadpoor A.A., *Relationship between unit cell type and porosity and the fatigue behavior of selective laser melted meta-biomaterials*, Submitted, 2014.

Articles in conference proceedings

- Kruth J., Deckers J., Yasa E., Wauthle R. *Assessing Influencing Factors of Residual Stresses in SLM using a Novel Analysis Method*. Proceedings of the 16th International Symposium on Electromachining. 16th International

Symposium on Electromachining (ISEM XVI). Shanghai, China, 19-23 April 2010 (pp. 531-537).

- Lauwers B., Wauthle R., Vanparys M., Vanderauwera W., Process *investigation and evaluation of vibration assisted turning of ceramic materials and turning of ecological steels*. Proceedings of MTTRF 2010 Meeting. MTTRF Meeting. San Francisco, CA, 7-8 July 2010 (pp. 127-144).
- Wauthle R., Kruth J.-P., Montero Sistiaga M., Thijs L., Van Humbeeck J., *New opportunities for using tantalum for implants with Additive Manufacturing*. European Cells & Materials: vol. 26. [MEET THE EXPERT – IMPLANTS] Materials – Surfaces – Manufacturing. Interlaken, 22-23 April 2013, Abstract No. 15.
- Vrancken B., Wauthle R., Kruth J.-P., Van Humbeeck J., *Study of the influence of material properties on residual stress in selective laser melting*. Proceedings of the Solid Freeform Fabrication Symposium. Solid Freeform Fabrication Symposium. Austin, Texas, USA, 12-14 August 2013 (pp. 393).
- Pellens E., Wauthle R., Lambrechts T., Bourgine P., Appeltans I., Colsoul B., Holsbeeks I., Schrooten J., Bloemen V., *Comparison of different scaffold materials and different cell types in a 2D+ bioreactor system by LiMSy, a Live cell Monitoring System*. Belgian Symposium on Tissue Engineering. Leuven, 24-25 October 2013 (art.nr. 1-5).